MSc thesis

Experimental and numerical analysis of a silica gel packed bed for passive humidity control in museum rooms

A.T. de Nooijer

Delft University of Technology

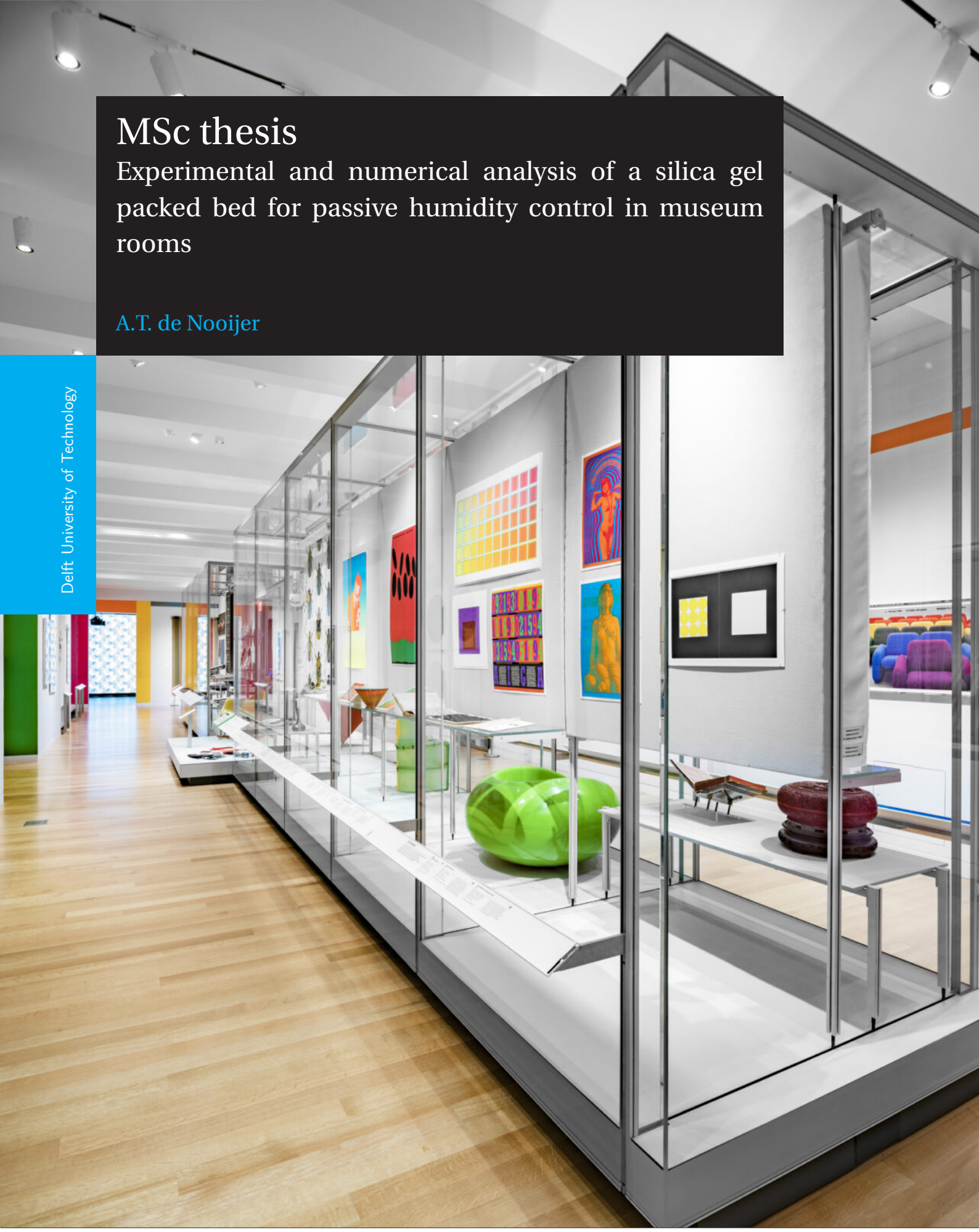

TU Delft Delft University of Technology

Challenge the future

Experimental and numerical analysis of a silica gel packed bed for passive humidity control in museum rooms

MSc thesis

by

A.T. de Nooijer

to obtain the degree of Master of Science
at the Delft University of Technology,
to be defended publicly on Thursday June 23, 2022 at 15.00.

Faculty of Civil Engineering and Geosciences
MSc Civil Engineering - track Building Engineering
specialisation Building Technology & Physics
Delft University of Technology
The Netherlands

In collaboration with:
ABT bv

June 13, 2022

Preface

This thesis marks the end of my master in Civil Engineering at TU Delft. The thesis work is executed in cooperation with TU Delft and ABT.

In this project I had the pleasure to combine the theoretical approach of model study, with the hands-on approach of executing experiments, something I really enjoyed. This project allowed me to combine skills acquired during my bachelor Mechanical Engineering, with new skills from the Building Physics & Technology master. It therefor feels like a satisfying end to my study career, and a strong basis to start my professional work career.

I want to thank all supervisors involved in the project, and other people who assisted in the lab work:

- Willem van der Spoel, for the close guidance during the project, and the interesting in-depth discussions.
- Zara Huybregts, for taking part in the graduation committee, and the critical questions during the progress meetings.
- Roel Schipper, for chairing the graduation committee, and constructive feedback during the progress meetings.
- Marco Poot, for his assistance in the lab work.

Arend-Jan de Nooijer
June 13, 2022

Personalia

Student

Arend-Jan de Nooijer
Student number 4474880
MSc track Building Engineering - specialisation Building Technology and Physics
Robijnstraat 44B
3051VN Rotterdam
A.T.deNooijer@student.tudelft.nl
+316 50512293

Graduation committee

dr.ir. H.R. Schipper - *chair*
TU Delft - Faculty of Civil Engineering and Geosciences
Section Structural Design & Building Engineering
H.R.Schipper@tudelft.nl

dr. ir. W.H. van der Spoel - *daily supervisor*
TU Delft / ABT
Faculty of Architecture and the Built Environment
Section Architectural Engineering and Technology
W.H.vanderSpoel@tudelft.nl

dr. ir. Z. Huijbregts
TU Delft - Faculty of Architecture and the Built Environment
Section Architectural Engineering and Technology
Z.Huijbregts@tudelft.nl

Nomenclature

Acronyms

EMPD	Effective Moisture Penetration Depth
MBV	Moisture Buffering Value
PGC	Pseudo Gas Controlled
SSR	Solid Side Resistance

Physical quantities

ϵ	Porosity [$-$]
μ_{air}	Dynamic viscosity of air [$N/s/m^2$]
ρ_{air}	Density of air [kg/m^3]
ρ_{gel}	Density of silica gel [kg/m^3]
τ	Half time of humidity cycle
θ	Temperature [^oC]
ξ	Hygroscopic capacity [$kg/m3$]
A	Surface area [m^2]
C	Water concentration in silica gel [g/dm^3]
c_{air}	Specific heat capacity of dry air [$J/(kg\ K)$]
c_{gel}	Specific heat capacity of dry silica gel [$J/(kg\ K)$]
c_{liq}	Specific heat capacity of liquid water [$J/(kg\ K)$]
$c_{p,e}$	Specific heat of humid air [$J\ kg^{-1}\ K^{-1}$]
c_{vap}	Specific heat capacity of water vapour [$J/(kg\ K)$]
D	Diameter packed bed [m]
d_b	Effective Moisture Penetration Depth
h_c	Convective heat transfer coefficient [$kg\ m^{-2}\ s^{-1}$]
h_m	Convective mass transfer coefficient [$W\ m^{-2}\ K^{-1}$]
H_{ads}	Heat of adsorption [$J\ kg^{-1}$]
L	Length packed bed [m]
p	Wetted perimeter [m^2]
P_v	Vapour pressure [Pa]
Q	Volumetric flow through packed bed [m^3/s]
R	Particle radius [m]
Re	Reynolds number [$-$]
T	Temperature [K]
U	Superficial air velocity [m/s]
V	Volume [m]
w	Water content [$kg/kg\ d.a$]
x	Humidity ratio [kg/kg]
RH	Relative humidity [$-$]

Subscripts

air	Air in packed bed
bed	Packed bed
cv	Control volume
gel	Silica gel
sat	Saturation
e	Outdoor air
EXP	Experimental data
i	Indoor room air
IN	Inlet air
NUM	Numerical data
OUT	Outlet air
p	Silica gel particle
room	Indoor room

The following convention is used in this report:

- Adsorption of water in silica gel $\equiv$ dehumidification of air: $+\Delta w \equiv -\Delta x_{air}$
- Desorption of water from silica gel $\equiv$ humidification of air: $-\Delta w \equiv +\Delta x_{air}$

Abstract

In this thesis the passive humidity control of indoor air is laid under review. This is primarily interesting for museum rooms, where strict requirements apply to the indoor air humidity. Passive humidity control is promising to contribute to stabilizing the relative humidity levels in a room. Besides, the use of passive humidity control can potentially reduce energy demand for (de)-humidification, and reduce HVAC dimensions as a consequence. This work has zoomed in on the (de)-humidification of air lead through a packed bed with silica gel beads. Silica gel is very promising to use as a buffer material for humidity control as a result of its high hygroscopic capacity, or slope of sorption isotherm.

The work started with uptake rate measurements on different silica gel samples, referred to as Experiment 1. This has yielded adsorption and desorption isotherm between 20 and 80 %RH. The obtained isotherms provide insight in the sorption capacity of different samples, as well as the presence of sorption hysteresis.

Samples with promising sorption and desorption behaviour were selected to include in an experiment with a packed bed. In this experiment, referred to as Experiment 2, silica gel was contained in a packed bed (column) and exposed to cyclic input: alternating high and low levels of relative humidity, using a step function. Both short (1h/1h) as well as long (8h/16h) cycles are executed in the experiment. In both types of experiments, significant dehumidification and humidification of air in the packed bed was measured.

Next to experiments, a numerical model of the packed bed is developed. The results of this model are compared to experimental data from literature and to the experimental data obtained in Experiment 2. The model proves to be able to simulate the course of both temperature and humidity of outlet air exiting the packed bed in a reliable way. The main discrepancy between model and experimental results is found in the response time of the model: it reacts faster to changing inlet compared to measurements. Furthermore the model is sensitive to the inputted isotherm polynomial, $RH(w)$. This polynomial describes the equilibrium of gaseous water in the air and adsorbed liquid water in the silica gel. This equilibrium applies at the interface of air and silica gel surface.

Experiment 2 has shown silica gel is able to both adsorb and desorb water in the humidity range of 40 to 60 %RH. An important observation in the long runs of Experiment 2 is that more water is adsorbed than desorbed in the first cycles. Two issues can be mentioned to explain this: the samples can experience 'primary' hysteresis: some water is permanently retained in silica gel during the first adsorption/desorption cycle. This is a plausible explanation for the difference in primary and secondary isotherms. The other potential explanation is 'sway-in behaviour': it takes some time before the effect of initial conditions is eliminated in a cyclic experiment. In this

case, it is possible that some water is stored in the deeper layers of a silica bead. The moisture uptake and release by silica gel converges to an equal value.

The performance in buffering moisture is expressed in the Moisture Buffering Value (MBV) in [g/m^3/%RH]. This MBV$_\tau$ accounts for the time period of the expected humidity fluctuations. The maximum, or theoretical, MBV$_\infty$ is derived from the equilibrium isotherm. For a given time period of the expected humidity fluctuations, the part of the hygroscopic capacity of silica gel that is effectively used is expressed as:

$$\xi_{effective} = \frac{MBV_\tau}{MBV_\infty} \cdot \xi_{theoretical} \tag{1}$$

The MBV$_\tau$ is determind based on experimental results in this project. The numerical PGC model can serve as a tool to simulate MBV (and $\xi_{effective}$) for different geometries of the silica gel container and different humidity input.

Concluding, silica gel is well able to reduce fluctuations in relative humidity of indoor air. It is important that the silica gel is well reachable by indoor air. Uniform utilization of the silica gel will increase the effective part of the (theoretical) hygroscopic capacity, $\xi_{effective}$ in [kg/m^3], of the silica gel. It is best to avoid long lengths of silica, since the effectiveness of 'upper' silica gel is reduced.

Relative humidity fluctuations can occur either due to changes in absolute humidity (hygric loads) or due to temperature fluctuations in a room. If relative humidity fluctuations are due to changes in absolute humidity, performance of the packed bed could be improved by cooling the silica during adsorption (dehumidification of air) and heating during desorption (humidification of air). Energy demand for temperature control of the silica gel should be limited, to not mitigate the profits in energy demand for passive humidity control.

Contents

1 Introduction

This report starts with a general introduction to the subject. It presents properties of silica gel, and why this is promising for application in a museum room.

1.1 Silica gel as a promising passive humidity buffer

The use of silica gel as a passive humidity buffer is a known application [25]. The main beneficial property is the equilibrium isotherm, which expresses the equilibrium moisture content of silica gel (% or kg/kg) versus the relative humidity of ambient air (%). An example of an isotherm is shown in Figure 1.1, for the commercial ProSorb. It is sold as a humidity buffer to be used in museum display cases.

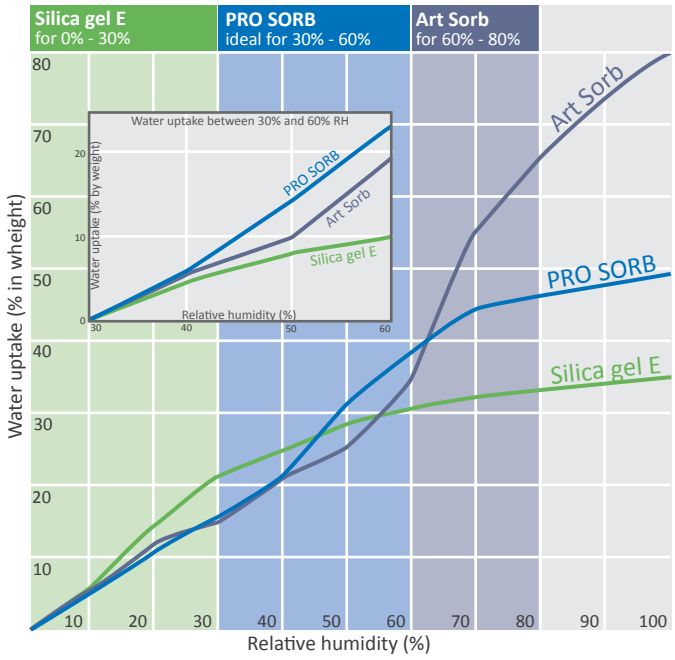

Figure 1.1: Equilibrium isotherm of ProSorb, retrieved from *llfa.eu*

Silica gel is a highly porous material. The inner surface area of ProSorb is approximately $750\ m^2/g$. If the relative humidity of ambient air, exceeds the relative humidity corresponding to the current moisture content, following from the isotherm, adsorption will take place: gaseous water from the air adheres to the (inner) surface area of the silica gel. Vice versa, desorption will occur if air relative humidity is lower than the relative humidity corresponding to the current moisture content.

Adsorption of water from ambient air will thus reduce the air humidity. Desorption of water from silica gel will increase the air humidity. In this way, the silica is expected to act as a buffer for room air humidity. The higher the slope of the isotherm, the higher the amount of moisture adsorbed by the silica gel, for a small change in relative humidity. This process is the main working principle of silica gel as a passive humidity buffer [25].

On the one hand, the process of water adsorption in silica gel is determined by a resistance to the transfer of gaseous water from air to the silica gel surface, as adsorbed water. On the other hand, the process is determined by the diffusion rate in the silica gel [12]. In the display case application, ProSorb is placed in an air-tight display case, impacting a delimited volume. This creates a micro-climate, that may differ from that in the museum room outside the display case.

In the application considered in this thesis, the buffer material is brought into contact with the *total* volume of room air. The room air is lead through a packed bed of silica gel. Using this forced air flow, the resistances to moisture exchange are expected to be reduced. In this way, it is believed silica gel can impact the relative humidity levels of a complete room [15].

This hypothesis is based on the conclusions of the thesis research by Lanwen Zhang [27]. In this research a combined thermal and hygric model of an exhibition room was developed. Yearly simulations of indoor temperature and humidity showed the silica gel is effective in reducing indoor air relative humidity fluctuations. Besides, the yearly simulations indicated a reduction in energy demand for (de)-humidification.

Reducing fluctuations in relative humidity is very important in museum rooms. Fluctuations impose a severe hazard to art works, for several reasons which will be mentioned in Section 2.2. It usually requires installation of large HVAC installations. Even then, it is a heavy task to prevent fast fluctuations in relative humidity, which might occur as a consequence of fast temperature changes or high hygric loads, for example by visitors. The ability to prevent rapid and heavy fluctuations in relative humidity, could result in smaller required HVAC capacity to maintain the same indoor climate [15].

1.2 Research questions and objectives

The *objective* of this research project is to contribute to the development of passive humidity buffering by silica gel in two ways. First, it focuses on validation of the moisture buffering principle. It addresses the level of the material: is the water uptake and release by silica gel as expected, and is it suitable for moisture buffering?

The second way to contribute is by presenting the guidelines and boundary conditions for application of silica gel in a museum room. These guidelines can be taken as a starting point for further design efforts. These design efforts should in the end lead to the development of a moisture buffering device or installation.

In these two ways, this thesis work aims to contribute to the larger goal: reduction of required HVAC capacity by application of passive humidity control. The dimensions of HVAC installations can be smaller as a consequence. Moreover, the energy demand for (de)humidification of air in museum rooms is expected to be reduced.

The first research objective is captured in Research Question 1:

> ***Is a silica gel packed bed able to dampen fluctuations in air relative humidity and how can it be modelled?***

The second research objective involves drawing up a list of design guidelines to guide the design of a prototype. This objective is captured in the second research question:

> ***What can a preliminary prototype for a moisture buffering device for use in museum rooms look like, and what is the performance?***

Both aspects, model validation and design, play a role at each of the three levels mentioned before. The answers to the two research questions are obtained by answering the sub-questions, presented below.

Research question 1

At material level the aim is to represent the silica gel response to changes in relative humidity as close as possible. This means an accurate isotherm has to be applied in the model. Besides the equilibrium isotherm, values for the coefficients describing the moisture uptake and moisture transfer in the silica gel have to be determined and applied in a numerical model. Sub-questions:

1. *How can the equilibrium isotherm for water vapour - silica gel be determined and integrated in the packed bed model?*

2. *How can the values for the coefficients describing water uptake in silica gel be determined, and applied in the model?*

On the level of a packed bed, the following sub-questions need to be addressed:

3. *How can water vapour diffusion resistance in the adsorbent particles be accounted for in the packed bed model?*

4. *How accurate do numerical results match experimental results for a cyclic RH-step input to a silica gel packed bed?*

The packed bed model can be integrated in a model describing energy performance of a room. This is helpful to assess the expected impact at room level. The sub-question left at room level is:

5. *What is the impact on relative humidity levels and energy demand in the room model?*

Research question 2

Regarding design, the first issue is the choice of a suitable silica gel.

6. *Which type of silica gel can best be used in the device?*

At device and room level design guidelines have to be drawn up:

7. *Which technical and aesthetical design guidelines apply for packed bed moisture buffering devices in museum rooms?*

The final sub-question intends to answer how the performance of the device can be specified:

8. *How can the performance of a moisture buffering device be specified?*

1.3 Research methodology

Equilibrium sorption isotherms for water vapour - silica gel can be determined experimentally. The answer to sub question 1 is found by executing Experiment 1. Theoretical relations for the sorption isotherm are encountered in literature [9]. Experimental determination is preferred due to the dependence on manufacturing conditions of silica gel. For application of the isotherm in a numerical model, the sorption isotherm can be fitted. This is done by Pesaran and Mills [12]. The answer to sub-question 2 is derived from literature. Pesaran and Mills have presented correlations for the needed coefficients describing water uptake by the adsorbent [12]. To answer sub-question 3, the first thing is to decide on the complexity of the model. A careful look should be given at the assumptions: which heat and mass transfer modes are included and which are neglected in the model? It is important to reach a balance between the desired accuracy of the model versus the complexity of the computational solution.

Sub-question 4 is answered by executing Experiment 2. In this experiment a cyclic step in relative humidity is inputted in an experimental setup of a packed bed containing silica gel. The numerical results are compared to the results from Experiment 2, to give the answer to sub-question 4. The packed bed model developed in sub-question 3 can be integrated in the numerical model of a room. This model is developed in a previous thesis work [27]. The model makes yearly simulations of the indoor air (relative) humidity and the energy demand for heating, cooling and (de)humidification. The numerical results will be used to answer sub-question 5.

The answer to sub-question 6 is based on the results from Experiment 1. For application in museum rooms, most suitable type of silica gel has steep isotherm between 40 and 60 %RH and has a high rate of moisture transfer. This means a large amount of water is adsorbed and desorbed in this range (mind hysteresis) per change in %RH. Additionally, a high diffusivity or short time to reach equilibrium is desired.

Question 7 should provide a set of design guidelines for a device. These include the technical design guidelines for a packed bed known from literature, for example the relations to calculate pressure drop over a packed bed. Other important phenomena related to packed bed adsorption processes mentioned by Ruthven [19] are axial dispersion, axial heat conduction and heat transfer to the packed bed wall. The ASHRAE guidelines, discussed in Section 2.2 form the basis for a set of technical design guidelines for a room. Aesthetic design guidelines are hard to capture in a generic set of design guidelines. This can best be assessed in a case study. This is not included in this thesis work.

Finally, to answer sub-question 8, common practice to express moisture buffering performance of materials is investigated in literature. The answer to sub-question 8 is based on further analysis of the results of Experiment 2.

The relations between all sub-questions is displayed in the research framework, see Figure 1.2. Vertical arrows indicate which knowledge has to be combined. Horizontal arrows indicate the chronological order of work.

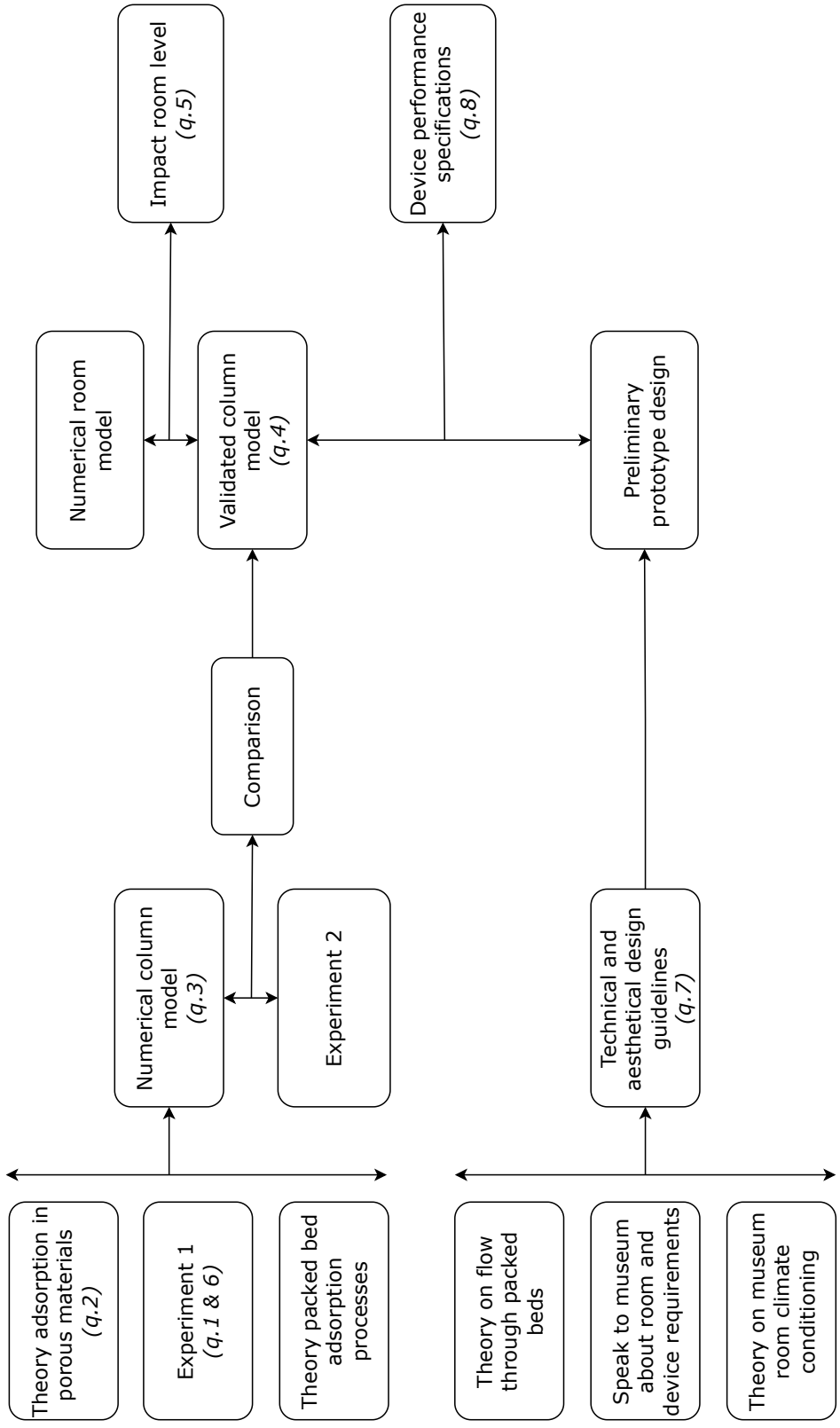

Figure 1.2: Research framework: vertical arrows indicated which knowledge has to be combined. Horizontal arrows indicate the chronological order of work.

2 | Literature study

The topic of this research can be divided into three levels: room level, device level and material level. The goal is to stabilize relative humidity levels and make a saving in energy demand at room level. The different levels and relevant literature are discussed in this chapter. The literature section starts with an overview of the relevant psychrometric equations.

2.1 Psychrometric equations

The relation between humidity ratio and vapour pressure is given by: [2]

$$\text{humidity ratio } x_v \ = 0.622 \ \frac{P_{v,sat} * RH}{P_{atm} - P_{v,sat} * RH} \qquad [kg/kg \ d.a.] \tag{2.1}$$

The denominator is simplified to $P_{atm} - P_{v,sat} * RH \approx P_{atm} = 10^5$. The relation is simplified to:

$$x_v = 0.622 * 10^{-5} * P_{v,sat} * RH = 0.622 * 10^{-5} * P_v \qquad [kg/kg \ d.a.] \tag{2.2}$$

In these equations P_v is the vapour pressure, P_{atm} is the ambient pressure and $P_{v,sat}$ is the saturation pressure for specified temperature.

The saturation pressure can be determined using a psychrometric chart (or Mollier diagram). For modelling purposes it is convenient to express in a correlation. θ is used for temperature expressed in degrees Celsius:

$$P_{v,sat} = 611 \ exp \left\{ \frac{17.27 \ \theta_e}{238.3 + \theta_e} \right\} \qquad [Pa] \tag{2.3}$$

The relative humidity is expressed as follows. Equation 2.4 shows the exact equation for relative humidity. Equation 2.5 shows the approximation used in this thesis. Here, equation 2.4 is simplified to the fraction of humidity ratios.

$$RH = \frac{\frac{x_v}{x_{sat}}}{1 - (1 - \frac{x_v}{x_{sat}}) \frac{p_{sat}}{p_{air}}} \approx \frac{x_v}{x_{v,sat}} \tag{2.4}$$

$$RH = \frac{P_v}{P_{v,sat}} \approx \frac{x_v}{x_{v,sat}} \tag{2.5}$$

2.2 Humidity control in museum rooms - room level

Two goals are associated with the control of indoor climate in museums: provide suitable conditions for the preservation of art pieces and building interior, and create a thermally comfortable indoor environment for occupants [24]. In a PhD thesis [15] Padfield states people are relatively indifferent to humidity levels in a room, in contrast to temperature. For this reason, humidity is usually not controlled in houses and offices. This does not apply to museums and art galleries, which accommodate objects much more sensitive to relative humidity levels. Padfield states low energy strategies for indoor relative humidity control are less developed than for the control of heat. In principle, the same strategies for collecting and storing of heat in thermal mass can be applied to moisture: storage of moisture in hygric mass.
The control of relative humidity levels in museum rooms is important for the preservation of art pieces, for multiple reasons. Organic materials are expanding and contracting due to humidity fluctuations, introducing shear stresses in the material. The amount of expansion and contraction is much higher than for temperature differences. At lower relative humidity values materials become stiff and even more prone to damage due to shear stress. Higher relative humidity levels increase the rate of oxidation, as well as the growth of living organisms, like moulds [15].
Hygric mass can be added to a room in the form of hygroscopic finishing materials in walls and ceiling. Gypsum plaster and wood show equally good moisture adsorption capacity. These materials are able to stabilize indoor relative humidity significantly, provided the air change rate is less than 1 per hour ($ACH < 1$). In practice, a minimum amount of ventilation is often needed to ascertain indoor air quality. Ventilation is counteracting possible passive moisture buffering by hygroscopic materials. Controlling relative humidity is therefor even more challenging in occupied rooms. A common approach is to control relative humidity by conditioning of air in a HVAC installation [15].
There is no deep knowledge on the impact of relative humidity fluctuations on deterioration of art works. Quantitative data is lacking. Thomson states in the future museums should feel responsible to record occuring damage together with quantitative data on the indoor environment. Currently it is hard to say what variation in relative humidity is acceptable regarding damage to art works. The current approach is based on the performance that can be achieved with HVAC installations [21].
The requirements for the indoor climate are laid out by ASHRAE, specifying class AA (precise control) up to class D (limited control). Most museums opt for the most stable indoor climate, resulting in huge energy demands for (de)humidification [24]. In the ASHRAE guidelines, the setpoint voor RH and T control is determined by the historic annual average of an art piece. For loan exhibitions, this is often set at 21 $^{\circ}C$ and 50 %RH, which is a good starting point for this research [6]. The ASHRAE guidelines for classes AA up to B are shown in Table 2.1. Variant As allows a seasonal change in RH setpoint. Variant Ad allows no seasonal change in setpoint, but allows larger daily fluctuations.

Class	Short fluctuations and space gradients	Seasonal adjustments in system set point
AA	± 5 %RH, ± 2 K	RH constant, up 5 K and down 5 K
As	± 5 %RH, ± 2 K	up and down 10 %RH, up 5 K and down 10 K
Ad	± 10 %RH, ± 2 K	RH constant, up 5 K and down 10 K
B	± 10 %RH, ± 5 K	up and down 10 %RH, up 10 K, but not above 30 $°C$

Table 2.1: Indoor climate conditions for ASHRAE classes AA up to B

For a specific museum case, the simulated indoor temperature and relative humidity under control class AA, Ad, As and B are shown in Fig. 2.1.

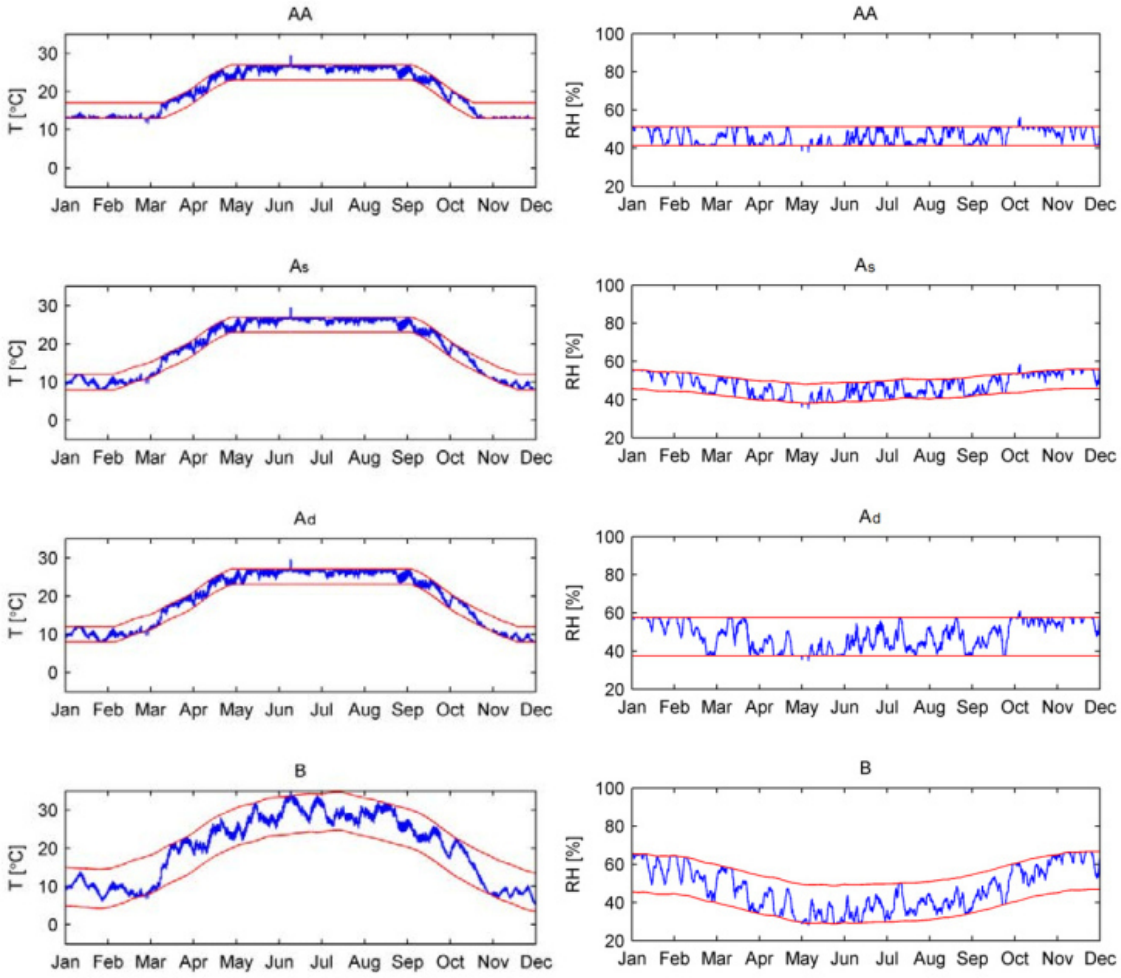

Figure 2.1: Resulting indoor T (left) and RH (right) conditioned at ASHRAE classes AA, Ad, As and B, for a museum with QoE = 3 [23].

Guidelines for optimal indoor climate in museums

An important question to be asked by collection curators is: what is an optimal indoor climate? Experience has shown the optimal indoor climate is not per se the most strict indoor climate. Schellen [11] has mentioned the realisation of an indoor climate suitable for collection preservation, might be conflicting with the preservation of a monumental building.

Four principles are listed to steer museum curators to formulate an optimal indoor climate:

1. **Valuation collection and building**: what are the risks related to the current indoor climate? What risks are present after proposed adaptations are applied? For example, display cases in a historical area are decreasing current value of the exposition. The risk reduction have to be weighed against costs, which include costs related to the adaptations, but also related to the value reduction of the exposition.

2. **Possibilities of building**: a building, in particular the enclosure, imposes limitations on the indoor climate that can be maintained in a building. For example: maintaining 50%RH in an old building is not possible without applying insulation and better air-tightness. The risk of condensation on cold surfaces is high.

3. **Collection risks**: three types of processes are distinguished: chemical, physical and biological degradation. These different processes help in defining what exactly is a wrong RH value.

4. **Type of climate control**: a choice has to be made to not intervene, intervene with passive measures, intervene partly by (de)humidification or heating, or complete air handling. Passive measures are beneficial regarding energy usage and robustness.

The process of finding the right type of intervention requires balancing the first three principles. This can be time consuming and demands experience. Important takeaways from this publication are that striving for one single relative humidity in a building is impossible, and moreover risky! Besides, the costs for maintaining a strict climate in a building with poor enclosure are unacceptably high.
The publication is concluded with emphasizing the need to research possibilities for local climate control. A common approach is to isolate an art object from the bigger space, which can be disadvantageous for the visitors experience. Local climate control can limit the need for complete room air handling [11].

Local room RH controllers

In a book on the indoor environment in museums, Thomson [21] distinguishes two levels of humidity control. The lower level focuses on keeping temperature and humidity within the boundaries. Stated different: its goal is to eliminate the major dangers. The lower level is often realised by the central HVAC installation. The higher level focuses on keeping a stable temperature and relative humidity throughout the year. The higher level is often realised by means of local RH controllers. Traditionally, this type of equipment is either humidifying or dehumidifying. This is acceptable since depending on the climate and the season, either humidifying or dehumidifying

is demanded. This equipment is highly reliant on an accurate humidistat, the equivalent of a well known thermostat.

The novelty of a silica gel packed bed lies in the possibility to both humidify and dehumidify. The silica gel adsorption behaviour is like wood, only the moisture transfer rate and sorption capacity are both higher. Whether it humidifies or dehumidifies is determined by the equilibrium state of the packed bed. The packed bed dries if incoming air is wet relative to the silica gel particles, and humidifies if incoming air is dry relative to the silica gel particles. In this way, the humidistat is physically integrated in the packed bed. Next to this moisture transfer behaviour silica gel is chemically inert and non-flammable, which are attractive properties for application in museums.

Quantitative assessment of indoor air humidity

Janssen [18] has proposed to use a room air moisture balance to predict the course of vapour pressure:

$$\frac{V_{room}}{R_v T_i}\frac{\partial p_{vi}}{\partial t} = (p_{ve} - p_{vi})\frac{nV_{room}}{3600 R_v T_i} + G_{vp} - G_{buf} \tag{2.6}$$

Where $\frac{V}{R_v T_i}$ in [kg/Pa] is the moisture capacity of the zone air, $p_{vi/e}$ the partial vapour pressure of interior/exterior air, n [1/h], the air change rate per hour, V [m^3] the volume of the zone, $R_v = 462$ [J/kg/K] the gas constant of water vapour, T_i [K] the interior air temperature, G_{vp} [kg/s] the interior vapour production and G_{buf} [kg/s] the moisture exchange between room air and room enclosure.

The moisture exchange with indoor finishes, G_{buf}, is often expressed by means of the *Effective Moisture Penetration* model. This model assumes only a thin surface layer is effectively used for moisture buffering: d_b The following expression can be used for G_{buf}:

$$G_{buf} = A \cdot d_b \cdot \xi \frac{\partial}{\partial t}\left(\frac{p_{vb}}{p_{v,sat}(T_b)}\right) \tag{2.7}$$

The effective moisture penetration depth is determined based on a **storage** term, ξ in [kg/m^3] and a **transport** term, water vapour permeability δ_v in [s]. The resulting moisture penetration depth accounts for the time period of the expected humidity fluctuations [18].

The moisture buffering by silica gel, taking into account timed humidity fluctuations, can be assessed using an equivalent approach. Christoffersen [3] proposes to multiply the sorption isotherm (or ξ) with the penetration depth to account for given timed humidity fluctuations.

The approach to express moisture buffering by silica gel is to use equation 2.7 using the total volume and theoretical slope of isotherm. A reduction factor, rf, can be used to account for the time period of humidity fluctuations:

$$G_{buf} = V_{gel} \cdot rf \cdot \xi \frac{\partial}{\partial t}\left(\frac{p_{vb}}{p_{v,sat}(T_b)}\right) \tag{2.8}$$

2.3 Silica gel material properties - material level

Silica gel is commonly used as a desiccant material, for its physical properties. It has a high adsorption capacity at low temperatures and moderate vapour pressures, relative to other adsorbents, like zeolites, activated carbon or activated alumina. The hygroscopic capacity of silica gel is expressed in an equilibrium isotherm, which describes the relation between relative humidity of the air in equilibrium with the desiccant particle and the water content of the particle [9].
Resistances to heat and mass transfer exist both at the gas side and at the solid side. For heat transfer, it is allowed to assume the heat transfer is solely determined by a single resistance in the gas film adjacent to the desiccant surface, because the heat transfer Biot number is small for packed bed situations [2]. For mass transfer however, the solid side resistance to mass diffusion is significant. Diffusion coefficients are hard to measure or predict theoretically. Besides, including both resistances in the model adds to the complexity of numerical solutions. Therefor, in a pseudo-gas-controlled (PGC) model, gas side resistance is modified to account for intra-particle diffusion resistance: a lumped capacitance model. Calculations are done using the average water content [12], [2]. In a solid-side resistance (SSR) model, both resistances are included in the calculation. Fig. 2.2 shows both models.

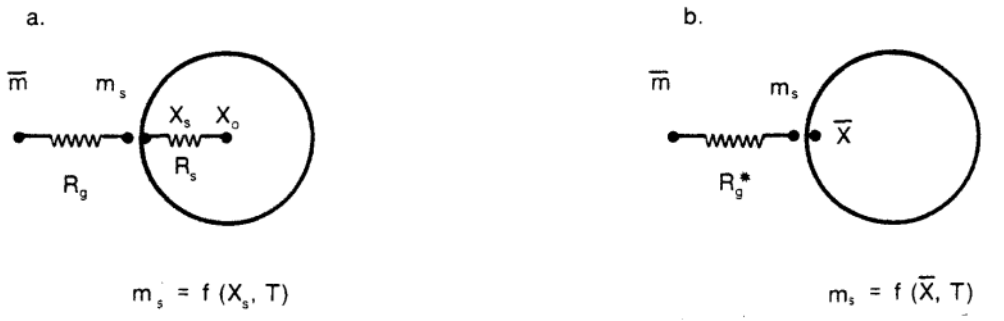

Figure 2.2: (a) Solid-side resistance (SSR) model (b) Pseudo gas-controlled (PGC) model, obtained from [2].

Intra-particle diffusion of water vapour in the pores of silica gel happens by three mechanisms: molecular diffusion, Knudsen diffusion and surface diffusion. The relative contributions depend heavily on the pore structure. Vapour flux through the solid is neglected [19]. According to Pesaran and Mills [12] molecular diffusion is negligible in silica gel at atmospheric pressure.

The concentration distribution in a sphere is described by Fick's diffusion law for a sphere, displayed in Equation 2.9 in general form.

$$\frac{\partial C}{\partial t} = \frac{1}{r^2}\frac{\partial}{\partial r}\left(Dr^2\frac{\partial C}{\partial r}\right) \tag{2.9}$$

If a closer look is given at the micropore, the total water content of a silica gel particle consists of water vapour in the micro-pore air, c, and adsorbed water on the micro-pore surface, q. The vapour part diffuses by Knudsen diffusion, the adsorbed part diffuses by surface diffusion. Fick's law for intra-particle diffusion in silica gel is described as: [22]

$$\epsilon_p\frac{\partial c}{\partial t} + \rho_p\frac{\partial q}{\partial t} = \frac{1}{r^2}\frac{\partial}{\partial r}\left[D_K r^2\frac{\partial c}{\partial r}\right] + \frac{\rho_p}{r^2}\frac{\partial}{\partial r}\left[D_s r^2\frac{\partial q}{\partial r}\right] \tag{2.10}$$

The adsorption step is fast, relative to the diffusion rate in silica gel. For this reason, the water vapour in the micro-pore air can be assumed in equilibrium with the adsorbed phase. This is expressed by the equilibrium sorption isotherm:

$$q = f(c) \rightarrow dq = f'(c)dc \tag{2.11}$$

The expression $\partial c = \frac{\partial q}{f'(c)}$ can be substituted in (2.10):

$$\epsilon_p\frac{\partial c}{\partial t} + \rho_p\frac{\partial q}{\partial t} = \frac{\rho_p}{r^2}\frac{\partial}{\partial r}\left[\frac{D_K}{\rho_p f'(c)}\ r^2\ \frac{\partial q}{\partial r}\right] + \frac{\rho_p}{r^2}\frac{\partial}{\partial r}\left[D_s\ r^2\ \frac{\partial q}{\partial r}\right] \tag{2.12}$$

The two contributions can be combined in an effective diffusivity D_{eff}:

$$D_{eff} = \frac{D_K}{\rho_p}\frac{1}{f'(c)} + D_s \tag{2.13}$$

This will lead to the description of intra-particle diffusion in silica gel:

$$\epsilon_p\frac{\partial c}{\partial t} + \rho_p\frac{\partial q}{\partial t} = \frac{\rho_p}{r^2}\frac{\partial}{\partial r}\left[D_{eff}\ r^2\ \frac{\partial q}{\partial r}\right] \tag{2.14}$$

Silica gel material properties like average particle diameter, surface area and pore volume depend heavily on the manufacturing conditions, such as pH values, gelling and dehydration temperatures. These properties affect the dynamic adsorption properties. This fact makes it necessary to determine the water vapour - silica gel isotherm prior to further modelling of the packed bed. [9]

Equilibrium isotherm

The quantity of moisture contained in a hygroscopic materials depends on the relative humidity of surrounding air. For a specified relative humidity, the moisture content will reach an equilibrium. This relation between equilibrium moisture content (EMC) and target relative humidity is expressed in an equilibrium isotherm. The EMC is usually expressed as a percentage of the dry weight. The EMC depends on temperature as well, although the influence of temperature variations is relatively small compared to relative humidity variations. So it is assumed the temperature has no influence on the water vapour - silica gel equilibrium isotherm in the museum room temperature range [25].

From the isotherm, the buffering capacity of silica gel can be determined. This buffering capacity M is expressed as the amount of moisture (grams) gained or lost by 1 kg of silica gel per 1 % change in RH. The value of M depends on the location on the isotherm, and more important, if measured on the sorption or desorption isotherm. The difference in sorption and desorption isotherm shows the effect of hysteresis in the silica gel.

Silica gel experiences hysteresis over the RH domain. Sorption hysteresis means the equilibrium moisture content of the silica gel is higher for desorption than adsorption, at the same relative humidity. For a pure desorption process the EMC follows the main desorption isotherm. For a pure adsorption process the EMC follows the main adsorption isotherm [20].

The value of M can be corrected to account for hysteresis. This corrected value can be obtained theoretically as well as experimentally. In the theoretical way, the value of the desorption isotherm for the lower limit of RH range can be connected to the value of the sorption isotherm for the upper limit of RH range. This leads to a new slope, that relates to the corrected buffer capacity, displayed in Figure 2.3. This approach does is only applicable for RH regions exceeding 25 %RH. For small RH variations this approach is not applicable [17].

In the experimental method, multiple cycles over the desired RH range, are applied to the silica, to the point where equilibrium moisture content at RH limits is constant [25].

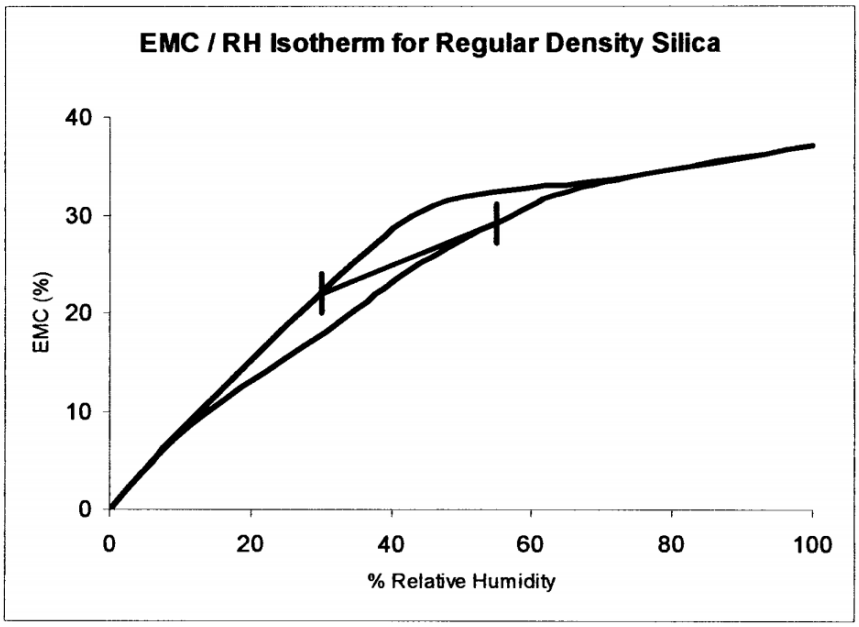

Figure 2.3: Hysteresis and determination of corrected buffering capacity, obtained from [25].

With the design of a device in mind, it is also interesting to review the buffering capacity per volumetric unit: amount of moisture (grams) gained or lost by 1 litre of silica gel per 1 % change. This expression, is known as ξ in other works: [27].

Hysteresis in water vapour - silica gel sorption

Rao has investigated the hysteresis loop in silica gel [17] by applying repeated cycles of sorption and desorption. The results show a large offset in sorption and desorption in the first cycle. These

sorption and desorption isotherms are labelled *primary isotherms*. All later cycles show similar sorption and desorption isotherms, as shown in Figure 2.4. The third up to nineteenth isotherms, are identical to the second cycle, concluding the hysteresis loop is permanent and reproducible.

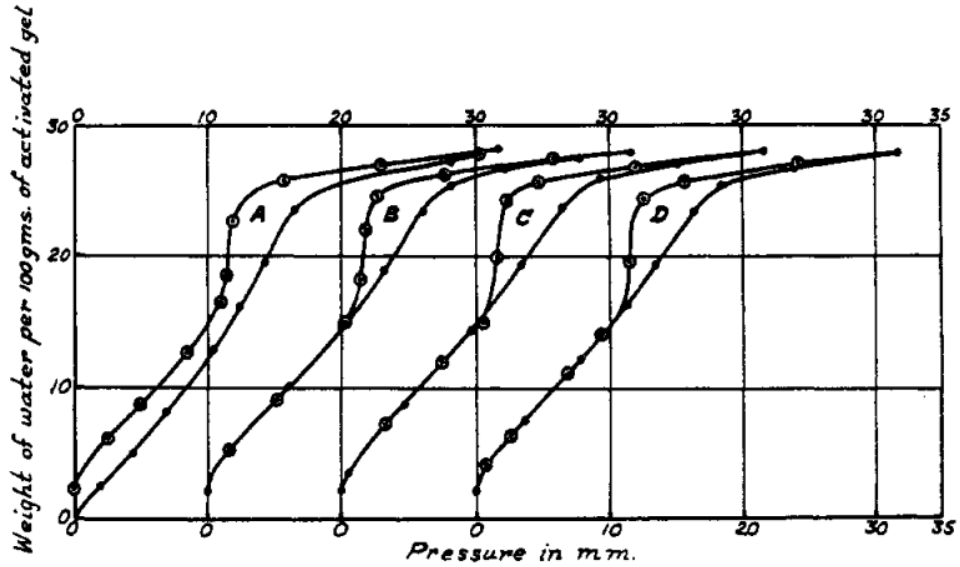

FIG. 1. Hysteresis loop in the sorption of water by silica gel. A, first sorption (●) and desorption (⊙); B, second sorption (●) and desorption (⊙); C, third sorption (●) and desorption (⊙); D, nineteenth sorption (●) and desorption (⊙).

Figure 2.4: Sorption and desorption isotherms for repeated RH cycles, obtained from [17].

Rao [17] has zoomed in at the hysteresis loop as well. The main outcome is: if starting from the main sorption curve, desorption is applied, the curve crosses the hysteresis loop and reaches the main desorption curve, as shown in Figure 2.5(a). However, if starting from the main desorption curve, sorption is applied, the curve reaches the main sorption curve at the top of the hysteresis loop, as shown in Figure 2.5(b).

Hysteresis is encountered in other hygroscopic materials, like wood. More literature is available on the sorption hysteresis phenomena in wood. The curves crossing the hysteresis loop are called *scanning* curves. When sorption follows desorption (in the hysteresis loop) the EMC follows a unique path through the hysteresis loop. Correlations for the isotherm of hygroscopic materials are usually the average of sorption and desorption isotherms. Correction factors will be introduced to the models to account for the error introduced by using average isotherm expressions. Salin mentions identical behaviour of scanning isotherms within the hysteresis loop as Rao [20].

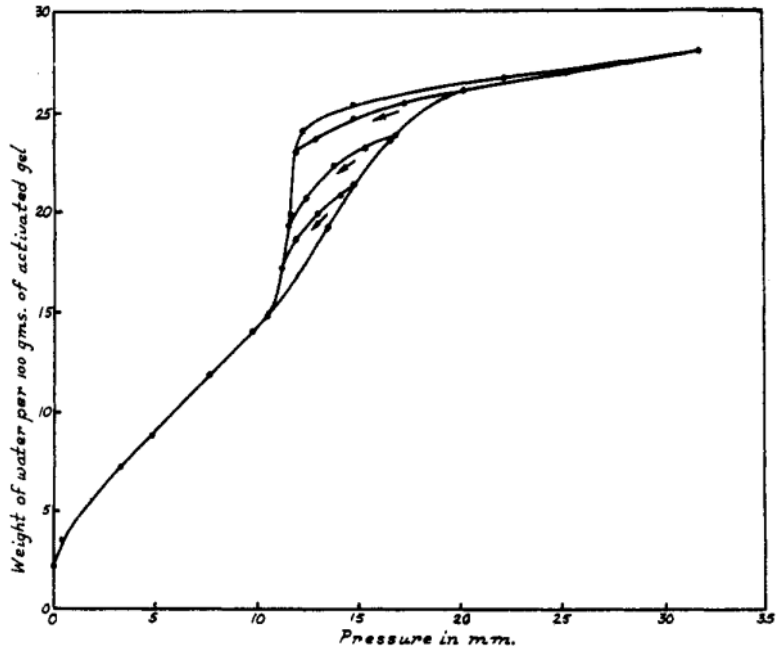

FIG. 2. Scanning of the hysteresis loop in the sorption of water on silica gel

(a)

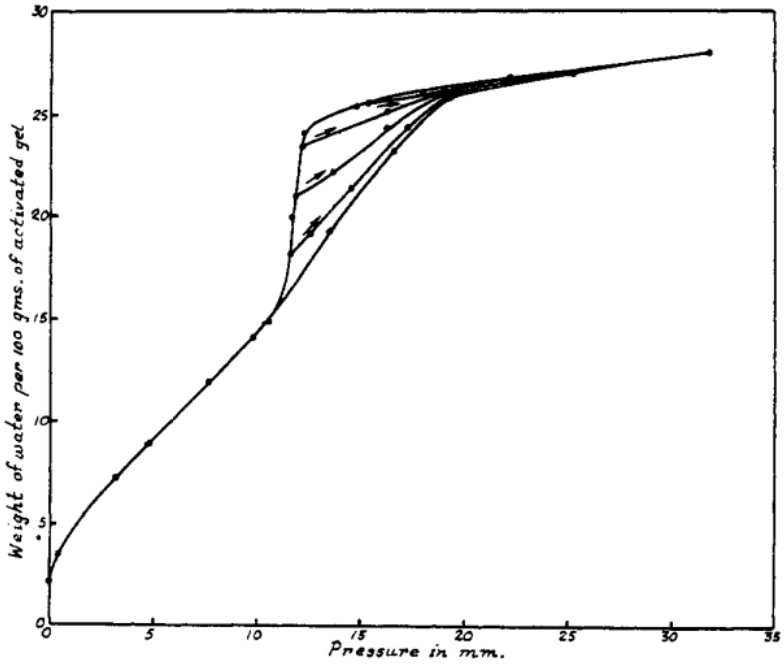

FIG. 3. Scanning of the hysteresis loop in the sorption of water on silica gel

(b)

Figure 2.5: Scanning of the hysteresis loop: (a) desorption from the sorption curve (b) sorption form the desorption curve, obtained from [17].

2.4 Adsorption in packed beds - device level

This section starts with presenting the governing set of equations for a packed bed with silica gel, as presented by Pesaran and Mills [12]. Thereafter, experimental and numerical results obtained by De Antonellis are presented [8]. At the end, the applicable relations for fluid flow through a packed bed are presented.

Governing set of equations, presented by Pesaran [12]

Hygroscopic materials are often addded to a room to provide moisture buffering capacity. The principle under review in this research is to add hygric mass in the form of a packed bed containing an adsorbent material. Water vapour is adsorbed by the adsorbent when the incoming air is wet relative to the bed. Ideally, water vapour is again desorbed from the adsorbent when the incoming air is dry relative to the bed.

A quick response to hourly variations can possibly reduce the required ventilation rates of the HVAC installation. As a consequence the energy demand for (de)humidification is lower. Peak capacity of the HVAC installation is likely lower, which means it can have smaller dimensions.

Pesaran and Mills have presented a set of governing relations describing the transient response of a silica gel packed bed to changes in inlet air conditions, for both a SSR and a PGC model. The governing equations for a SSR model are equations (21), (22a), (23), (28), (31) and (32) from [12], respectively given below. Symbols unique for this set of equations are declared separate from the Nomenclature in Table 2.2. In an experimental study both model types are verified by experiments. The conclusion is that for both models numerical results agree with experimental results, but in general the SSR model agrees better. These coupled non-linear equations have six unknowns: water vapour mass fraction at particle surface s: $m_{1,s}(z,t)$, water vapour mass fraction in flowing air: $m_{1,e}(z,t)$, water content in silica particles: $W(z,r,t)$, average water content in silica particles: $W(z,t)$, temperature of particle surface s: $T_s(z,t)$ and temperature of flowing air: $T_e(z,t)$. The proposed solution method is discretization of the set of equations.

$$\dot{m}_G * \frac{\partial m_{1,e}}{\partial z} = K_G(m_{1,s} - m_{1,e})(1 - m_{1,e})p \tag{21}$$

$$\frac{\partial W}{\partial t} = \frac{1}{r^2}\frac{\partial}{\partial r}(r^2 D \frac{\partial W}{\partial r}) \tag{22a}$$

$$m_{1,s}(z,t) = \frac{0.622\ RH\ \times P_{sat}(T_s)}{P_{total} - 0.378\ RH \times P_{sat}(T_s)} \tag{23}$$

$$W_{avg} = \frac{\int_0^K 4\pi r^2 W \rho_p dr}{(4/3)\pi R^3 \rho_p} \tag{28}$$

$$c_{p,e}\dot{m}_G \frac{\partial T_e}{\partial z} = -p[h_c + c_{p1}K_G(m_{1,s} - m_{1,e})] * (T_e - T_s) \tag{31}$$

$$A\rho_b c_b \frac{\partial T_s}{\partial t} = p[h_c(T_e - T_s) - H_{ads}K_G(m_{1,s} - m_{1,e})] \tag{32}$$

Symbol	Physical quantity	Units
m	humidity ratio	[kg vapour/ kg dry air]
K_G	gas-side mass transfer coefficient	[kg m^{-2} s^{-1}]
h_c	convective heat transfer coefficient	[W m^{-2} K^{-1}]
W	water content	[kg water / kg silica gel]
z	axial distance	[m]
r	radial coordinate in particle	[m]
c_{p1}	specific heat of water vapour	[J/(kg K)]
m_G	mass flow rate of gas mixture	[kg/s]

Symbol	Subscript
e	air
s	silica gel
b	bed, bulk
p	particle

Table 2.2: Nomenclature to set of equations by Pesaran [12]

In case of the PGC model, equations (22a) and (28) are replaced by equation (22b), shown below.

$$A\rho_b \frac{W_{avg}}{\partial t} = -K_{G,eff}(m_{1,s} - m_{1,e})p \tag{22b}$$

Model parameters

The governing equations need values for different parameters. Below are the values as proposed by Pesaran and Mills [12].
For the gas-side mass transfer coefficient K_G:

$$K_G = 1.70\ G_a\ Re^{-0.42} \qquad \text{kg m}^{-2}\ \text{s}^{-1} \tag{2.15}$$

For the convective heat transfer coefficient h_c

$$h_c = 1.60\ G_a\ Re^{-0.42}\ c_{p,e} \qquad \text{W m}^{-2}\ \text{K}^{-1} \tag{2.16}$$

G_a is the air mass flow rate per unit area in [kg m^{-2} s^{-}1], which is equal to the product of air density and superficial air velocity: $G_a = U * \rho_{air}$. Re is the dimensionless Reynolds number.

In case the PGC model is applied, the above coefficients are corrected to discount for diffusion:

$$K_{G,eff} = 0.704\ G_a\ Re^{-0.51} \qquad \text{kg m}^{-2}\ \text{s}^{-1} \tag{2.17}$$

$$h_{c,eff} = 0.683\ G_a\ Re^{-0.51}\ c_{p,e} \qquad \text{W m}^{-2}\ \text{K}^{-1} \tag{2.18}$$

For the heat of sorption, different correlations are mentioned in [12], depending on silica gel density and range of water content.

The total effective diffusivity, from equation (22a), is given by:

$$D_{eff} = D_{S,eff} + D_{K,eff} \frac{g'(W)}{\rho_p} \qquad m^2\ s^{-1} \tag{2.19}$$

In which, the effective Knudsen diffusivity $D_{K,eff}$ is given by:

$$D_{K,eff} = \frac{\epsilon_p}{\tau_g} D_K \tag{2.20}$$

$$D_K = 22.86\ a\ (T + 273.15)^{1/2} \qquad m^2\ s^{-1} \tag{2.21}$$

In the above equations, ϵ_p represents the particle porosity, τ_g the gas tortuosity factor, a the cylindrical pore radius in meters and T the temperature in degrees Celsius.

The effective surface diffusivity $D_{K,eff}$ is expressed as:

$$D_{S,eff} = \frac{1}{\tau_s} D_S \tag{2.22}$$

$$D_S = D_0\ exp\left[-0.974 \times 10^{-3}\ \times \frac{H_{ads}}{T + 273.15}\right] \tag{2.23}$$

D_0 is estimated at $1.6 \times 10^{-6}\ m^2\ s^{-1}$. τ_s is the surface tortuosity.

The specific heat of humid air $c_{p,e}$ is given by:

$$c_{p,e} = 1884\ m_{1,e} + 1004(1 - m_{1,e}) \qquad J\ kg^{-1}K^{-1} \tag{2.24}$$

The specific heat of the bed c_b is expressed as:

$$c_b = 4186\ W_{avg} + 921 \qquad J\ kg^{-1}\ K^{-1} \tag{2.25}$$

Experiments and model study by De Antonellis [8]

Experiments on a silica gel packed bed are executed by De Antonellis et al. [8]. Their aim is to develop a passive system for humidifying air in an Air Handling Unit, by alternatively crossing two silica gel packed beds. In the first packed bed, humid indoor air is dehumidified before exhausted to outside; the packed bed is loaded. Outdoor air, before entering the room is humidified by crossing the loaded packed bed. After a while the flow is alternated. Their design activities have started by examining the behaviour of a single packed bed.

In their model, they have adopted a PGC model, following the set of equations presented by Pesaran [12]. In their experiment, the bed, of length 5.5 cm and diameter 25 cm is alternatively crossed by following air flows:

- $T = 32.3\ ^{\circ}C$ and $x = 7.9\ g/kg$ at $v = 0.60\ m/s$
- $T = 55.7\ ^{\circ}C$ and $x = 7.1\ g/kg$ at $v = 0.55\ m/s$

The packed bed in the research by De Antonellis should fulfill similar function as in current research: dehumidify wet air, by storing water in the silica gel, to humidify dry air later. Since De Antonellis has executed cyclic experiments, it serves as a good reference for the experiments executed in this research. Experimental results compared to numerical results are shown in Fig. 2.6.

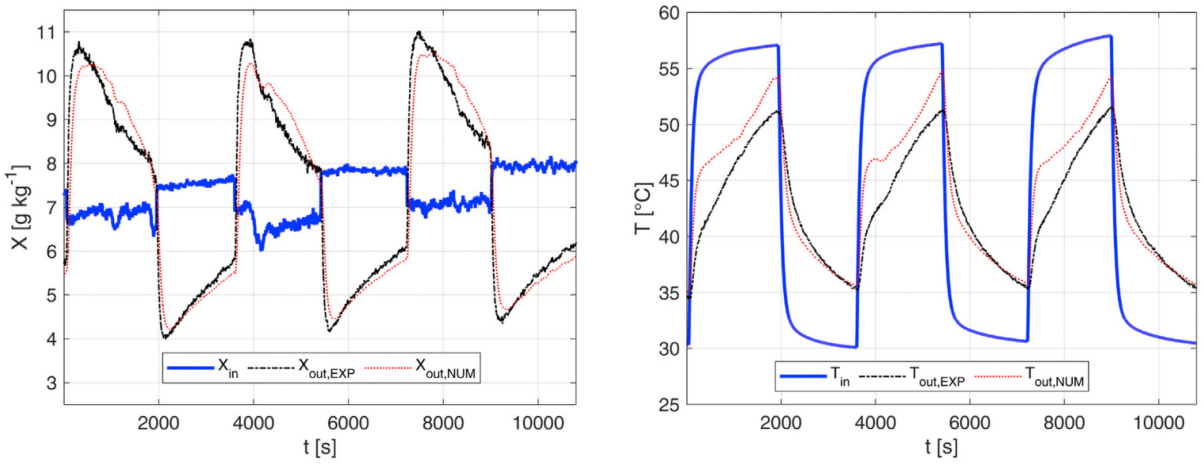

(a) (b)

Figure 2.6: PGC-model results by [8] for: (a) response of outlet air humidity to changing inlet air absolute humidity and (b) response of outlet air temperature to changing inlet air temperature.

A different approach to modelling moisture transfer in a packed bed is applied by Ramzy et al [10]. They have applied a semi-analytical solution to the set of equations for a PGC model. The author mentions the adsorption resistance at the bead surface is small compared to the diffusion resistance inside the bead, thus a local equilibrium can be assumed at the surface of the bead. It is also mentioned the lumped capacitance model, or PGC model, is acceptable for smaller particle diameters.

The main assumption in the semi-analytical model is that water content and surface temperature of silica gel, w and T_s are constant for height increment dz. Therefor the equations describing air humidity ratio and air temperature are partial differential equations with respect to only height z: $\frac{\partial m_e}{\partial z}$ and $\frac{\partial T_e}{\partial z}$. At a certain height z the air properties are assumed constant for time step dt, thus the equations describing water content and surface temperature are partial differential equations with respect to only t: $\frac{\partial m_s}{\partial z}$ and $\frac{\partial T_e}{\partial z}$. Equations (24), (27), (29), (34) and (35) in reference [10] are the analytical solutions to the PGC model equations.

Next to the semi-analytical approach, Ramzy et al. have developed a numerical model. The set of PGC model equations is discretized in space and time. The equations are solved by Runge Kutta Fehlberg and forward finite difference method. The numerical and semi-analytical results are both compared to experimental results from Pesaran and Mills, for single blow adsorption and desorption experiments. A clear overview of the runs is presented in Figure 2.7. The authors concluded both numerical and semi-analytical model results agree well with experimental results, for both adsorption and desorption experiments. These results are later compared to results from the model developed in this thesis [10].

Table 1
Bed and flow conditions for experiments conducted by Pesaran and Mills [17].

Run	Gel type	Process kind	d_p [mm]	L [cm]	q_0 [kg $_w$/kg $_s$]	T_{s0} [°C]	T_{ai} [°C]	w_{ai} [kg $_v$/kg $_a$]	v [m/s]	t [sec]
1	RD	Des	5.2	5.0	0.26	25.4	25.4	0.0007	0.67	1200
2	RD	Des	5.2	5.0	0.368	25.0	25.0	0.0051	0.4	1800
3	RD	Ads	3.88	7.75	0.0417	23.3	23.3	0.01	0.21	1800
4	RD	Ads	2.54	6.5	0.041	24.7	24.7	0.0106	0.39	1800
5	RD	Des	5.2	5.0	0.37	23.8	23.5	0.009	0.65	1200
6	RD	Ads	5.2	5.0	0.0668	25.6	25.6	0.01093	0.4	1800
7	ID	Ads	3.88	7.75	0.005	24.4	24.4	0.0063	0.67	1200
8	ID	Ads	3.88	7.75	0.0088	23.7	23.7	0.0097	0.45	1200

Figure 2.7: Experiment parameters for single blow experiments by Pesaran and Mills [12], obtained from [10].

Flow through packed beds

The following correlations are obtained from Ruthven. [19] The pressure drop over a packed bed is given by:

$$f = \left(\frac{2\ R_p}{L}\right) \frac{\Delta p}{\rho_f (U_s)^2} \tag{2.26}$$

Ergun's correlation describes the friction factor for flow through a packed bed:

$$f = \left(\frac{1-\epsilon}{\epsilon^3}\right) \left[\frac{150}{Re^*} + 1.75\right] \tag{2.27}$$

The dimensionless Reynolds number in a packed bed is indicated by Re^*. U_s is the superficial fluid velocity, calculated by $U_s = \frac{Q}{A}$. The factor ϵ is the bed porosity, μ is the dynamic viscosity of the humid air, and ρ_f is the density of humid air.

$$Re^* = \frac{2R_p\ U_s\ \rho_f}{\mu\ (1-\epsilon)} \tag{2.28}$$

Equalizing equations 2.26 and 2.27, and rewriting for pressure drop yields:

$$(\Delta p) = L\ \frac{\rho_f\ (U_s)^2}{2\ R_p} \left(\frac{1-\epsilon}{\epsilon^3}\right) \left[\frac{150}{Re^*} + 1.75\right] \tag{2.29}$$

Dimensional analysis:

$$\left[\frac{N}{m^2}\right] = [m] \frac{\left[\frac{kg}{m^3}\right] \left[\frac{m^2}{s^2}\right]}{[m]} [-][-] \tag{2.30}$$

$$\left[\frac{N}{m^2}\right] = [m] \frac{\left[\frac{kg}{m.s^2}\right]}{[m]} = \left[\frac{kg}{m.s^2}\right] = \left[\frac{kg.m}{m^2.s^2}\right] = \left[\frac{N}{m^2}\right] \tag{2.31}$$

2.5 Sorption hysteresis in numerical modelling

The phenomenon of hysteresis in sorption is mainly known from studies on wood. The boundary adsorption and desorption isotherms can not be used in applications where small fluctuations in relative humidity are applied to a material. In that case, where desorption follows adsorption halfway along the hysteresis loop, or vice versa, equilibrium moisture content follows a scanning curve, unique for the starting point [1].

Research effort has been done by Mualem [14], by developing a phenomenological model, referred to as Independent Domain model. An other approach is followed by Pedersen [16], who has developed an empirical model. Several researchers have applied and evaluated the phenomenological model [1], or both models [4], [5]. Carmeliet [5] concludes both models are able to predict the trend of scanning curves. The experimental model agrees better than the phenomenological model.

The phenomenological model uses two independent variables H_{12} and H_{21} for adsorption and desorption relative humidities. These relative humidities are expressed as distribution functions along vertical and horizontal axis, visualized in Fig.2.8. The water content as a function of relative humidity is given by:

$$M = \int\int w(H_{12}, H_{21}) dH_{21} dH_{12} \tag{2.32}$$

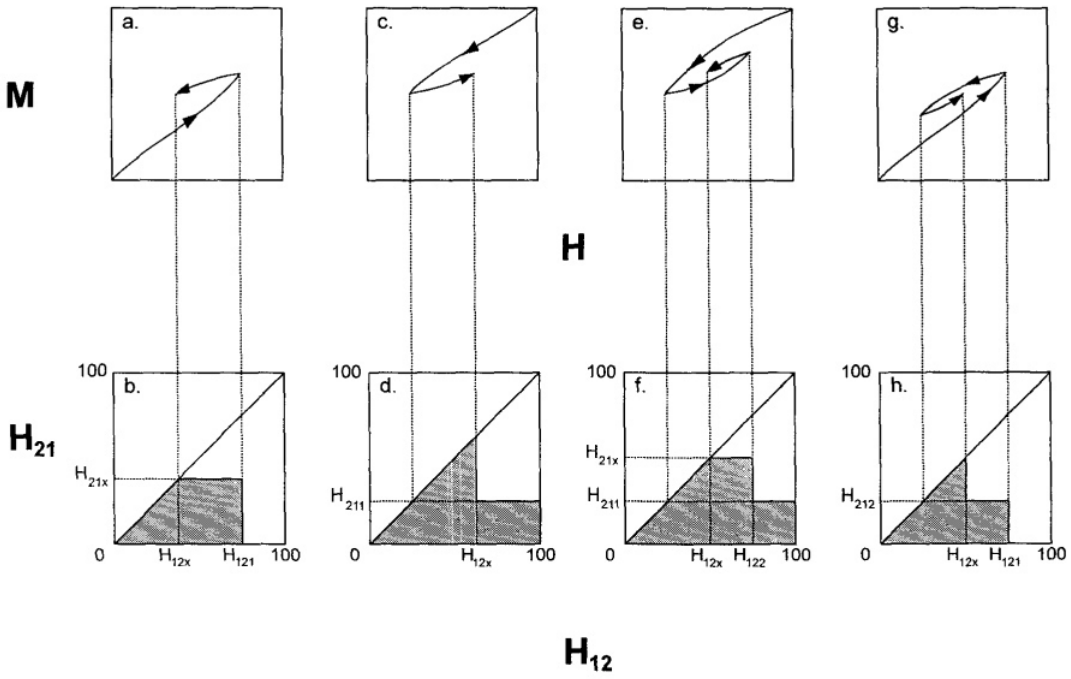

Figure 2.8: Consecutive: (a) Ads - Des, (b) Des - Ads, (c) Des - Ads - Des, (d) Ads - Des - Ads, and corresponding states of both domains, obtained from [1].

The experimental method determines the slope of the isotherm ξ using the weighted values for adsorption and desorption. This requires the expressions for boundary adsorption $w_{ads}(\phi)$ and

desorption $w_{des}(\phi)$ curves are known, and consequent slopes:

$$\xi_{ads} = \frac{\partial w_{ads}}{\partial \phi} \quad , \quad \xi_{des} = \frac{\partial w_{des}}{\partial \phi} \tag{2.33}$$

ϕ in this case is identical to RH. The slope of the scanning curve for adsorption and desorption after a cyclic process, are given respectively by:

$$\xi_{hys,ads} = \frac{\gamma_{ads}(w - w_{ads})^2 \xi_d + (w - w_{des})^2 \xi_{ads}}{(w_{des} - w_{ads})^2} \tag{2.34}$$

$$\xi_{hys,des} = \frac{(w - w_{ads})^2 \xi_{des} + \gamma_{des}(w - w_{des})^2 \xi_{ads}}{(w_{des} - w_{ads})^2} \tag{2.35}$$

The equilibrium condition of a numerical model can thus not be a single sorption isotherm. For a time step, the new water content w can not be determined from the function value of $w(RH)$. Instead, the new value of w is determined from the current value, the slope ξ of the isotherm and the differential step in RH.

The parameters γ_{ads} and γ_{des} can be fitted based on the experimental determination of scanning curves. The parameters ensure the course of the scanning curves follow adsorption or desorption, following from theory in section 2.3, and displayed in Figure 2.5(a).

It is important to note that the model lacks physical background. Frandsen [4] states: *'the ID models and Pedersen's model are both very cumbersome to implement into a numerical method such as the finite element method, since the prevailing scanning curve must be evaluated numerically for each step forward in time.'*

3 | Experiment 1: Uptake Rate Measurements

This chapter presents the experimental procedure followed in Experiment 1. Experiment 1 concerns the determination of the equilibrium sorption isotherm of water vapour - silica gel.

The following topics are addressed:

- Objective
- Experimental method
- Experiment design
- Results
- Discussion of Experiment 1
- Conclusion of Experiment 1

3.1 Objective

The objectives from Experiment 1 are listed concisely below:

- determine a suitable silica gel type from a collection of samples.
- provide sorption data to fit the isotherm polynomial, as input for the packed bed model.
- assess the possible presence of hysteresis.

3.2 Experimental method

Equilibrium isotherm can be determined by means of gravimetric determination in a Dynamic Vapour Sorption (DVS) apparatus, or uptake rate measurements in a climatic chamber. DVS measurements would take 3-5 days per sample. Uptake rate measurements would take 14 - 28 days for all fourteen samples. Since DVS availability was limited, the applied method in Experiment 1 is executing *uptake rate measurements*.

Sorption *isotherm* means the equilibrium moisture content is determined at a single constant temperature. This temperature is fixed throughout the experiment. The target relative humidity of the air is controlled, and changed in steps of 10 %RH. Sample mass is registered at equilibrium for all steps in relative humidity to construct the sorption isotherm. When the sample mass reaches (close to) equilibrium, the target relative humidity is raised with a step of 10 % RH. To have an idea whether the sample mass is close to equilibrium or not, the sample mass is measured multiple times, preferably at 2 to 3-hour interval. The measured mass change rate should indicate whether equilibrium is close.

In this experiment, the isotherm between 20 and 80 %RH is constructed. The reverse process from 80 to 20 %RH is executed as well, in order to construct the desorption isotherm.

3.3 Experiment design

This experiment is executed in a climatic cabinet, in the Macrolab of the faculty of Civil Engineering and Geosciences. 14 samples, listed in Table 3.1, are stored in small RVS containers. Approximately 20 gram of the samples is loaded, see Figure 3.1.

(a)

(b)

Figure 3.2: (a) setpoint T and RH (b) measured values of T and RH.

(a)

(b)

Figure 3.1: 14 silica gel samples in climatic cabinet.

The climatic cabinet can be set up at 0.1 %RH resolution. The climatic cabinet is expected to be stable, but not very accurate. The inside relative humidity and temperature are measured with the high accuracy Rotronic T/RH probe, hanging between the sample containers. Figure 3.2 shows the setpoints of the cabinet, as well as the measured values. The sample mass is measured manually by a calibrated laboratory scale, with resolution $0.001\ g$.

No.	**Name**	**Supplier**	**Type**	**Bulk density (kg/m3)**	**Beads / Irregular**	**Grain size (mm)**
1	SIOGEL, small pored, white	Oker-Chemie	microporous	620 - 800	Irregular	0.5 -1.5
2	SIOGEL, small pored, white	Oker-Chemie	microporous	620 - 800	Irregular	1.0 - 3.15
3	SIOGEL, small pored, white	Oker-Chemie	microporous	620 - 800	Irregular	3.0 - 6.0
4	SIOGEL, small pored, white	Oker-Chemie	microporous	680 - 780	Beads	0.5 - 1.5
5	SIOGEL, small pored, white	Oker-Chemie	microporous	680 - 780	Beads	1.0 - 3.15
6	SIOGEL, small pored, white	Oker-Chemie	microporous	680 - 780	Beads	2.5 - 4.0
7	SIOGEL, wide pored, white	Oker-Chemie	macroporous	380 - 450	Irregular	1.5 - 3.15
8	SIOGEL, wide pored, white	Oker-Chemie	macroporous	380 - 450	Irregular	5.0 - 8.0
9	SIOGEL, wide pored, white	Oker-Chemie	macroporous	350 - 500	Beads	1.5 - 2.5
10	SIOGEL, wide pored, white, *cracked beads*	Oker-Chemie	microporous	700 - 820	Cracked beads	1.0 - 3.0
11	SIOGEL, mesoporous, white	Oker-Chemie	mesoporous	500 - 600	Irregular	1.5 - 3.15
12	Silica Gel White	DDC	microporous	720	Beads	3.0 - 5.0
13	Silica Gel Orange	DDC	microporous	720	Beads	3.0 - 5.0
14	PROSorb	Long Life for Art	microporous	750	Beads	$\pm$ 3 - 5

Table 3.1: Silica gel types included in Experiment 1

3.4 Results

The results of Experiment 1A are shown in the Annex A to this report containing the experiment data. For each step a table is shown containing the raw data of the measured sample masses. Next, the curves fitted to the experimental data are shown. The Matlab script *results2030.m* is used for the case of a step from 20 to 30 %RH, shown in Appendix A. The following fitting equation is used to fit the experimental data:

$$f(x) = a * (1 - e^{-bx}) + c \tag{3.1}$$

When this equation is considered at $x = \infty$ the term e^{-bx} becomes 0. The final value of the fit is therefor: $f(\infty) = a * (1) + c$. This final value of the fitted curve is taken as a data point for equilibrium isotherm. The 'goodness of fit' is expressed by the sum of squares due to error (SSE), R-square, adjusted R-square and root mean squared error (RMSE).

The final values for all samples at all steps of the sorption phase are tabulated in Figure 3.3. From these final values the mass gain per kg (g/kg) and the mass gain per litre (g/dm3) relative to 20 %RH equilibrium are calculated. The same is done for the desorption phase, presented in Figure 3.4. These values are plotted against the target relative humidity to present the equilibrium isotherm of the samples, see Figure 3.4.

Figure 3.3: Final values of the *sorption* uptake rate measurements.

Sample mass at equilibrium (g)								
Target RH [%]		20,0	30,6	40,8	50,6	60,4	70,3	80,1
Sample no.		[g]	[g]	[g]	[g]	[g]	[g]	[g]
1		22,011	23,113	24,231	25,274	25,960	26,316	26,528
2		21,897	23,001	24,190	25,339	26,090	26,525	26,854
3		28,717	30,058	31,628	33,422	34,873	35,736	36,096
4		19,064	20,014	21,061	22,113	22,828	23,169	23,363
5		20,283	21,295	22,419	23,530	24,280	24,637	24,835
6		20,537	21,536	22,675	23,804	24,590	24,959	25,154
7		13,360	13,492	13,650	13,840	14,128	14,647	15,844
8		18,309	18,457	18,621	18,831	19,142	19,754	21,423
9		16,354	16,671	17,102	17,803	18,826	20,976	24,595
10		30,459	32,069	33,587	34,953	35,736	36,130	36,400
11		17,456	17,806	18,263	18,964	20,039	22,388	26,734
12		26,088	27,333	28,739	30,321	31,453	32,038	32,324
13		24,637	25,897	27,203	28,545	29,415	29,771	29,970
14		19,913	20,548	21,413	22,517	23,766	24,900	25,210
Mass gain (g/kg), rel. to. 20% at start sorption								
1		0,00	50,07	100,84	148,22	179,42	195,57	205,23
2		0,00	50,44	104,72	157,17	191,49	211,37	226,39
3		0,00	46,70	101,37	163,84	214,38	244,41	256,97
4		0,00	49,85	104,73	159,94	197,45	215,34	225,50
5		0,00	49,88	105,32	160,08	197,04	214,66	224,42
6		0,00	48,63	104,10	159,05	197,34	215,30	224,83
7		0,00	9,89	21,70	35,89	57,52	96,35	185,89
8		0,00	8,08	17,03	28,48	45,50	78,93	170,06
9		0,00	19,37	45,76	88,60	151,17	282,63	503,90
10		0,00	52,86	102,69	147,54	173,25	186,17	195,04
11		0,00	20,06	46,23	86,39	147,95	282,56	531,50
12		0,00	47,70	101,60	162,26	205,64	228,06	239,05
13		0,00	51,15	104,15	158,60	193,94	208,38	216,45
14		0,00	31,90	75,34	130,74	193,48	250,42	266,01
	Bulk density (kg/dm3)	Mass gain (g/dm3), rel. to. 20% at start						
1	***0,620***	0,00	31,04	62,52	91,90	111,24	121,25	127,24
2	***0,620***	0,00	31,27	64,93	97,44	118,72	131,05	140,36
3	***0,620***	0,00	28,96	62,85	101,58	132,92	151,54	159,32
4	***0,680***	0,00	33,90	71,21	108,76	134,27	146,43	153,34
5	***0,680***	0,00	33,92	71,62	108,86	133,99	145,97	152,61
6	***0,680***	0,00	33,07	70,79	108,16	134,19	146,40	152,88
7	***0,380***	0,00	3,76	8,25	13,64	21,86	36,61	70,64
8	***0,380***	0,00	3,07	6,47	10,82	17,29	29,99	64,62
9	***0,350***	0,00	6,78	16,02	31,01	52,91	98,92	176,37
10	***0,700***	0,00	37,00	71,88	103,28	121,28	130,32	136,53
11	***0,500***	0,00	10,03	23,12	43,19	73,97	141,28	265,75
12	***0,720***	0,00	34,35	73,15	116,83	148,06	164,20	172,12
13	***0,720***	0,00	36,83	74,99	114,19	139,64	150,03	155,84
14	***0,750***	0,00	23,93	56,50	98,06	145,11	187,82	199,51
Mass gain between steps (g/dm3)								
			20-30	**30-40**	**40-50**	**50-60**	**60-70**	**70-80**
1			+31,04	+31,48	+29,37	+19,34	+10,01	+5,99
2			+31,27	+33,66	+32,51	+21,28	+12,33	+9,32
3			+28,96	+33,89	+38,73	+31,34	+18,62	+7,78
4			+33,90	+37,32	+37,54	+25,51	+12,16	+6,91
5			+33,92	+37,70	+37,24	+25,13	+11,99	+6,64
6			+33,07	+37,72	+37,37	+26,04	+12,21	+6,48
7			+3,76	+4,49	+5,39	+8,22	+14,76	+34,02
8			+3,07	+3,40	+4,35	+6,47	+12,70	+34,63
9			+6,78	+9,24	+15,00	+21,90	+46,01	+77,45
10			+37,00	+34,88	+31,40	+17,99	+9,05	+6,21
11			+10,03	+13,09	+20,08	+30,78	+67,31	+124,47
12			+34,35	+38,80	+43,68	+31,24	+16,14	+7,91
13			+36,83	+38,16	+39,20	+25,44	+10,39	+5,81
14			+23,93	+32,57	+41,56	+47,05	+42,70	+11,69

Figure 3.4: Final values of the *desorption* uptake rate measurements.

Sample mass at equilibrium (g)								
Target RH [%]		80,0	70,0	60,0	50,0	40,0	30,0	20,0
Sample no.		[g]	[g]	[g]	[g]	[g]	[g]	[g]
1		26,202	26,052	25,879	25,655	25,367	23,471	22,351
2		26,430	26,237	25,973	25,628	25,175	23,232	22,047
3		35,513	35,278	34,999	34,646	33,543	30,381	28,948
4		23,060	22,923	22,758	22,550	22,284	20,296	19,275
5		24,529	24,389	24,214	24,001	23,736	21,569	20,500
6		24,829	24,684	24,513	24,303	24,041	21,777	20,717
7		15,905	14,755	14,086	13,791	13,627	13,490	13,368
8		21,559	20,119	19,199	18,864	18,675	18,511	18,361
9		24,457	23,204	20,464	18,142	17,155	16,707	16,413
10		35,983	35,788	35,548	35,272	34,936	32,835	31,134
11		26,368	24,925	21,410	18,924	18,153	17,725	17,433
12		31,941	31,736	31,505	31,188	30,534	27,911	26,402
13		29,893	29,731	29,540	29,313	29,024	26,653	24,939
14		25,208	25,068	24,892	24,486	22,729	20,625	19,908
Mass gain (g/kg), rel. to. 20% at start sorption								
1		190,40	183,59	175,75	165,54	152,48	66,33	15,46
2		207,01	198,21	186,16	170,38	149,70	60,96	6,83
3		236,65	228,49	218,76	206,47	168,07	57,95	8,04
4		209,61	202,45	193,76	182,88	168,91	64,64	11,05
5		209,34	202,41	193,81	183,32	170,22	63,39	10,70
6		208,99	201,95	193,58	183,39	170,61	60,39	8,77
7		190,49	104,43	54,37	32,28	19,95	9,74	0,61
8		177,51	98,83	48,60	30,33	19,98	11,04	2,86
9		495,48	418,83	251,30	109,31	49,00	21,58	3,64
10		181,36	174,96	167,09	158,02	146,99	78,02	22,16
11		510,54	427,90	226,49	84,11	39,94	15,39	-1,30
12		224,36	216,50	207,64	195,48	170,42	69,90	12,02
13		213,34	206,75	199,02	189,79	178,06	81,84	12,25
14		265,91	258,87	250,03	229,65	141,44	35,74	-0,25
	Bulk density (kg/dm3)	Mass gain (g/dm3), rel. to. 20% at start						
1	0,620	118,05	113,82	108,96	102,64	94,54	41,13	9,59
2	0,620	128,35	122,89	115,42	105,64	92,81	37,80	4,23
3	0,620	146,73	141,66	135,63	128,01	104,20	35,93	4,99
4	0,680	142,53	137,66	131,76	124,36	114,86	43,96	7,51
5	0,680	142,35	137,64	131,79	124,66	115,75	43,10	7,28
6	0,680	142,11	137,32	131,63	124,70	116,02	41,06	5,97
7	0,380	72,39	39,68	20,66	12,27	7,58	3,70	0,23
8	0,380	67,45	37,56	18,47	11,53	7,59	4,20	1,09
9	0,350	173,42	146,59	87,96	38,26	17,15	7,55	1,27
10	0,700	126,95	122,47	116,96	110,62	102,89	54,61	15,51
11	0,500	255,27	213,95	113,25	42,06	19,97	7,69	-0,65
12	0,720	161,54	155,88	149,50	140,75	122,70	50,32	8,66
13	0,720	153,60	148,86	143,29	136,65	128,20	58,92	8,82
14	0,750	199,43	194,16	187,52	172,24	106,08	26,80	-0,19
		Mass loss between steps (g/dm3)						
			80-70	70-60	60-50	50-40	40-30	30-20
1			-4,23	-4,86	-6,33	-8,10	-53,41	-31,54
2			-5,46	-7,47	-9,79	-12,82	-55,02	-33,56
3			-5,06	-6,03	-7,62	-23,81	-68,27	-30,95
4			-4,87	-5,91	-7,39	-9,50	-70,90	-36,44
5			-4,71	-5,85	-7,14	-8,91	-72,65	-35,83
6			-4,79	-5,69	-6,93	-8,69	-74,95	-35,10
7			-32,71	-19,02	-8,40	-4,69	-3,88	-3,47
8			-29,90	-19,09	-6,94	-3,93	-3,40	-3,11
9			-26,83	-58,63	-49,70	-21,11	-9,60	-6,28
10			-4,48	-5,51	-6,35	-7,73	-48,28	-39,10
11			-41,32	-100,70	-71,19	-22,09	-12,28	-8,35
12			-5,65	-6,38	-8,75	-18,05	-72,37	-41,67
13			-4,74	-5,57	-6,65	-8,45	-69,28	-50,10
14			-5,27	-6,63	-15,29	-66,16	-79,28	-26,99

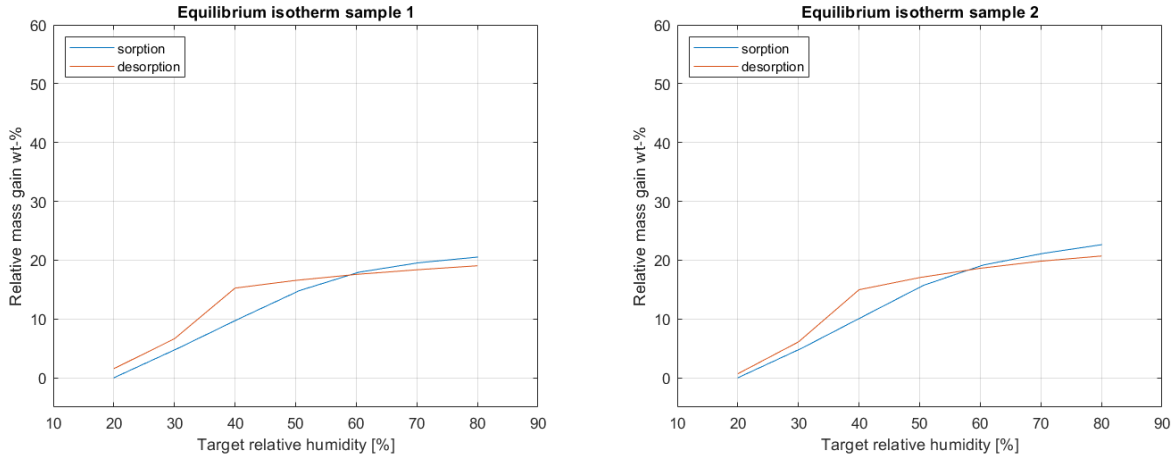

(a)

(b)

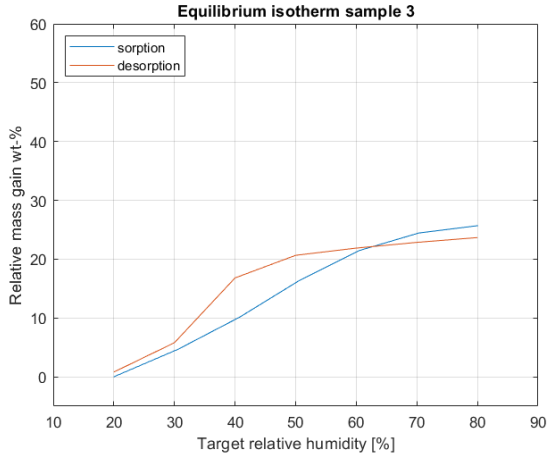

(c)

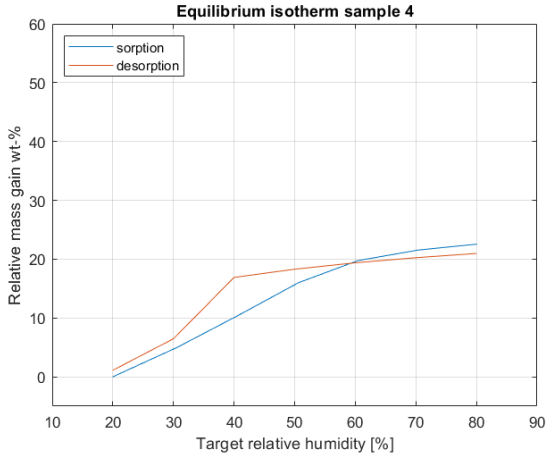

(d)

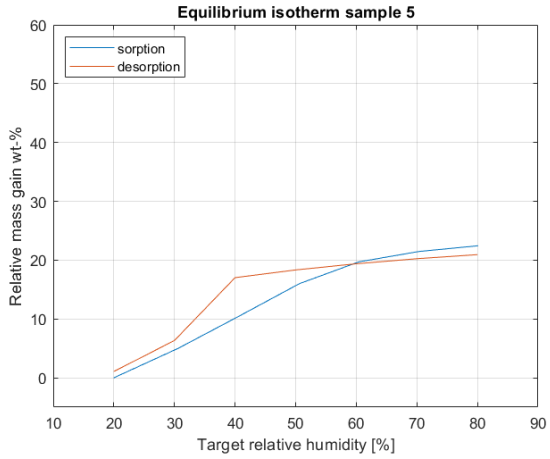

(e)

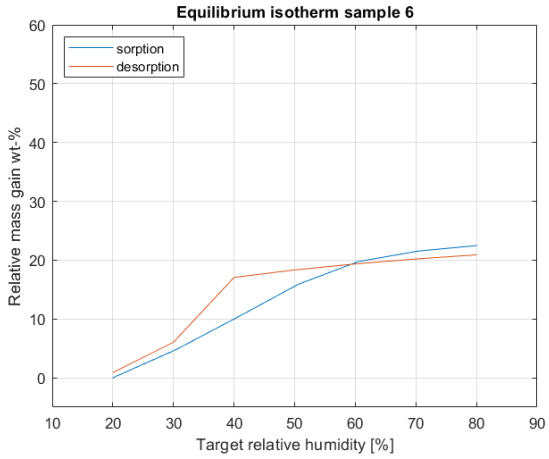

(f)

Figure 3.4: Isotherms of samples 1 to 14.

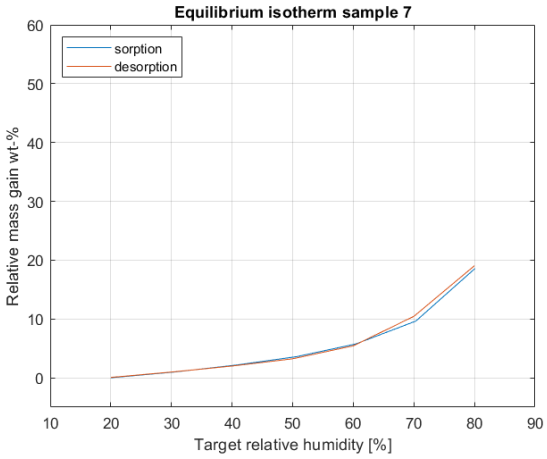

(g)

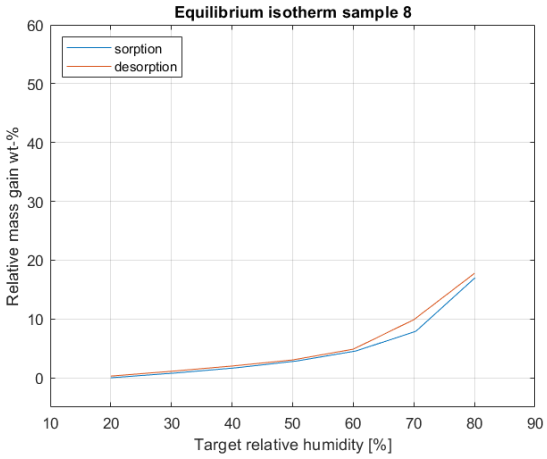

(h)

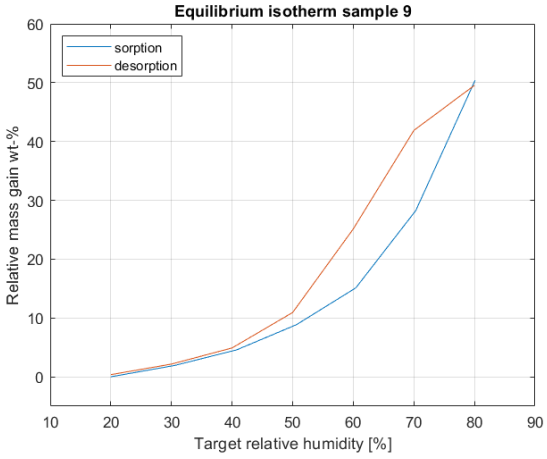

(i)

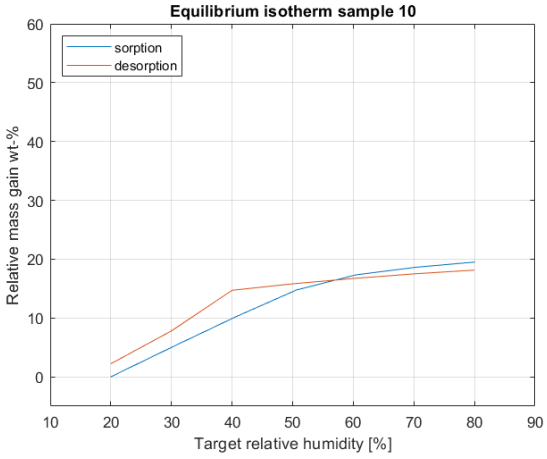

(j)

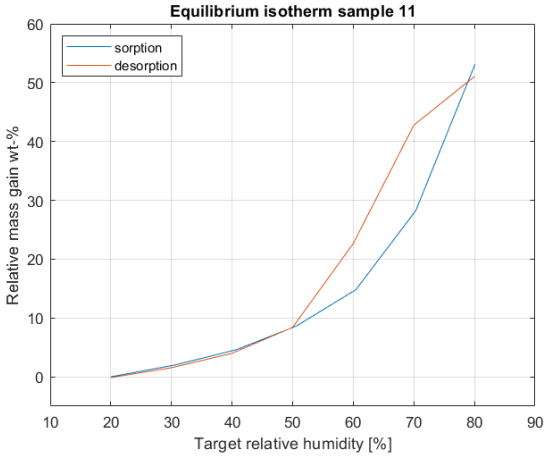

(k)

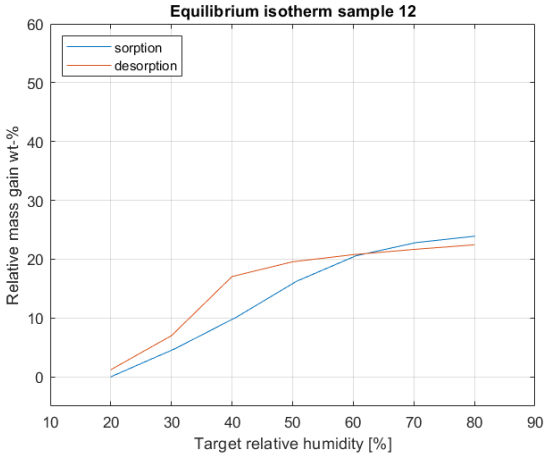

(l)

Figure 3.4: Isotherms of samples 1 to 14. *(cont.)*

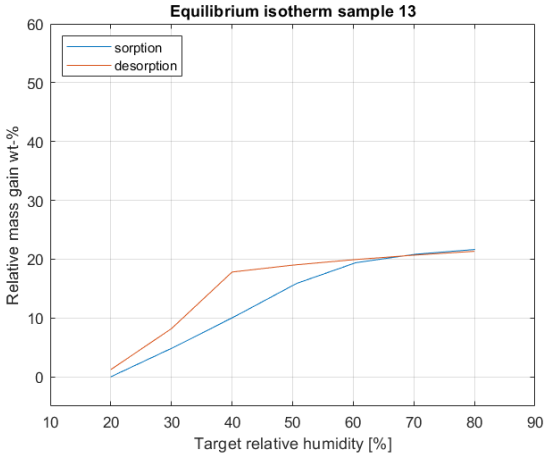

(m)

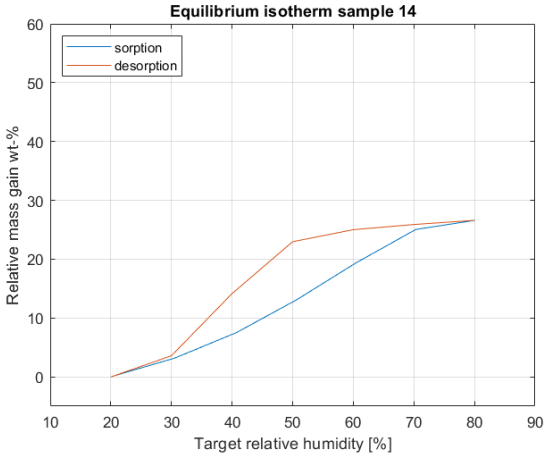

(n)

Figure 3.4: Isotherms of samples 1 to 14. *(cont.)*

3.5 Discussion of Experiment 1

For all steps in relative humidity the fit equation fitted the acquired data well. This leads to a high confidence in the resulting end value, or the equilibrium sample mass. For time's sake, during a step the measurements are not continued until all samples have reached their equilibrium mass. Often, the next step is taken when most of the samples are in equilibrium, and when the acquired data points allow a good fit and end value calculation. The fact that samples might not be completely in equilibrium, could influence the next step. The absolute gain or loss in the next step will likely be higher. This does not influence the isotherms in the end, since only end values are used to construct isotherms.

Due to technical issue with the climatic cabinet, the relative humidity has made a few cycles between approximately 35 and 80 %RH. This has happened inbetween the sorption and desorption measurements. The experiment is started with dry samples, except for Sample 14 (ProSorb) which is conditioned at 50 %RH. These facts mean that the determined sorption isotherm is *primary*, but the desorption isotherm is *secondary*. This combination of *primary* sorption and *secondary* desorption isotherm leads to an offset in both curves; the desorption isotherm has higher moisture content than the sorption isotherm at low RH. At high RH, the desorption isotherm has lower moisture content than the sorption isotherm.

This observation seems to agree with the theory from Rao [17] and Weintraub [25]: the slope of the secondary isotherms is flattened compared to the primary isotherms, or: the overall buffering capacity is reduced compared to the primary isotherms. Would this experiment have been continued with sorption, the (secondary) sorption isotherm would have likely matched desorption isotherm at endpoints. This is supported by the fact that the sorption and desorption isotherm of sample 14 (ProSorb) do match at endpoints. This sample is (pre)-conditioned at 50 %RH, so in this case the presented sorption isotherm is not *primary*.

Following the theory of Salin [20], strictly speaking, the isotherms obtained in Experiment 1 are *scanning* curves, because the samples do not reach fully dry and fully saturated state. The samples are only tested in the range 20 to 80 %RH.

3.6 Conclusion Experiment 1

Based on the mass gain or loss during the 40-50 and 50-60 %RH steps, and reversed, sample 11, 12, and 14 are chosen to include in Experiment 2. Sample 6 is added, since this is the silica gel used in the research of Antonellis. This set of samples includes micro- and mesoporous silica gels. This allows to compare the performance of different types. Beside, the set includes relatively large particle diameters (sample 12, 14), small diameters (sample 11), and inbetween (sample 6). An overview of the selected samples is given in Table 3.2

No.	**Name**	**Supplier**	**Type**	**Bulk density (kg/m3)**	**Beads / Irregular**	**Grain size (mm)**
6	SIOGEL, small pored, white	Oker-Chemie	microporous	680 - 780	Beads	2.5 - 4.0
11	SIOGEL, mesoporous, white	Oker-Chemie	mesoporous	500 - 600	Irregular	1.5 - 2.5
12	Silica Gel White	DDC	microporous	720	Beads	3.0 - 5.0
14	PROSorb	Long Life for Art	microporous	750	Beads	$\pm$ 3 - 5

Table 3.2: Silica gel types selected for Experiment 2

Figure 3.5 shows the isotherms of silica gel samples 1 - 11, as provided by Oker-Chemie GmbH. The isotherms obtained in Experiment 1 follow comparable trend. Samples 7 and 8 compare to the wide porous SIOGEL (*purple*), samples 1 to 6 compare to the small porous SIOGEL (*green*) and sample 11 compares to the mesoporous (*blue*), cf. Figure 3.4.

Experiment 1 indicates hysteresis is present in all samples, yet very limited in the macroporous samples. Sample 14 shows considerable hysteresis. Besides, Experiment 1 made clear the deviation of the *primary* isotherms compared to second and consecutive, or *secondary isotherms*.

The procedure of fitting polynomials to the isotherm data of Experiment 1 is explained in Section 5.1.

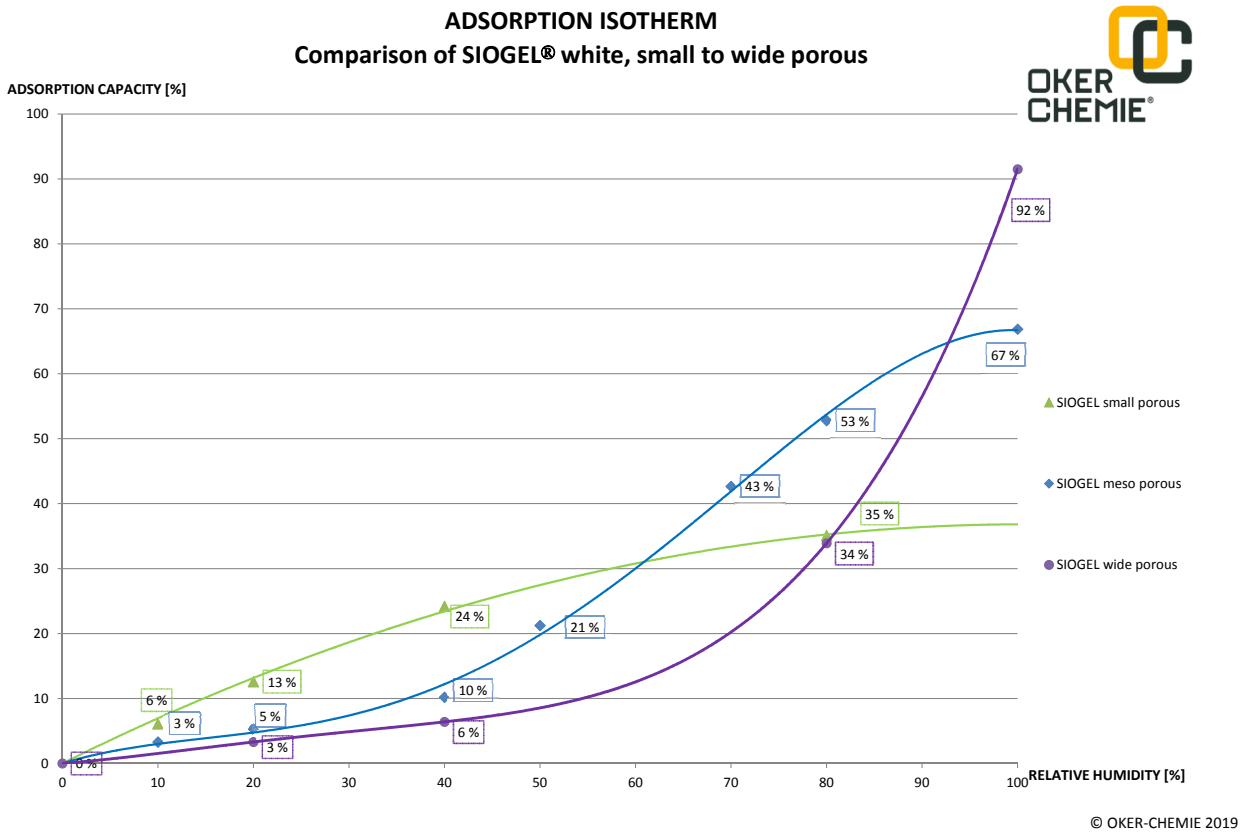

Figure 3.5: Comparison of macroporous, mesoporous and microporous SIOGEL, retrieved from Oker-Chemie GmbH.

4 | Experiment 2: Packed Bed

In experiment 2, the (de)humidification performance of a packed bed with silica gel beads is investigated. An experimental setup is built to measure the response of this packed bed to a changing RH input. In the packed bed, the incoming air, outgoing air and intermediate air at multiple points is measured. Beside the temperature and relative humidity, the flow discharge is measured by a gas flow meter.

The following topics are addressed:

- Objective
- Experimental method
- Experiment design
  - Parameter study
  - Materials
  - Experimental setup
  - Data acquisition
- Results
- Discussion of Experiment 2
- Conclusion of Experiment 2

Further analysis of the results from Experiment 2 is presented in Chapter 6.

4.1 Objective

The objectives of Experiment 2 are listed concisely below:

- indicate the time scale at which silica gel reaches new equilibrium.
- indicate the performance of moisture uptake and release.
- show the possible influence of hysteresis.

4.2 Experimental method

The variation in inlet air flow is realised in the following way: the complete setup is placed in a climatic cabinet. This climatic cabinet is able to control temperature and relative humidity up to $0.1\ \%RH$ and $0.1\ ^oC$. The air from the climatic cabinet is inputted directly in the fan, and blown through the packed bed. The cabinet can take a step of $10\ \%RH$ within approximately 1 minute. The pipe of the packed bed has an extended exit length to prevent the output temperature and relative humidity being affected by the cabinet temperature and relative humidity.

The state of different input air flows is stated per experiment run. Run A up to D are executed to discover the response of a packed bed to a change in RH input.

- Run A: Sample 12, step from 20 to 46 %RH, 22 ^oC
- Run B: Sample 12, cyclic between 46 and 56 %RH.
- Run C: Sample 11, cyclic between 36 and 56 %RH.
- Run D: Sample 11, cyclic between 40 and 60 %RH.

Based on the findings in this initial runs the following set of experiment runs is planned:

- Short cycle (1h) between 40 and 60 %RH.
  - Experiment duration: 8 hours.
  - Starting at 50 %RH equilibrium.
  - For sample 6, 11, 12 and 14.
- Long cycle between 60 % (8h) and 50 %RH (16h).
  - Three runs of 24 hour duration.
  - Starting at 50 %RH equilibrium.
  - For sample 6, 11, 12 and 14.

4.3 Experiment design

Prior to executing the experiment, careful design calculations are made to determine packed bed dimensions. Packed bed dimensions and particle diameter are highly influencing the pressure drop over the packed bed. The pressure drop ΔP over the packed bed and the flow discharge Q are key parameters for the choice of a ventilator.

The desired particle diameter can be based on the rate of diffusion. If the rate of diffusion is limiting the moisture uptake, it is wise to choose a small particle diameter. In this way, the full hygric mass of the silica gel can be utilized. Smaller particle diameter does increase the surface where moisture is exchanged, however it does increase the pressure drop.

The governing equations from Section 2.4 are coded in Matlab, see Appendix C, to have an indication of the expected pressure drop over the packed bed. The resulting pressure drops plotted against a range of volumetric flow rates for different bed diameters are shown in Fig. 4.1. Figure (a) shows results for particle radius $R_p = 0.001$ m and (b) for particle radius $R_p = 0.002$ m. From this results it can be seen that the pressure drop heavily depends on particle size.

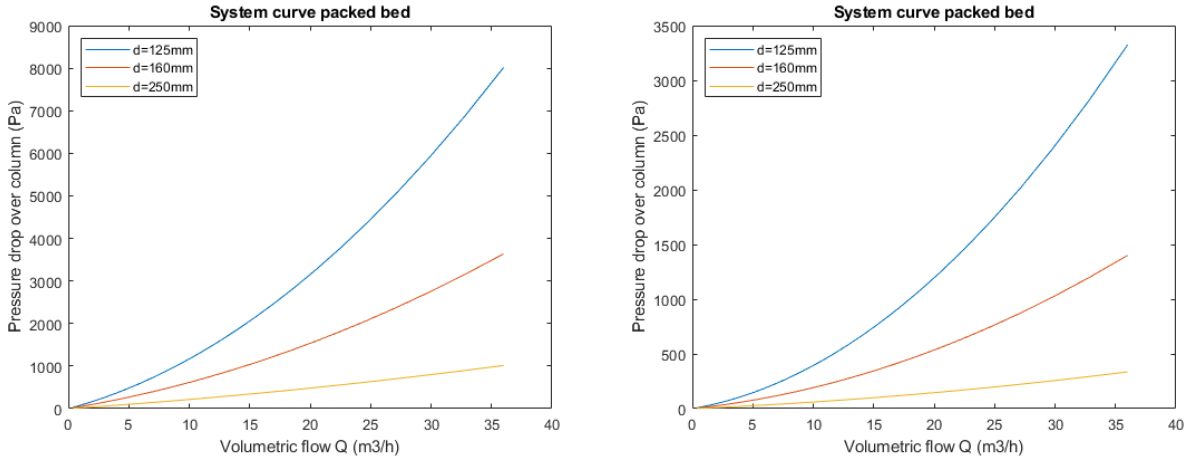

(a) (b)

Figure 4.1: Pressure drop over packed bed of $L = 50\ cm$ and particle radius (a) $R_p = 0.001$ m, (b) $R_p = 0.002$ m

Parameter study and design approach

An inventory is made of the parameters involved in the design of Experiment 2. An overview is shown in Figure 4.2. Later individual parameters are discussed in more detail. First of all the independent variables are mentioned. Independent means they can be freely chosen in the experiment design. They do however influence each other. Therefor, the order in which these variables are defined is presented in addition.

In a practical application the required flow discharge would be normative, and the bed geometry would be adjusted. In the experiment the bed geometry is fixed for practical reasons, and the flow discharge follows.

The **geometry** of the bed is chosen first. It is favorable to chose a bed diameter of at least 100 mm to ease installation of T/RH sensors. Regarding pressure drop it is desired to maximize the ratio $\frac{d}{L}$. Since PVC material with diameter 125 mm is widely available in stores, this is the applied diameter.

Bed length = $40\ cm$ *and diameter* = $125\ mm$. *Resulting volume* = $4.91\ dm^3$

The **input air flows** are defined by the temperature and relative humidity of the two alternating air flows. The rate at which they alternate is defined by the half cycle time τ. Both the change in RH and the half cycle time should be based on values that can reasonably be expected in a museum indoor climate. This determines the absolute amount of moisture to be taken up by the silica gel in that time span.

The expected fluctuation is from 40 *to* $60\ \%RH$ *at* $21\ ^oC$ *over 1 hour. The air flows have absolute humidity of* 9.4 *and* $6.2\ \frac{g}{kg\ d.a.}$ *The amount of moisture to regulate is* $9.4 - 6.2 = 3.2\ \frac{g}{kg\ d.a.}$

The third choice is a **type of silica gel**. This can be *macro-*, *meso-* or *microporous*. A combination of steep equilibrium isotherm and large diffusion coefficient is desired in the range between 40 and 60 $\%RH$. Based on the expected time needed for concentration differences to settle over the radius of a silica gel particle, the particle radius can be chosen. Mind, this particle radius has a high impact on pressure drop over the packed bed. It defines the bed porosity as well.

Based on Experiment 1 samples 6, 11, 12 and 14 are included in Experiment 2. They have either high mass gain or loss in the range of 40-60 %RH. It are micro- and mesoporous silica gels with varying particles diameters.

The superficial **air velocity** can be regulated by the fan. Based on the before set geometry, the expected amount of moisture to regulate and the performance of the silica gel, the required air velocity (= flow discharge) can be determined.

In practice the design of a device should aim for a low pressure drop. For this reason the pressure drop is designed low as well in the experiment. For a packed bed of length $40\ cm$ and diameter $125\ mm$, the needed flow discharge for 3 seconds residence time equals $5.89\ m^3/h$. A flow discharge of $5.00\ m^3/h$ will lead to a pressure drop of $\Delta P = 120 Pa$ over the packed bed.

Finally a **fan type** should be found that matches the system characteristics curve, shown before in Figure 4.1. A quick search for fan types learns the system characteristic curve is unusual; a very small flow discharge relative to the pressure drop over the system. For this reason, the strategy is to chose a fan that is able to generate sufficient pressure. The intended flow discharge is reached by a practical workaround: excess flow can be leaked deliberately before the packed bed.

As mentioned earlier, the intervening variable is the pressure drop over the packed bed. This is a function of the particle radius and bed porosity, bed length and diameter and the superficial air velocity. The dependent variables are to be measured in this experiment. It is the temperature and relative humidity of air at both exit and intermediate points.

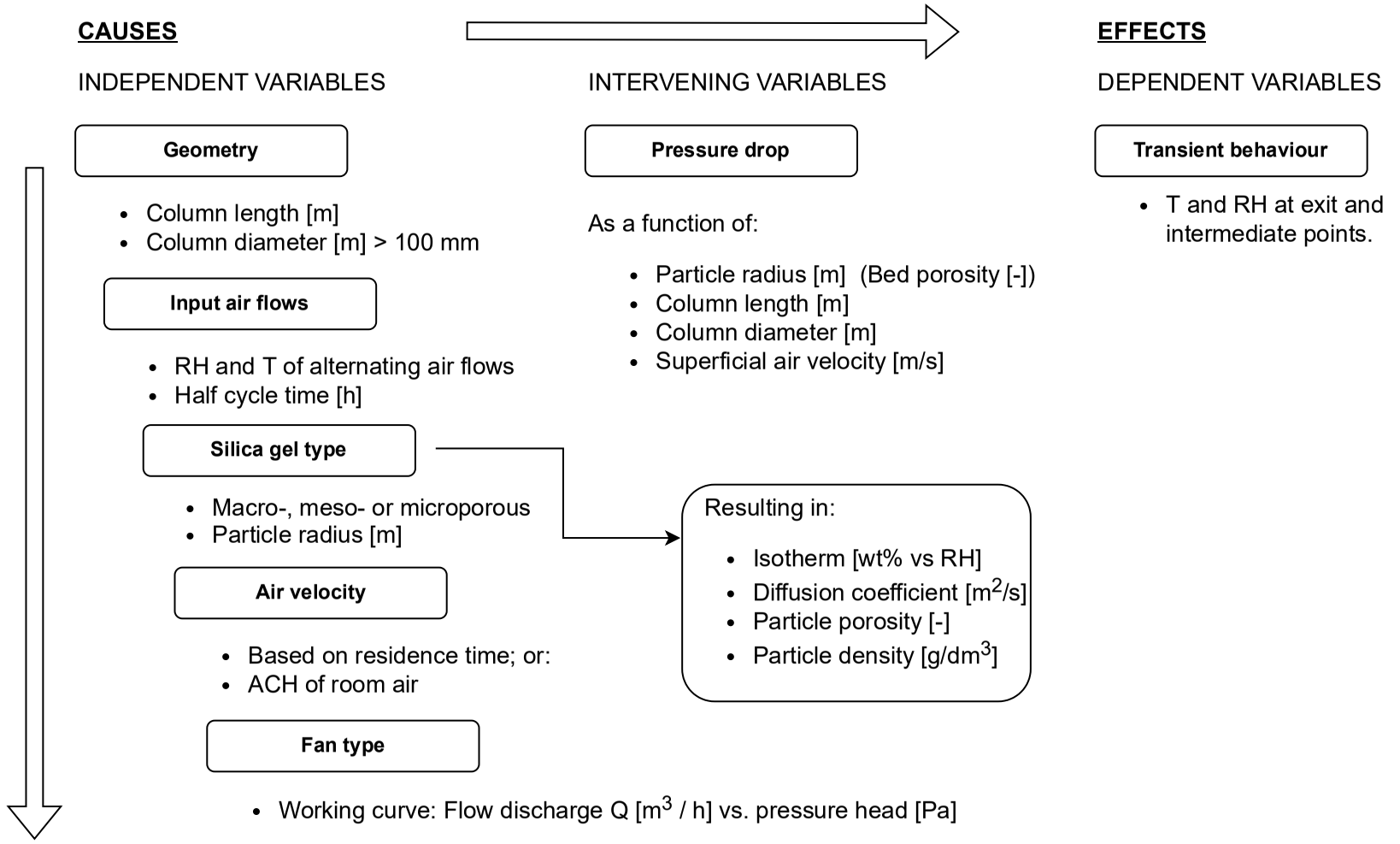

Figure 4.2: Parameter study for the design of experiment 2.

Materials

The materials needed for the setup of Experiment 2 are listed below:

Part	Supplier	Quantity	Note
Silica gels			
SIOGEL white, small pored, beads, 2.5 -4.0 mm	Oker-Chemie GmbH	5 kg	Sample 6
SIOGEL white, wide pored, 1.5 - 3.15 mm	Oker-Chemie GmbH	5 kg	Sample 9
SIOGEL white, mesoporous, beads, 1.5 - 2.5 mm	Oker-Chemie GmbH	5 kg	Sample 11, but beads!
Silica Gel White	DDC	4 kg	Sample 12
ProSorb	Long Life for Art	4 kg	Sample 14
Sensors			
Rotronic HF T/RH transmitter	Acin Instrumenten BV	1 pce.	
Rotronic HygroClip HC2S-A T/RH probe	Acin Instrumenten BV	1 pce.	Accuracy: 0.8 %RH / 0.1 K
T9602 T/RH sensors	Mouser Electronics	5 pcs.	Accuracy: 2.0 %RH / 0.5 K
Sensirion SFM3003 gas flow meter	Mouser Electronics	1	-
ESP32 development boards	Otronic.nl	4 pcs.	-
Pump and PVC pipe			
Fan CK100 C (EC)	Inatherm BV	1 pce.	20 m3/h at 300 Pa
Transparent PVC tube 125 mm	PVC Hoogeveen	50 cm	
Additional			
Climatic cabinet	TU Lab		For input air and sensor calibration
Wood for frame, PVC connections, Y piece,	Hornbach, Gamma		
Cable glands, control valves, flexible tubes 20, 50 mm, PVC connections	Wildkamp.nl, Arestho.nl, PVC24.nl		

Table 4.1: Materials used in Experiment 2

Experimental setup

Figure 4.3 shows a sketch of the experimental setup of Experiment 2. Figure 4.4 shows pictures of the built experimental setup.

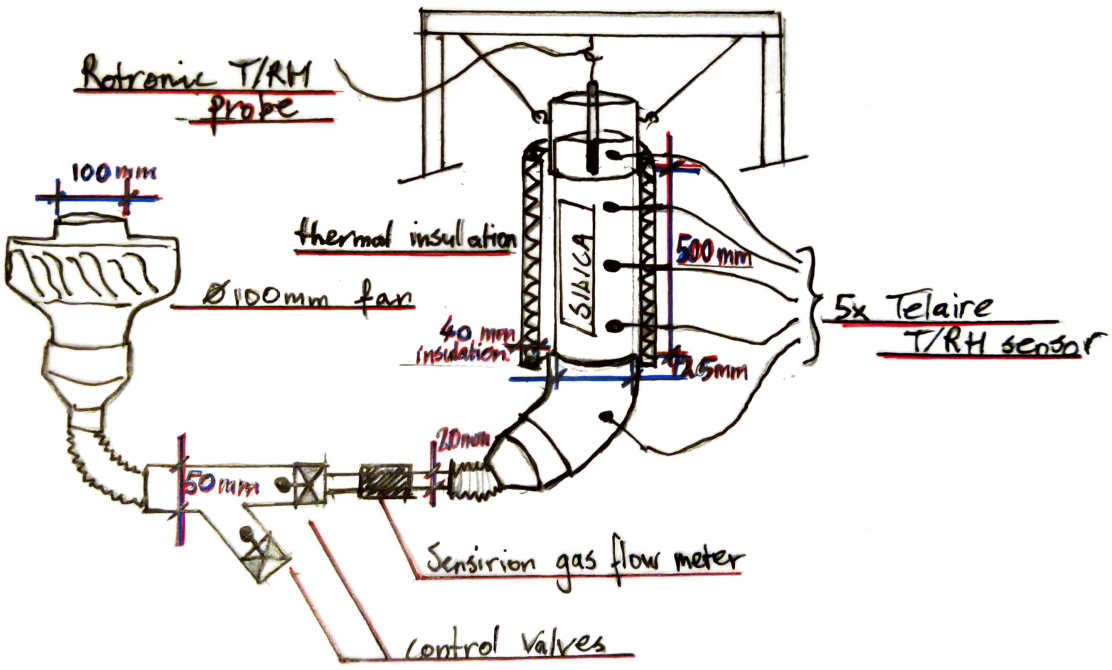

Figure 4.3: Sketch of experimental setup built for Experiment 2.

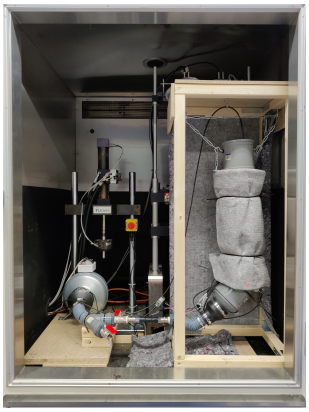

(a)

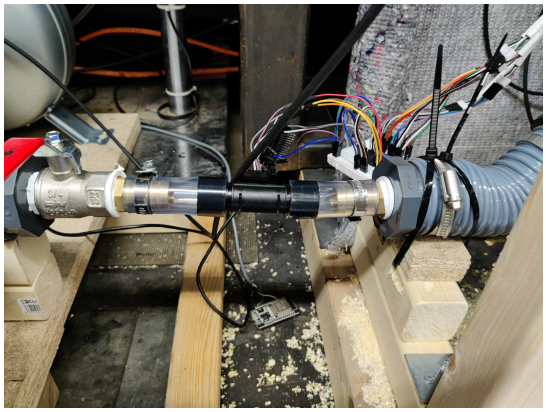

(b)

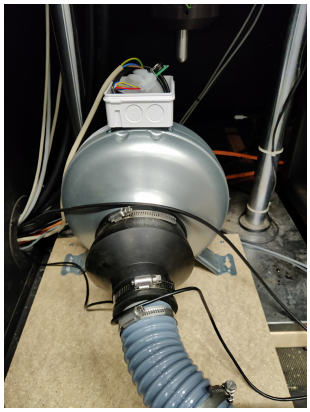

(c)

(d)

(e)

(f)

Figure 4.4: (a) Complete setup (b) air flow sensor (c) fan (d) Y piece to regulate air flow (e) packed bed inlet (f) filled packed bed and cable glands.

Data acquisition

The high accuracy Rotronic T/RH probe is not logged in the experiments. The smaller Telaire T/RH sensors as well as the Sensirion gas flow meter are digital sensors, controlled via I2C protocol. The sensors are wired to an ESP32 microcontroller board.

A script is written in Arduino/C++ and uploaded to the ESP32 board to read the sensors, and subsequently send a string of sensor data to a laptop via serial communication (USB). A Matlab script, presented in Appendix E, is written to read the serial port of the laptop and store the sensor data in a *.txt* file and the Matlab workspace.

Calibration of T/RH sensors

The Telaire T9602 T/RH sensors can be purchased for a reasonable price. The sensors have accuracy of 2.0 %RH and 0.5 K. The high accuracy temperature and relative humidity sensor, Rotronic HF4 transmitter with HC2A-S probe, is used as a benchmark for calibration of other T/RH sensors. This probe has an accuracy of 0.8 %RH and 0.1 K

The Telaire T9602 temperature and relative humidity sensors are calibrated as follows: all sensors are hanged close together in the climatic cabinet together with the high accuracy probe. The climatic cabinet itself has limited accuracy of approximately 3 %RH, hence the need for the high accuracy probe. Unhandled sensor output is measured at two distinct points of temperature and relative humidity. This allows to determine a linear fit equation which describes the function to apply to the sensor data to obtain physical units.

A third point is measured to ensure the sensor output is indeed linear. Besides, it adds more confidence to the linear fit. After the conversion equations are applied to the microcontroller, sensor readings are observed at two arbitrary points to judge the conversion equations. The detailed calibration procedure is described in Appendix D.

4.4 Results

In Annex B the data acquired in Experiment 2 is presented. This includes the following experiment runs:

- **Trial runs:**
  A. Sample 12, step input 20 to 50 %RH
  B. Sample 12, cyclic input between 50 and 60 %RH
  C. Sample 12, cyclic input between 36 and 56 %RH
  D. Sample 12, cyclic input between 40 and 60 %RH

- **Short cycle (1h / 1h), between 40 and 60 %RH:**
  1. Sample 6
  2. Sample 11
  3. Sample 12
  4. Sample 14

- **Long cycle (8h / 16h), between 50 and 60 %RH:**
  5. Sample 6
  6. Sample 11
  7. Sample 12
  8. Sample 14

Relative humidity is directly related to temperature. For analysis, and later comparison to the model results, the measured relative humidity is recalculated to absolute humidity, using the temperature at corresponding time step. Per experiment run, four plots are presented:

- RH versus time, sensor data
- X versus time, calculated from RH and T
- T versus time, sensor data
- Flow versus time, sensor data

4.5 Discussion of Experiment 2

Discussion points specific to individual experiment runs are discussed in Annex B, in the section for the corresponding run. Here, generic observations are mentioned. The course of temperature, absolute and relative humidity is discussed.

Short cycle

Temperature of air and silica increases as a consequence of adsorption and decreases as a consequence of desorption.

Absolute humidity X of intermediate and outlet air follows the course of the absolute air humidity of the input air. The increase and decrease in absolute humidity (indicated with 1 in Figure 4.5) is caused by the increase and decrease in temperature. The difference in input and output is a direct effect from dehumidification (indicated with 2) and humidification (indicated by 3).

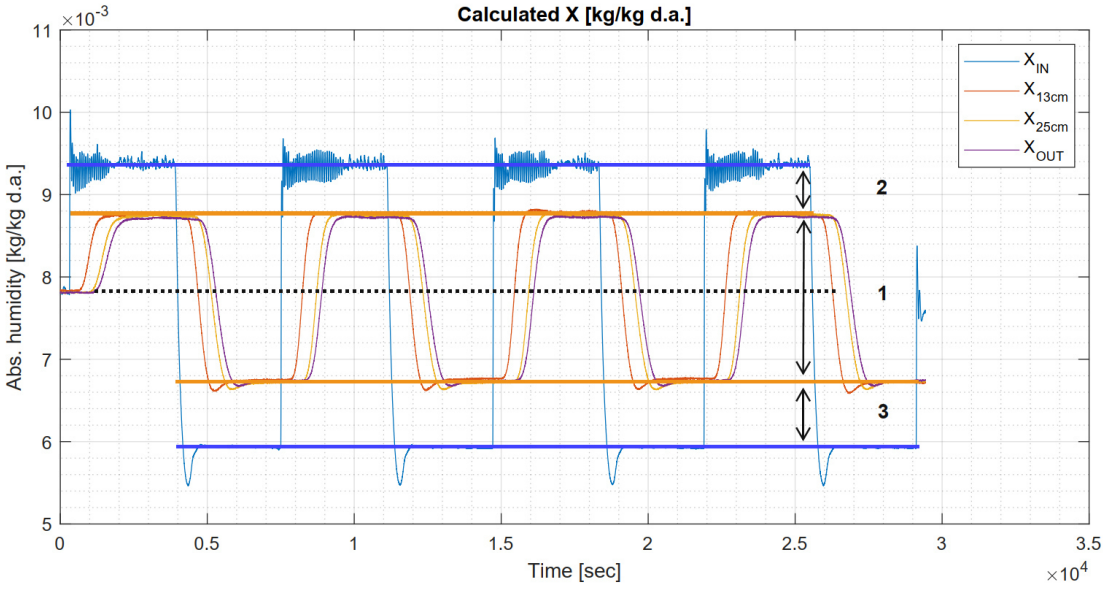

Figure 4.5: Discussion of absolute humidity changes in short cycle experiment.

Relative humidity is affected by temperature as well. As mentioned, the absolute humidity changes due to temperature changes. The relative humidity tends to follow the same course as absolute humidity. However, when in adsorption mode, the temperature increase leads to an increase in saturation humidity x_{sat}, and thus a decrease in relative humidity: This is best seen from the spike after a step to high input relative humidity, indicated with (1) in Figure 4.6. After the step to high input relative humidity, the relative humidity tends to increase, but decreases as soon as the temperature increases. The result is a spike in relative humidity.

Vice versa for the step to low input relative humidity, the relative humidity drops and tends to follow the absolute humidity course. Due to the decrease in temperature, the saturation humidity decreases and thus the relative humidity increases. A spike occurs, indicated with (2).

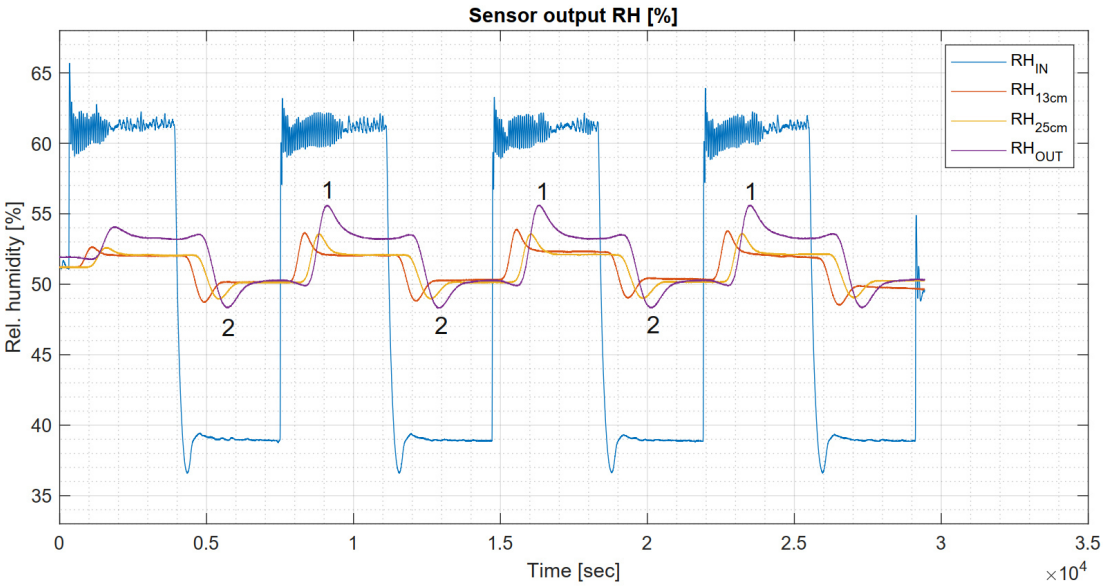

Figure 4.6: Discussion of relative humidity changes in short cycle experiment.

In all short runs, the absolute humidity remains constant after the initial step (due to temperature change). This indicates moisture is exchanged between air and silica gel. Only when the silica gel is saturating the absolute humidity of the air will start to rise (after the initial change due to temperature). Vice versa, the absolute humidity of the air will start to drop when no more water is desorbed from silica gel.

It is observed the outlet relative humidity stays very well within the inlet values. This means very good buffering performance is obtained.

No considerable change is observed in outlet air relative humidity between cycles 2 up to 4. This indicates hysteresis does not have a negative impact on the buffering performance.

Long cycle

The results from cycle 2 in run 5 are used to discuss the generic observations in the long cycle experiment. It is important to mention that the long cycle experiment runs start at 50 %RH. There is little data logged before the step to 60%RH.

After the step to high input humidity, the silica starts adsorbing, and thus silica and air temperature increases. As a consequence, the absolute humidity rises. The absolute humidity then stays constant for a while. When the silica is reaching new equilibrium (or 'saturating' at $\pm$ 60%RH) the air absolute humidity is starting to increase, indicated with 1 in Figure 4.7, for the first part of the packed bed.

When the step to low input relative humidity is taken, the absolute humidity decreases as well. The water stored during the 8 hours of high input relative humidity, is then slowly released during the 16 hours. This is why the absolute air humidity in the first part of the packed bed rises after the step (2), and a while later in the middle part (3), and finally in the last part of the packed bed. The input from the 8 hours exits *dampened* and *delayed*.

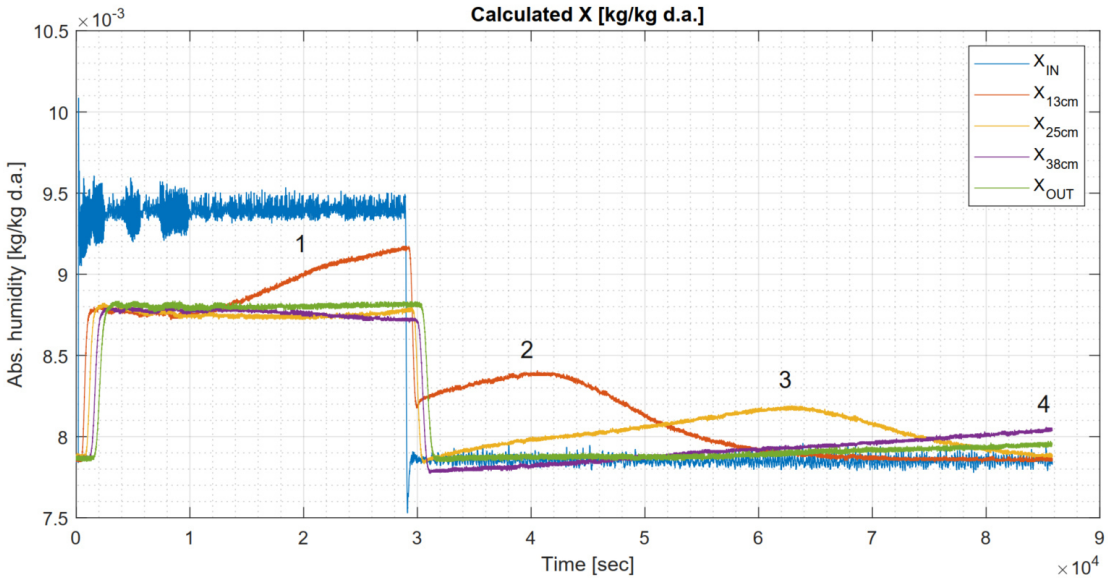

Figure 4.7: Discussion of absolute humidity changes in run 5, cycle **2**.

Temperature again changes when adsorption and desorption is happening, shown in Figure 4.8. Temperature rises when the silica has to adsorb water (1). When the silica is saturating, no more latent heat is released: the temperature starts decreasing to inlet value (2). After the reverse step, the temperature decreases instantly, and continues decreasing while water is desorbing (3). When desorption stops, no more heat is needed for the phase change of water; temperature rises to inlet value (4).

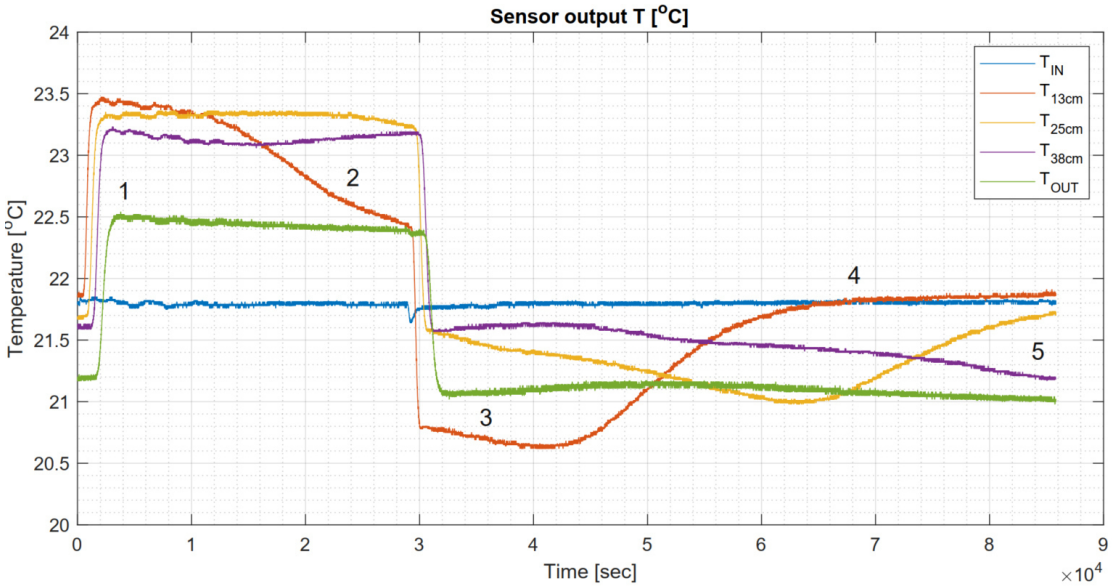

Figure 4.8: Discussion of temperature changes in run 5, cycle **2**.

At the start of the third cycle, the first part of the packed bed has reached initial temperature and humidity values. The last part of the packed bed has not reached initial conditions. In fact, the absolute humidity is higher than inlet air humidity, since water is desorbing from silica at this location: indicated with (4) in Figure 4.7. Since temperature decreases when desorption is happening, the temperature at the last part of the packed bed is lower than inlet air temperature: indicated with (5) in Figure 4.8.

The combination of high absolute humidity and low temperature (and thus low x_{sat} will lead to an increase in relative humidity. This is seen right after the step to 60 %RH, in cycle **3**, see (1) in Figure 4.10.

After the step in cycle **3**, the temperature in the last part of the packed bed continues to increase after the initial jump, indicated by (1) in Figure 4.11. This is explained by adsorption, but the higher temperature of the parts before could also contribute to the increase in temperature.

The absolute humidity does not change too much during the 8 hours of high relative humidity input in cycle **3**, see *purple* line in Figure 4.9. As the temperature is increasing in the last part of the packed bed, the relative humidity will drop during the 8 hours of high relative humidity, indicated by (2) in Figure 4.10. This seems counter-intuitive, but is explained by the transient behaviour of the packed bed: the output of the packed bed depends heavily on the historical input.

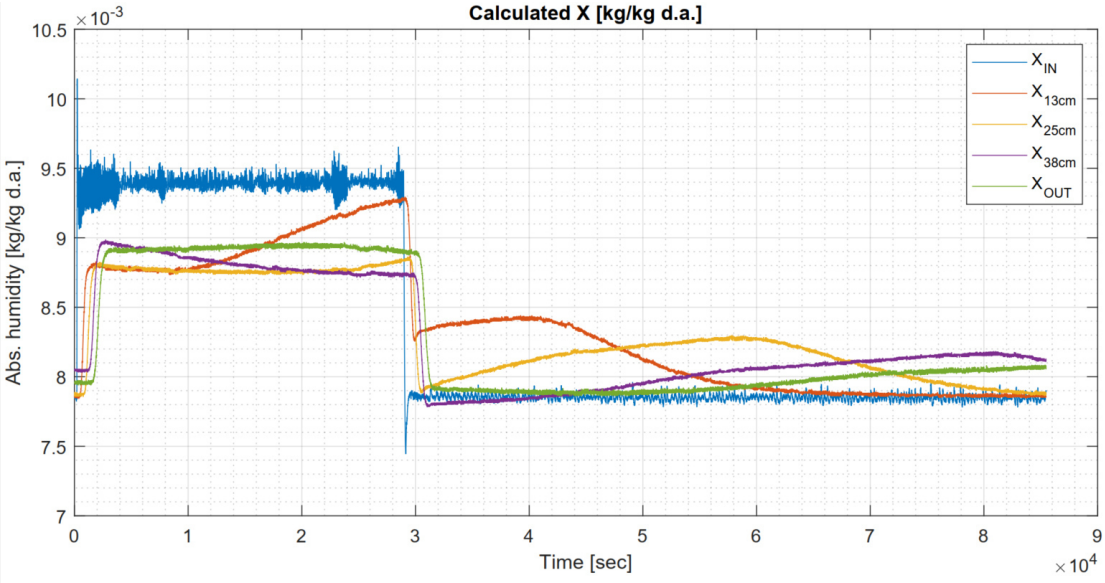

Figure 4.9: Discussion of absolute humidity changes in run 5, cycle **3**.

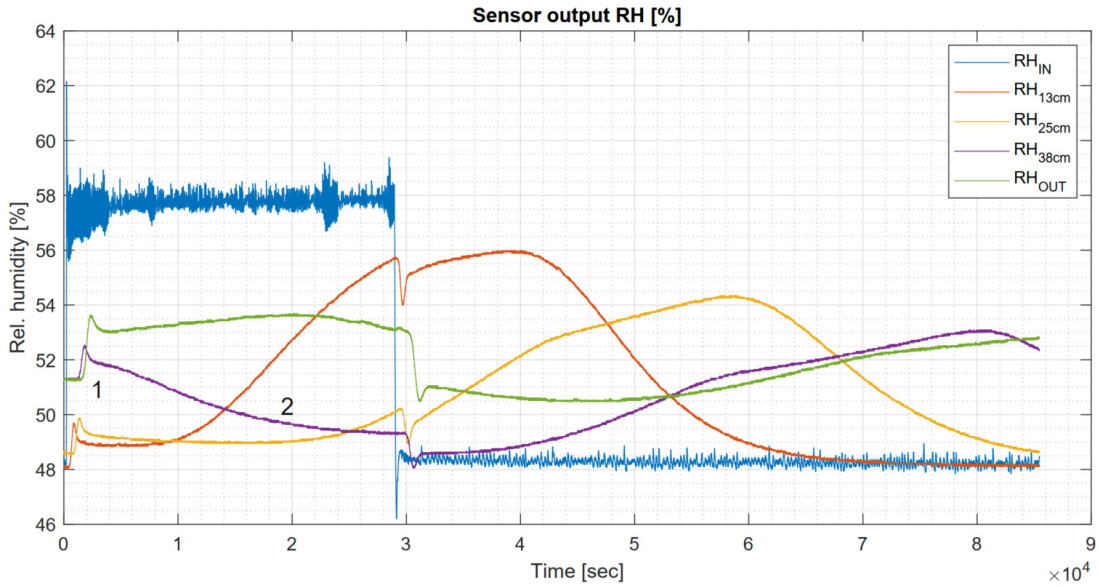

Figure 4.10: Discussion of relative humidity changes in run 5, cycle **3**.

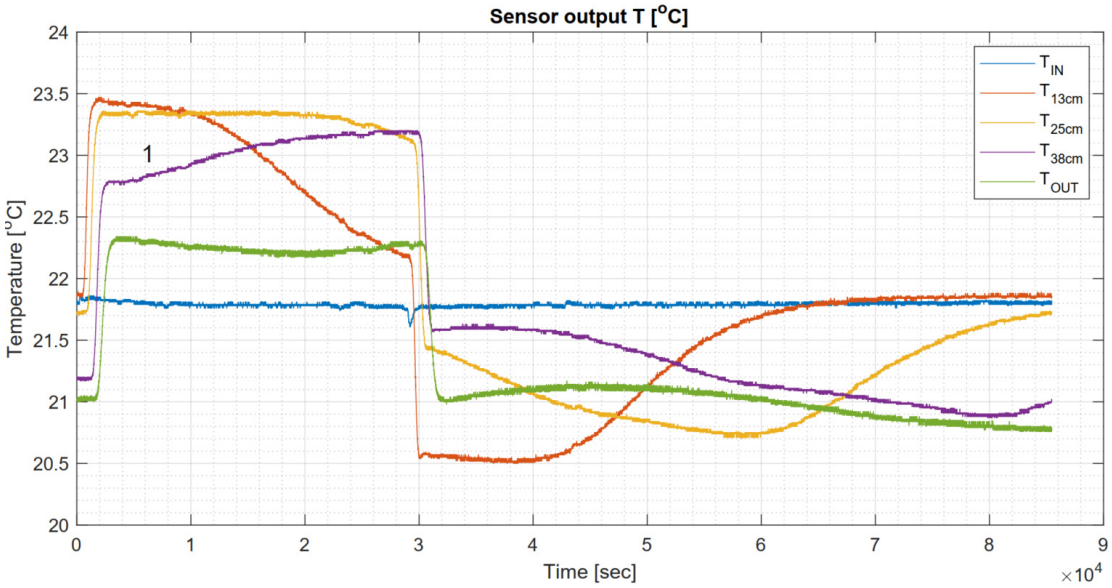

Figure 4.11: Discussion of temperature changes in run 5, cycle **3**.

Adsorption exceeds desorption in long runs

An important observation from the long runs is that adsorption seem to reduce in the first cycles, and desorption seems to increase in the first cycle. This is seen from the following facts:

- In cycle **1**, the absolute humidity does not rise in the first part of the packed bed during the high part of the cycle (indicated with (1) in Figure 4.12).

- During the low part of cycle **1**, limited moisture is released: the red peak in the low part of the cycle is not high (indicated with (2)).

- In cycle **2** of run 5, the absolute humidity does rise in the first part of the packed bed during the high part of the cycle, indicated with (1) in Figure 4.13.

- In cycle **3** the absolute humidity in the first part of the packed bed during the high part of the cycle does rise a bit more.

The fact that more moisture is adsorbed than desorbed in the long cycle experiments is supported by the water uptake and release numbers in Table 6.2.

Two issues are possible as an explanation for this observation, explained hereafter:

– 'primary' hysteresis between primary and secondary isotherms.

– sway-in behaviour: effect of initial conditions in cyclic experiment.

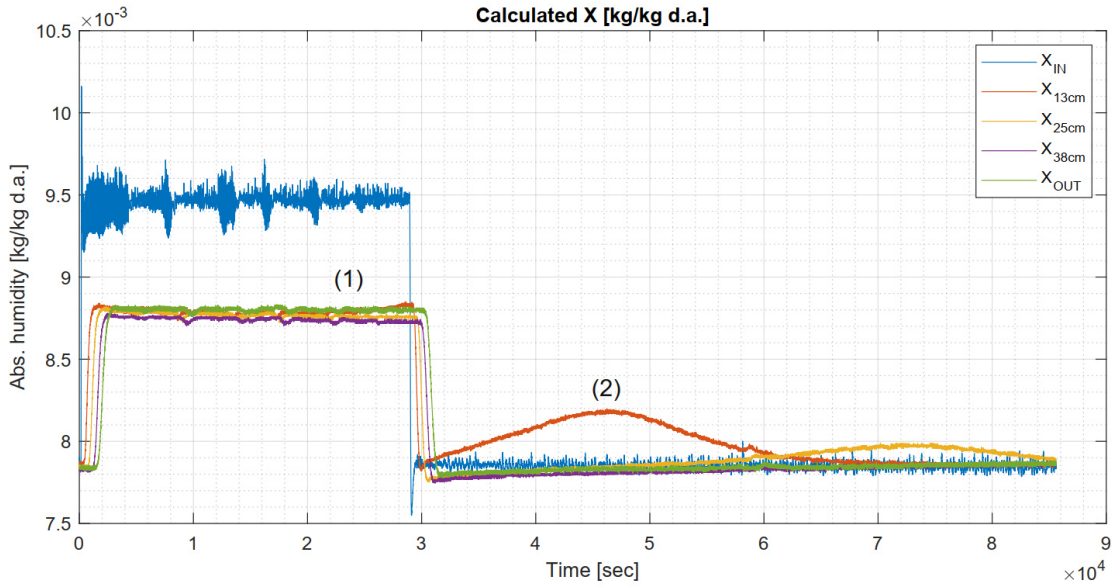

Figure 4.12: Absolute humidity measurements in run 5, cycle **1**.

The first possible explanation is the difference between *primary* and *secondary* isotherm. In run 5, sample 6 is loaded from a dry state and brought to equilibrium at 50 %RH. In the first adsorption/desorption cycle a part of the moisture is retained in the silica gel. The retention of water in silica gel blocks the pores, which is a potential and plausible explanation for the presence of hysteresis in silica gel [26], [17].

Some water is permanently retained in the silica gel. This causes the difference in *primary* and *secondary* isotherm. For clarity, in this thesis it is called 'primary' hysteresis. Retention of water in silica gel during consecutive adsorption causes 'continuous' hysteresis. However, this is the hysteresis that is reproducible; this hysteresis can be undone by exiting the hysteresis loop at the low RH side, via desorption. Adsorption then again follows *secondary* boundary adsorption isotherm. This phenomenon was described by Rao [17].

It is hard to conclude from Experiment 2 if there is an influence of 'continued' hysteresis as well. Continued cycles, starting from equilibrium, could provide information on the presence of 'continued' hysteresis.

The second possible explanation is the effect of initial conditions: the 'sway-in behaviour' of the cyclic experiment. Some time is needed before the effect of initial conditions is eliminated in a cyclic experiment. In the case of Experiment 2, the samples are in equilibrium at 50 %RH. During the first cycles, water might be stored in the hygric mass in the core of the silica gel beads.

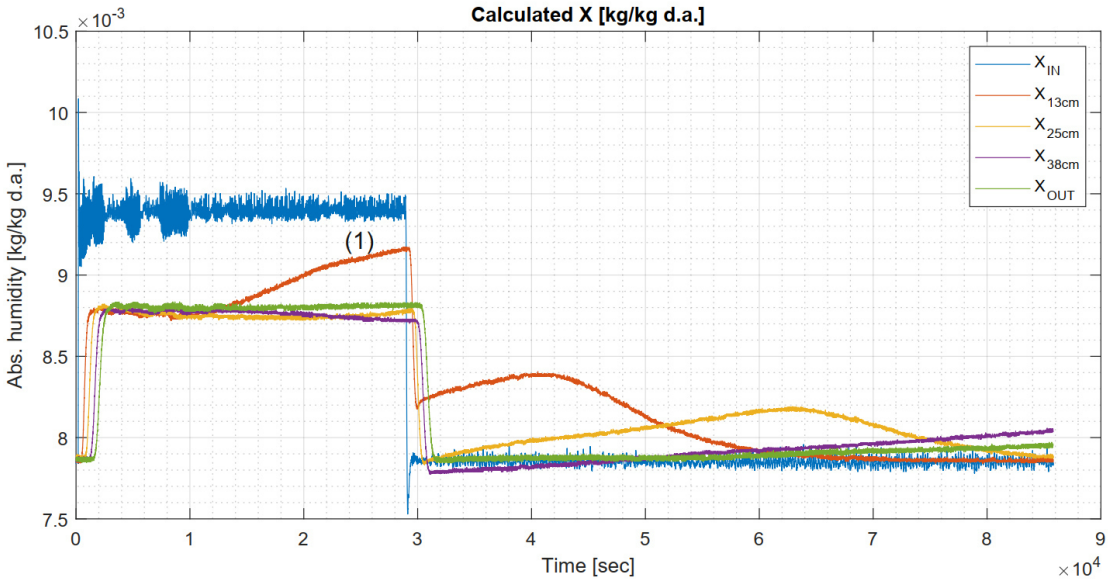

Figure 4.13: Absolute humidity measurements in run 5, cycle **2**.

Influence of experimental setup on results

The ventilator used in the experimental setup was able to produce sufficient pressure. It was not necessary to regulate air flows using the Y piece. Significant attention is paid to ensure the air-tightness of the experimental setup.

The calibration of the small Telaire T/RH sensors with help of the high accuracy T/RH probe has provided confidence in the measurement results.

The packed bed is thermally insulated during experiments. This is done to ensure the packed bed wall is theoretically adiabatic, which is an assumption in the numerical packed bed model. An indicative calculation is made, based on a derivation of Fourier's equation for radial heat conduction [13]:

$$Q = 2\pi k N \frac{(T_c - T_o)}{ln(r_o/r_c)} \tag{4.1}$$

Where Q [W] is the heat flow through the packed bed wall, N [m] is the length of the packed bed, k is the thermal conductivity of the insulation material, T_c and T_o are the temperatures at the packed bed wall and the insulation material, respectively. r_c and r_o are the radii, following from Figure 4.14.

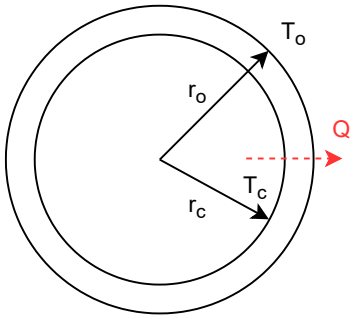

Figure 4.14: Calculation of radial heat conduction (insulation of pipe)

.

A quick search indicated the thermal conductivity of heavy cloth can be estimated at $k = 0,04$ [w/(m K)]. The applied thickness is ± 4 [cm]. The expected temperature difference is 4 ^oC. The calculated heat flow is low:

$$Q = 2\pi 0,04 \cdot 0,310 \frac{(24 - 20)}{ln(0,133/0,125)} = 5,02\ W \tag{4.2}$$

The applied amount of insulation is assumed sufficient since measured temperature of silica gel agrees with model results.

Measurements of temperature and relative humidity are stored every 2 seconds. This interval is quite small. It did not lead to issues regarding data storage.

4.6 Conclusion of Experiment 2

The short cycle experiment shows the capability of silica gel to reduce rapid fluctuations in air relative humidity. Improvement in buffering could be achieved when the change in temperature is reduced. Reducing the temperature change will reduce the change in absolute humidity. This means cooling the silica during adsorption (dehumidification of air) and heating the silica during desorption (humidification of air).

The short cycle experiment does not indicate any disadvantageous effect of hysteresis. Silica gel is not saturating during the 1 hour of high humidity input: this is seen from the fact that the absolute humidity does not rise during the high part of the cycle.

An important consideration regarding the length of the packed bed became clear in the long cycle. A long bed enhances the immediate dampening of a variation in RH. The longer the bed, the smaller the effect of inlet variations at exit. However a long bed introduces transient effects: higher parts of the packed bed can be in different desorbing or adsorbing mode. Air temperature will vary as a consequence of adsorbing or desorbing mode. The temperature directly influences the RH levels. Thus, a long packed bed may cause delayed rises or falls in RH.

5 | Numerical packed bed model

This chapter explains the structure of the developed model of the packed bed. It is a Pseudo-Gas Controlled model. Numerical results of the model are compared to experimental data from literature, with experimental parameters as input. Thereafter the numerical results of the PGC model are compared to the results of the simplified model from Zhang [27]. The chapter is concluded with the comparison of PGC model results to results from Experiment 2, and a discussion of the model.

5.1 Pseudo Gas Controlled model (PGC)

The numerical packed bed model is set up according to the Finite Volume method. The principle of the numerical packed bed model is visualized in Figure 5.1. In this approach the packed bed is divided in n_{bed} finite volumes. These finite volumes all contain a node for air, representing the total air volume in the macro-pore, and a node for silica gel, representing the total volume of silica beads in that finite volume.

The packed bed geometry is discretized in the following way: the packed bed is divided in n_{bed} control volumes, which each have volume $V_{cv} = A_{bed} * \frac{L_{bed}}{n_{bed}}$. Each control volume has a void part, representing the total air volume in a control volume, and a solid part, representing the volume of silica gel in a control volume. The assumed porosity equals $\epsilon = \frac{V_{air}}{V_{cv}} = 0.36$, yielding following volumes:

$$V_{gel} = (1 - \epsilon)\ V_{cv}, \qquad V_{air} = (\epsilon)\ V_{cv} \tag{5.1}$$

The volume and surface area of one silica gel particle are respectively:

$$V_p = \frac{4}{3}\pi\,(R_p)^3 \tag{5.2}$$

$$A_p = 4\pi\,(R_p)^2 \tag{5.3}$$

The number of particles in one control volume is determined as follows:

$$n_p = \frac{V_{gel}}{V_p} \tag{5.4}$$

Finally, the number of particles in one control volume multiplied by the surface area of one particle results in the surface area where moisture is exchanged, in one control volume. This is also referred to as *wetted perimeter* in literature: [8] [12]

$$p = n_p * A_p \tag{5.5}$$

The density of air flowing through the bed, ρ_{air}, is assumed constant. The mass flow is defined in the model by:

$$\dot{m} = \rho_{air} * Q \tag{5.6}$$

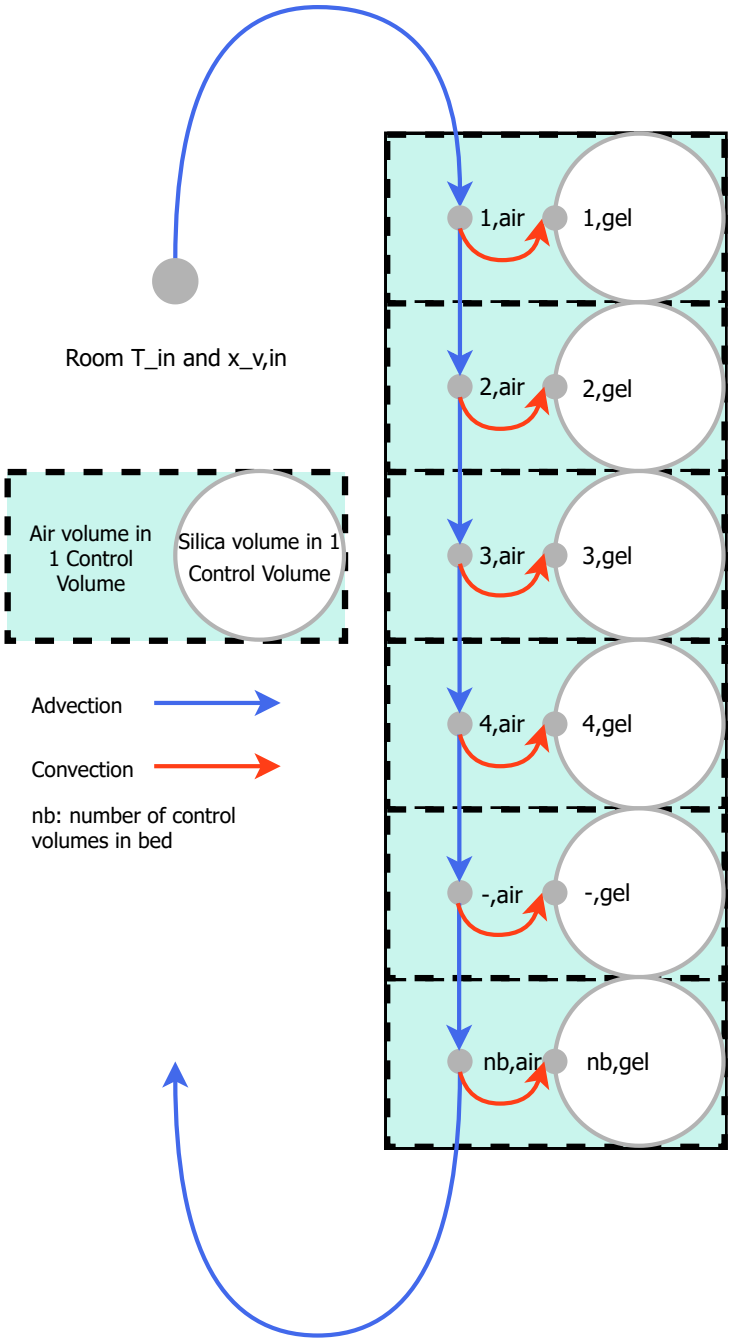

Figure 5.1: Schematic overview of the Pseudo-Gas-Controlled model.

For a given node all heat flows in and out of the corresponding volume are summed, to give the heat balance. Equivalenty, all mass flows are summed, to give the mass balance. At this point, the problem is discretized in space; the time derivatives of temperature and concentration are expressed by the heat and mass balances. *Matlab/Simulink* allows to simultaneously solve the four time derivatives; air temperature, air absolute humidity, particle temperature, particle water concentration.

The following assumptions are made in the model:

- No heat transfer through the bed wall;
- Air flows in 1 direction through the packed bed, modelled by Upwind Differencing scheme.
- Axial heat conduction is negligible in the air stream, as well as the silica particles.
- Axial water vapour diffusion is negligible in the air stream, as well as the silica particles.
- Silica particles have uniform temperature.
- The gaseous phase water near the particle surface is in equilibrium with the adsorbed phase water at the particle surface.

The exchange of mass and heat is displayed in Figure 5.2:

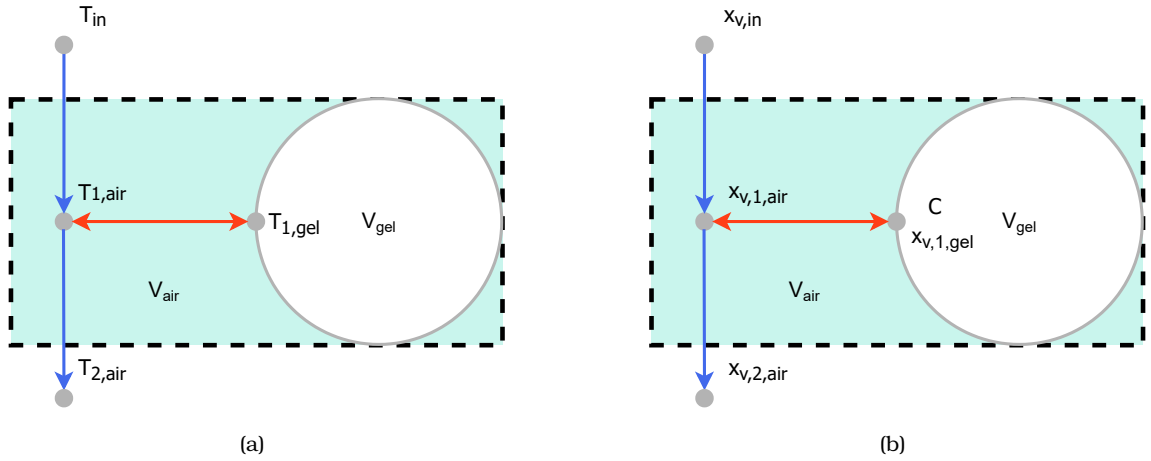

Figure 5.2: (a) Heat flows and (b) mass flows between nodes of finite volume.

The mass balance for silica gel is as follows:

$$V_{gel}\frac{\partial C}{\partial t} = h_m\ p(x_{1,air} - x_{1,gel}) \tag{5.7}$$

The right-hand side consists of the following terms:

1. Convective mass transfer between air and silica node.

The heat balance for silica gel is as follows:

$$\rho_{gel}(c_{gel} + w * c_{liq})V_{gel}\frac{\partial T_{1,gel}}{\partial t} = h_c\ p(T_{1,air} - T_{1,gel}) + H_{ads}h_m\ p(x_{1,air} - x_{1,gel}) \tag{5.8}$$

The left-hand side includes the storage of heat in the silica gel as well as storage of heat in adsorbed water. The right-hand side consists of the following terms:

1. Convective heat transfer due to temperature difference of air and silica gel.
2. Latent heat, released when moisture is adsorbed, or taken up when moisture is desorbed.

The mass balance for air in the macro-pore is as follows:

$$\rho_{air} V_{air} \frac{\partial x_{1,air}}{\partial t} = -h_m \; p(x_{1,air} - x_{1,gel}) + \rho_{air} Q (x_{v,in} - x_{1,air}) \tag{5.9}$$

The right-hand side includes the following terms:

1. Convective mass transfer between air and silica node.
2. Advective mass transfer between air nodes, following Upwind Differencing scheme.

Finally, the heat balance for air in the macro-pore is:

$$\rho_{air} c_{p,e} V_{air} \frac{\partial T_{1,air}}{\partial t} = +\rho_{air} Q c_{air} (T_{in} - T_{1,air}) - h_c \; p(T_{1,air} - T_{1,gel}) + c_{vap} h_m \; p(x_{1,air} - x_{1,gel})(T_{1,air} - T_{1,gel}) \tag{5.10}$$

The left-hand side includes storage of heat in humid air. The right-hand side consists of the following terms:

1. Advective heat flow via bulk air volume.
2. Convective heat transfer due to temperature difference of air and silica.
3. Transfer of heat contained in water vapour

The mass flux by convection between the air node and silica node is determined by the difference in humidity: $x_e - x_s$. This x_s is the absolute humidity ratio of the air *near* the silica surface. The adsorption resistance is small compared to the diffusion resistance inside the silica gel bead. For this reasons, it is assumed the gaseous water *near* the bead surface is in equilibrium with the adsorbed water *at* the bead surface. Thus, the humidity x_v *near* the surface is determined directly from w $[kg/kg]$ (calculated from C $[kg/m^3]$) using the equilibrium isotherm. This needs the following calculations:

1. Calculate w [kg water vapour / kg silica] from C [kg water vapour / m^3 water vapour]:

$$w = \frac{C}{\rho_{gel}} \tag{5.11}$$

2. Calculate apparent RH at surface from w using $RH(w)$ isotherm polynomial for silica gel, (*polynomial used by Pesaran [12]*):

$$RH(w) = 0.0078 - 0.05759w + 24.16554w^2 - 124.478w^3 + 204.226w^4 \tag{5.12}$$

3. Calculate saturation humidity for corresponding surface temperature T_{gel} of silica gel:

$$P_{sat}(T_{gel}) = 611 * exp\left\{\frac{17.27\;\theta_{gel}}{238.3 + \theta_{gel}}\right\} \qquad [Pa] \tag{5.13}$$

$$x_{v,sat}(\theta_{gel}) = 0.622 * 10^5 * P_{sat}(\theta_{gel}) \qquad [kg/kg\;d.a.] \tag{5.14}$$

4. Calculate the absolute humidity from RH and x_{sat}:

$$x_v(w, \theta_{gel}) = RH(w) * x_{v,sat}(\theta_{gel}) \qquad [kg/kg\ d.a.] \tag{5.15}$$

In the heat balance, the specific heat capacity for pore air $c_{p,e}$ depends on the absolute humidity of the air, according to the following equation:

$$c_{p,e} = 1884 * x_{air} + 1004 * (1 - x_{air}) \qquad [kJ\ kg^{-1}\ K^{-1}] \tag{5.16}$$

The used correlations for mass transfer coefficient h_m and h_c are found in Pesaran [12] and Antonellis [8], and are the ones adjusted to a PGC model:

$$h_c = 0.683 * U_{air}\ \rho_{air}\ c_{air}\ Re^{-0.51} \qquad [W/(m^2\ ^oC)] \tag{5.17}$$

$$h_m = 0.704 * U_{air}\ \rho_{air}\ Re^{-0.51} \qquad [kg/(m^2\ s)] \tag{5.18}$$

Where the term ($U_{air}\ \rho_{air}$) is the mass flow rate per unit area and U_{air} is the superficial fluid velocity: $U_{air} = \frac{Q}{A_{bed}}$. The Reynolds number can be determined with the relations shown in Section 2.4.

All time-invariant variables are defined in the Matlab script *PGCmodel.m*, shown in Appendix G. The Simulink script in Appendix H shows the visual interpretation of the governing differential equations. The Simulink script is solved using the *ode23tb* solver with a variable time step (max. $2\ s$).

Fit procedure for isotherm polynomial

The isotherm polynomial is obtained from polynomial fitting of the uptake rate measurements from Experiment 1. The resulting form is $RH(w)$. Experiment 1 has provided mass gain and loss relative to 20 %RH equilibrium. Y data for the fit is relative humidity in [-]. X data for the fit is water uptake in [kg/kg]. For example, for sample 6:

$$Y = RH = \begin{bmatrix} 0.20 & 0.30 & ... & 0.80 \end{bmatrix} \tag{5.19}$$

$$X = w = \begin{bmatrix} 0.0000 & 0.0486 & 0.1041 & 0.1591 & 0.1973 & 0.2153 & 0.2248 \end{bmatrix} \tag{5.20}$$

Since the polynomial used in the model needs absolute moisture uptake instead of relative, the moisture uptake data from Experiment 1 is offsetted. The offset is the water content at 20 %RH, obtained from silica gel datasheets. Using the data from Experiment 1 ensures the course of the isotherm agrees with the actual samples used in this research. However, the offset adds uncertainty to the retrieved polynomial.

The equilibrium moisture content of sample 6 (microporous) at 20 %RH is $6.0\ wt-\% \approx 0.06 kg/kg$. This is the offset for the X data.

$$X = w = \begin{bmatrix} 0.0600 & 0.1086 & 0.1641 & 0.2191 & 0.2573 & 0.2753 & 0.2848 \end{bmatrix} \tag{5.21}$$

Matlab toolbox *cftool* is used to fit Y versus X data. The interface is shown in Figure 5.3. The resulting 4^{th} order polynomial is:

$$RH(w) = 0.004955 + 0.5169w + 19.02w^2 - 80.81w^3 + 98.12w^4 \tag{5.22}$$

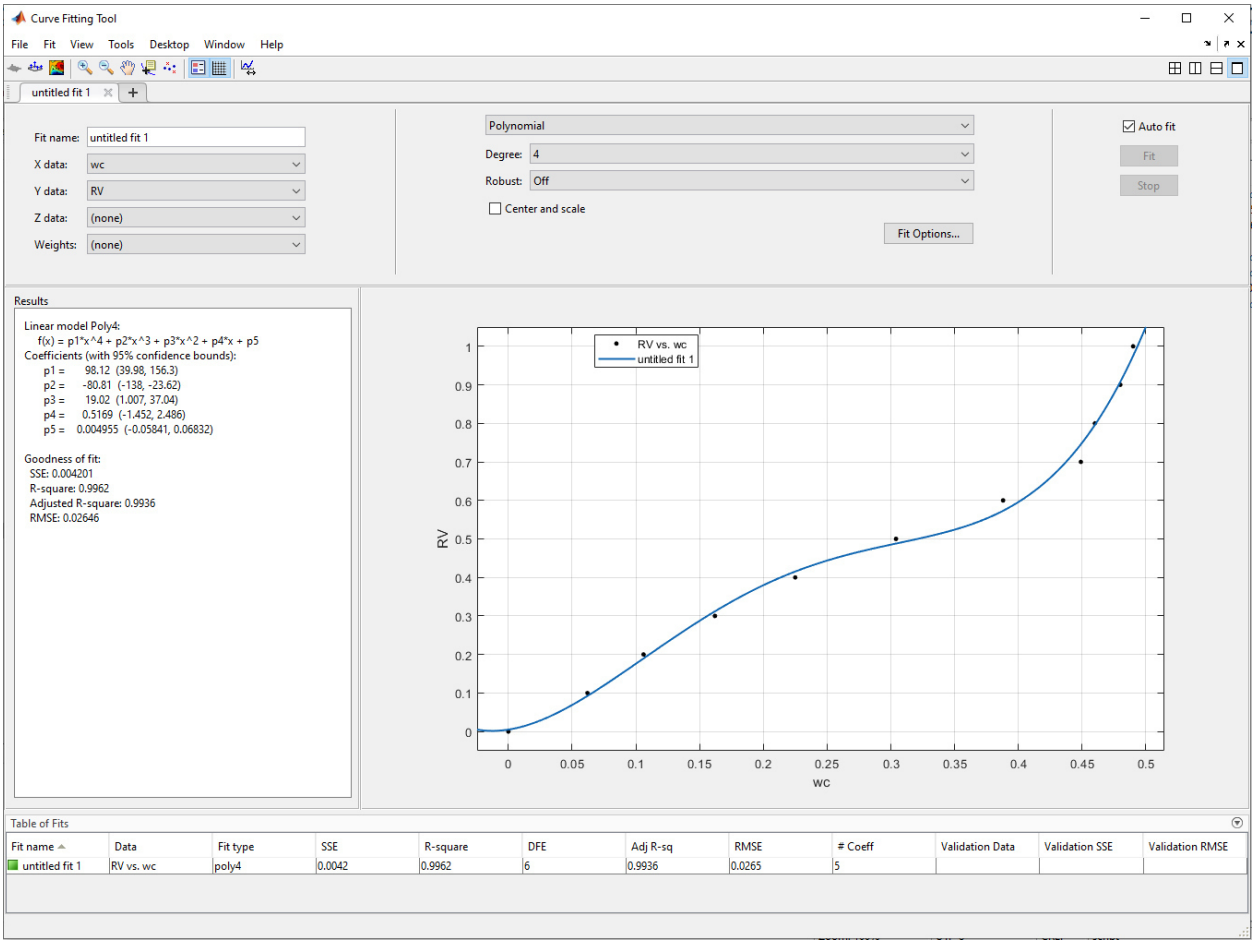

Figure 5.3: Polynomial fitting of $RH(w)$ using *cftool* in Matlab, with (offsetted) data from uptake rate measurements for sample 6.

Input parameters

The following values are used as input in the PGC model. The isotherm polynomial for every sample is given as well. Density of silica gel ρ_{gel} and particle radius R_p vary per sample.

Parameter	**Character**	**Value**	**Unit**
Diameter bed	D	0.120	m
Length bed	L	0.50	m
Bed porosity	ϵ_{bed}	0.36	[-]
Volumetric flow rate	Q	$\frac{97.5}{60*1000}$	m^3/s
Density air	ρ_{air}	1.1987	kg/m^3
Density silica gel	ρ_{gel}	700	kg/m^3
Dynamic viscosity of air	μ_{air}	$18.17 * 10^{-6}$	$Pa * s$
Specific heat air	c_{air}	1000	$J/(kg * K)$
Specific heat water vapour	c_{vap}	1860	$J/(kg * K)$
Specific heat silica gel	c_{gel}	1000	$J/(kg * K)$
Specific heat liquid water	c_{liq}	4184	$J/(kg * K)$
Particle radius	R_p	0.0015	m
Latent heat of vaporization of water	H_{ads}	$2.5 * 10^6$	J/kg
First input temperature	$T_{in,1}$		^oC
Second input temperature	$T_{in,2}$		^oC
First input humidity	$x_{in,1}$		kg/kg
Second input humidity	$x_{in,2}$		kg/kg
Initial temperature in packed bed	$T_{0,e}$		^oC
Initial air humidity in packed bed	$x_{0,e}$		kg/kg
Isotherm sample 6			
$RH(w) = 1.667 - 33.65w + 265.6w^2 - 845w^3 + 969.9w^4$			
Isotherm sample 11			
$RH(w) = 0.008263 + 4.145w - 9.279w^2 + 7.938w^3$			
Isotherm sample 12			
$RH(w) = 0.782 - 16.74w + 157.4w^2 - 556.8w^3 + 700.1w^4$			
Isotherm sample 14			
$RH(w) = 0.005046 + 0.5135w + 19.01w^2 - 80.69w^3 + 97.96w^4$			

Table 5.1: Input parameter values for the PGC model

5.2 Analysis of packed bed model

Comparison to experimental data from literature

The developed PGC model is used to simulate experimental data found in literature. The two used researches are:

- a cyclic experiment executed by Antonellis [8].
- single blow experiments executed by Pesaran [12], from a model study by [10].

Annex C presents the results from literature together with the results from the PGC model, for identical input as the experimental data.

The PGC model developed in this thesis shows the same response to temperature and humidity input as the mentioned experiments and model studies from literature.

Comparison to simplified model

In a previous thesis work [27], a numerical model of an exhibition room is developed. Within this model, a packed bed model is integrated. This simplified model is based on two differential equations, the heat and mass balances for air in the packed bed, modelled by Upwind Differencing scheme:

$$(1-\epsilon)*\xi*V_i*\frac{\partial \phi_i}{\partial t} = \dot{m}_{air}[x_{sat}(T_{i-1})\ \ \phi_{i-1} - x_{sat}(T_i)\ \ \phi_i] \tag{5.23}$$

$$\begin{aligned}[(1-\epsilon)*(c_{gel}\rho_{gel}+c_{liq}w_{gel})]*V_i*\frac{\partial T}{\partial t} &= \dot{m}_{air}[c_{air}T_{i-1}+x_{sat}(T_{i-1})\phi_{i-1}*(L_{lv}+c_{vap}T_{i-1})] \\ &\quad - \dot{m}_{air}[c_{air}T_i+x_{sat}(T_i)\phi_i*(L_{lv}+c_{vap}T_i)]\end{aligned} \tag{5.24}$$

The model describes the $RH(w)$ relation solely by the slope of the equilibrium isotherm: $\xi = \frac{\partial w_{gel}}{\partial RH}$. The isotherm is thus assumed linear, which is a reasonable assumption in the range of 40 to 60 %RH.

The PGC model results for a step input from 20 to 50 %RH are compared to the results from the simplified model. Both results are shown in Figure 5.4. The simplified model reacts faster than the PGC model; it reaches inlet values earlier in time. The overall course of the humidity and temperature do agree with measurements.

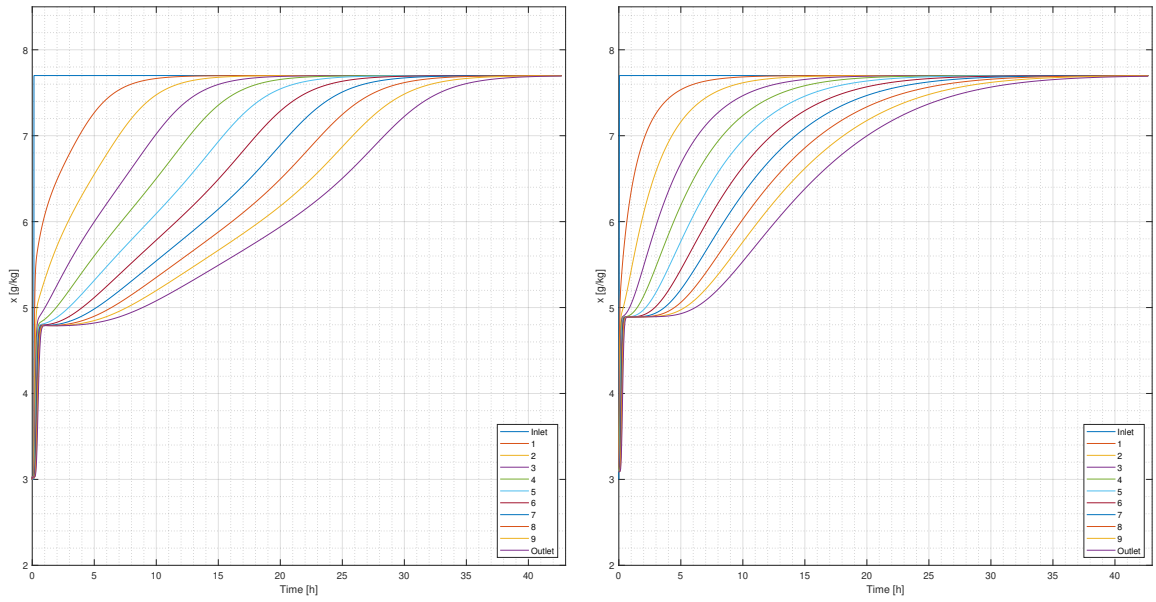

(a) (b)

Figure 5.4: Numerical results for a step input from 20 to 50 %RH, obtained with (a) PGC model and (b) simplified model.

The PGC and simplified model are compared for the short cycle experiment as well. The results are identical, and presented in Figure 5.5.

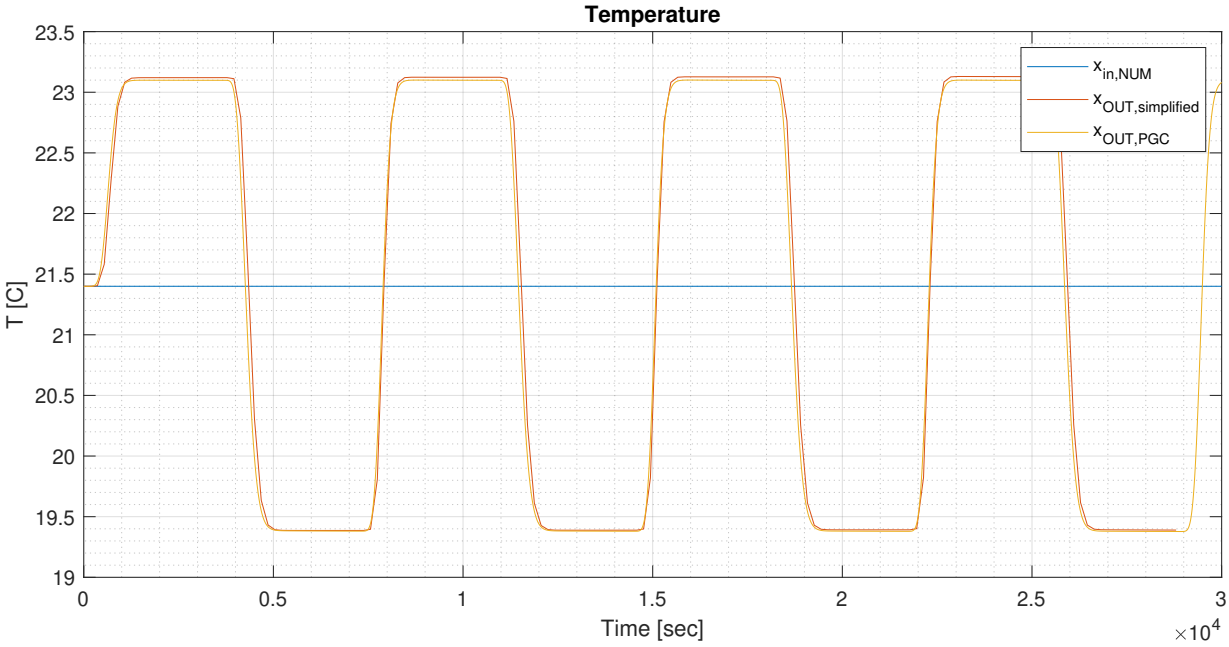

(a)

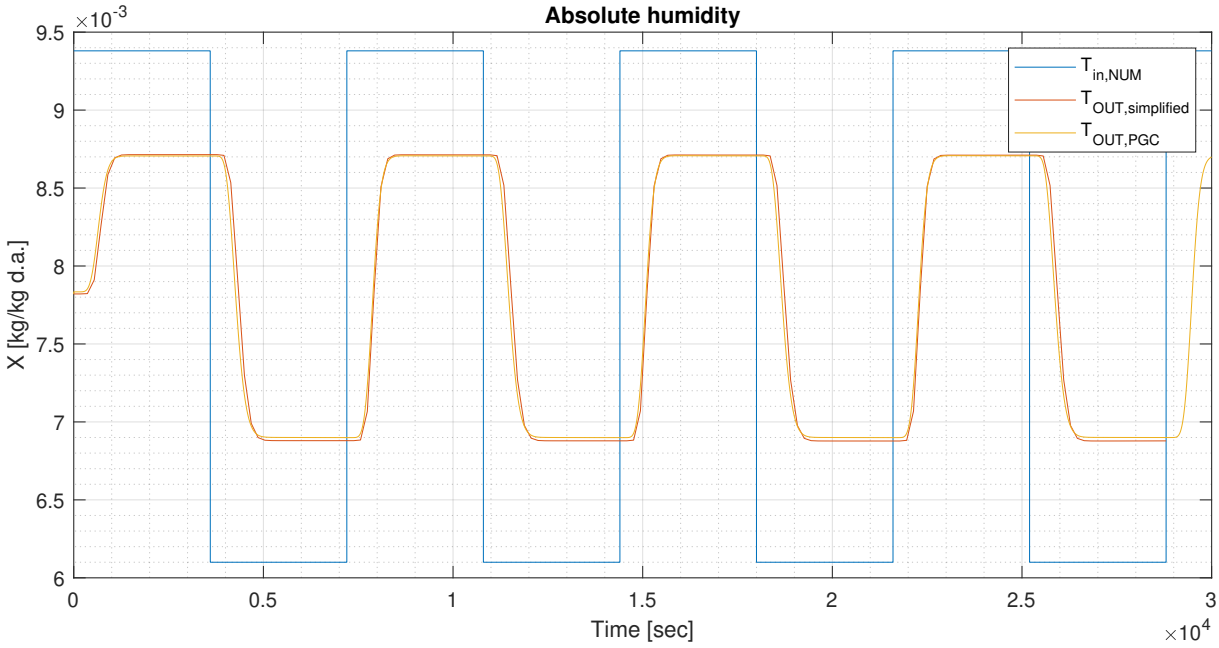

(b)

Figure 5.5: Comparison of PGC model and simplified model results for (a) temperature and (b) absolute humidity in run 2 of Experiment 2.

Finally, the PGC and simplified model are compared for a long experiment run. Both models show similar course of temperature and humidity. Desorption appears faster in the simplified model. Results are shown in Figure 5.6.

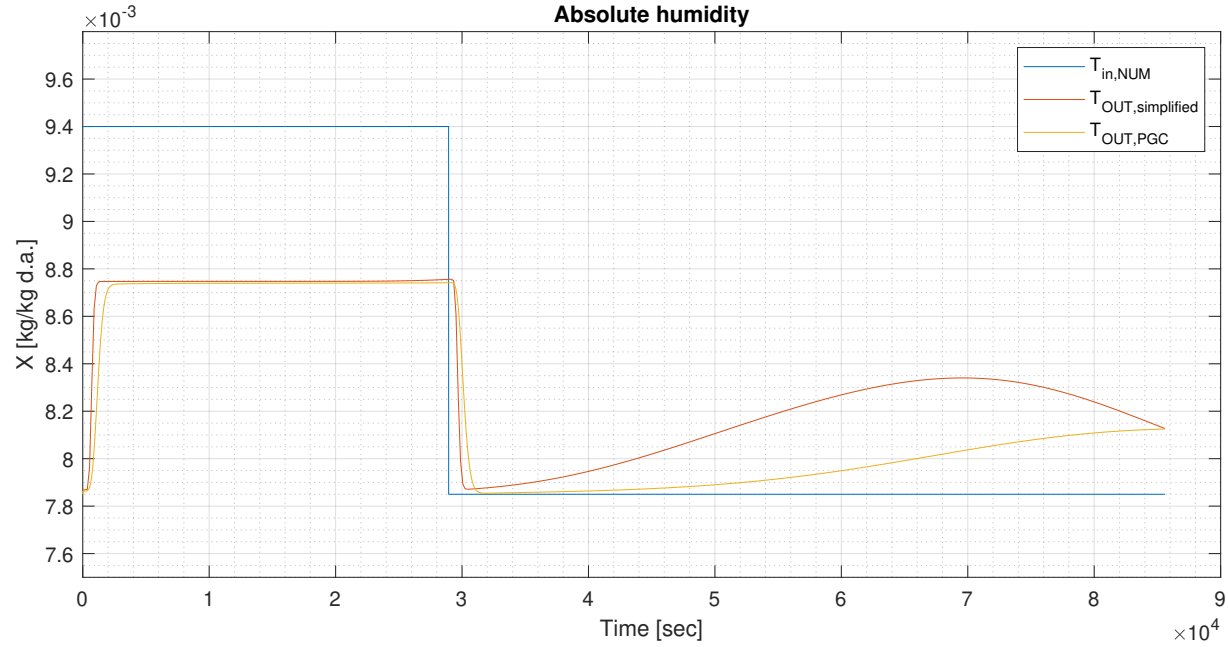

(a)

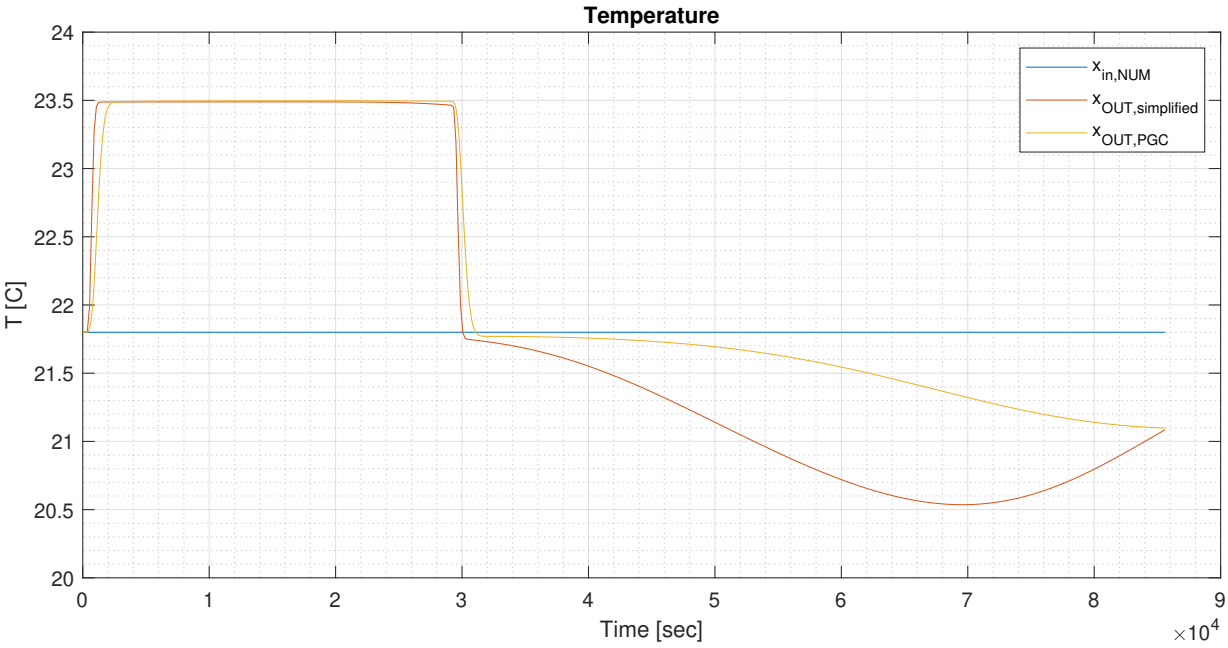

(b)

Figure 5.6: Comparison of PGC model and simplified model results for (a) temperature and (b) absolute humidity in run 2 of Experiment 2.

Comparison to Experiment 2

Step from 20 to 50 %RH

First the PGC model from this thesis is compared to run A from Experiment 2. Both the model results and experimental results are shown in Figures 5.7 up to 5.10. The PGC model is a bit faster: the initial step in absolute humidity happens faster, and the humidity reaches inlet value (or equilibrium) earlier.

The PGC model reacts faster to a step input than measured in the experiments. The simplified model reacts even faster than the PGC model. It is important to mention the sample used in the step experiment follows primary isotherm. Numerical results are expected to match better to experimental results if the sample would follow secondary isotherm: sorption would then be less, and outlet air would reach equilibrium earlier.

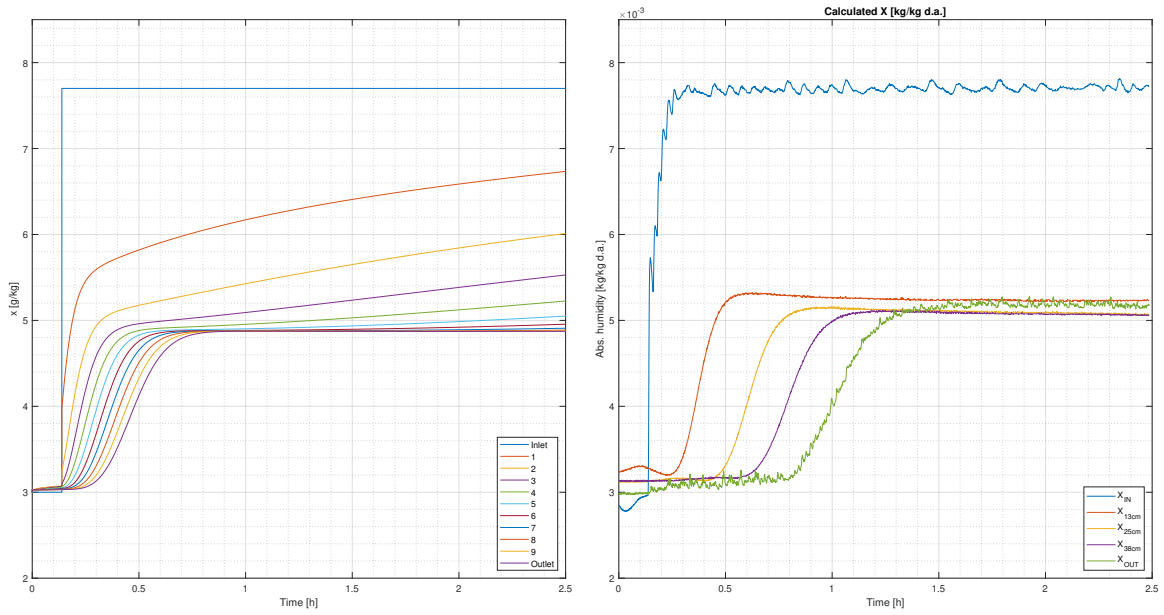

(a) (b)

Figure 5.7: Step input from 20 to 50 %RH: (a) PGC model results and (b) experimental results.

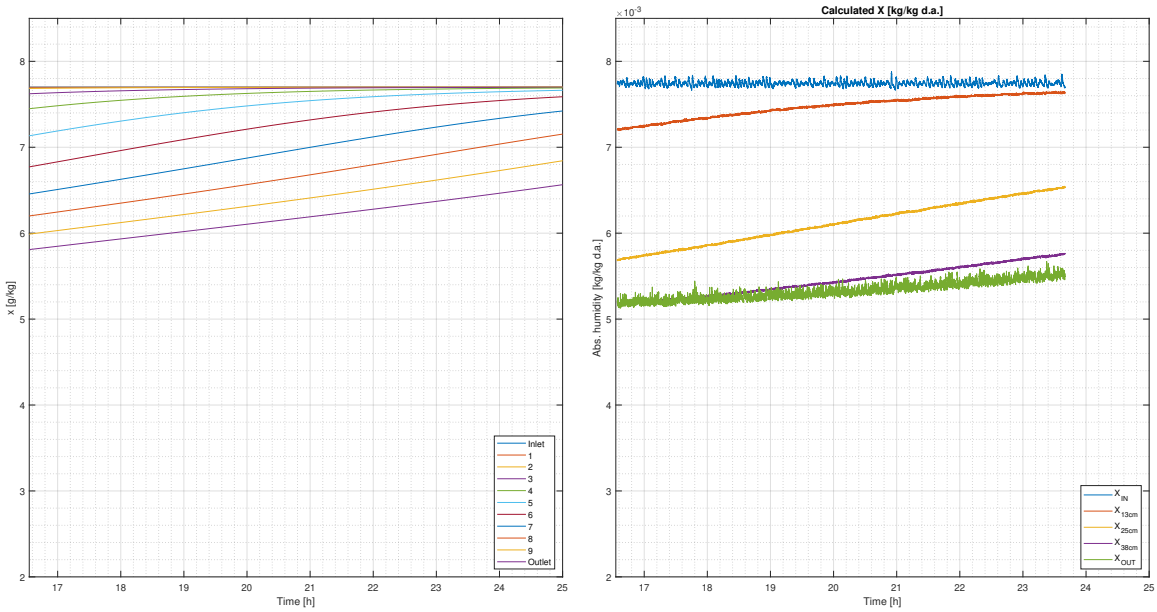

(a) (b)

Figure 5.8: Step input from 20 to 50 %RH: (a) PGC model results and (b) experimental results.

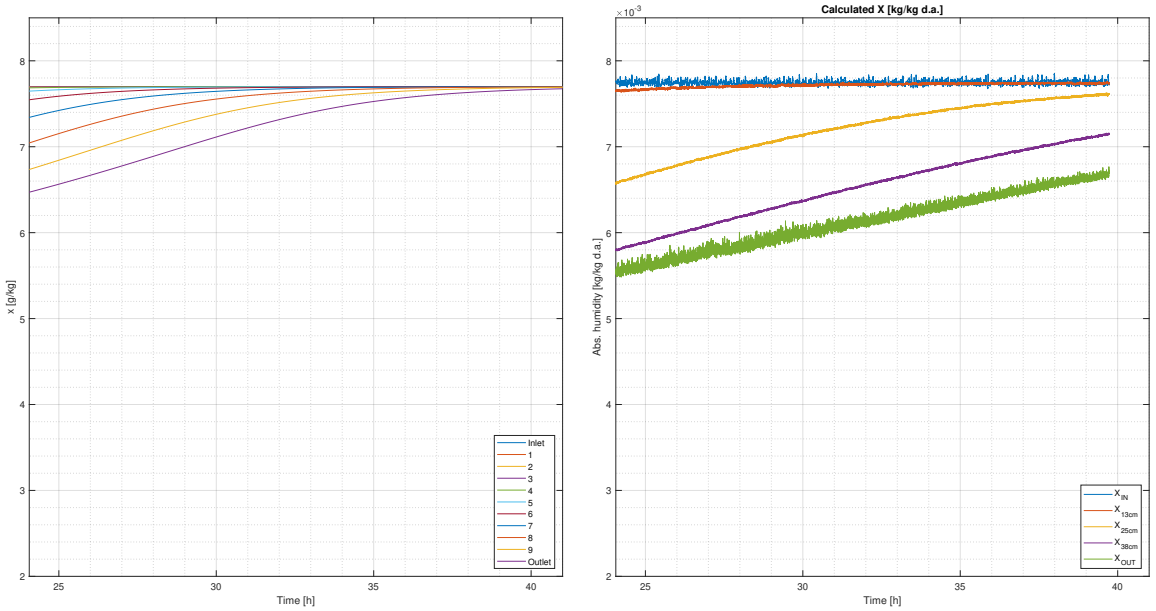

(a) (b)

Figure 5.9: Step input from 20 to 50 %RH: (a) PGC model results and (b) experimental results.

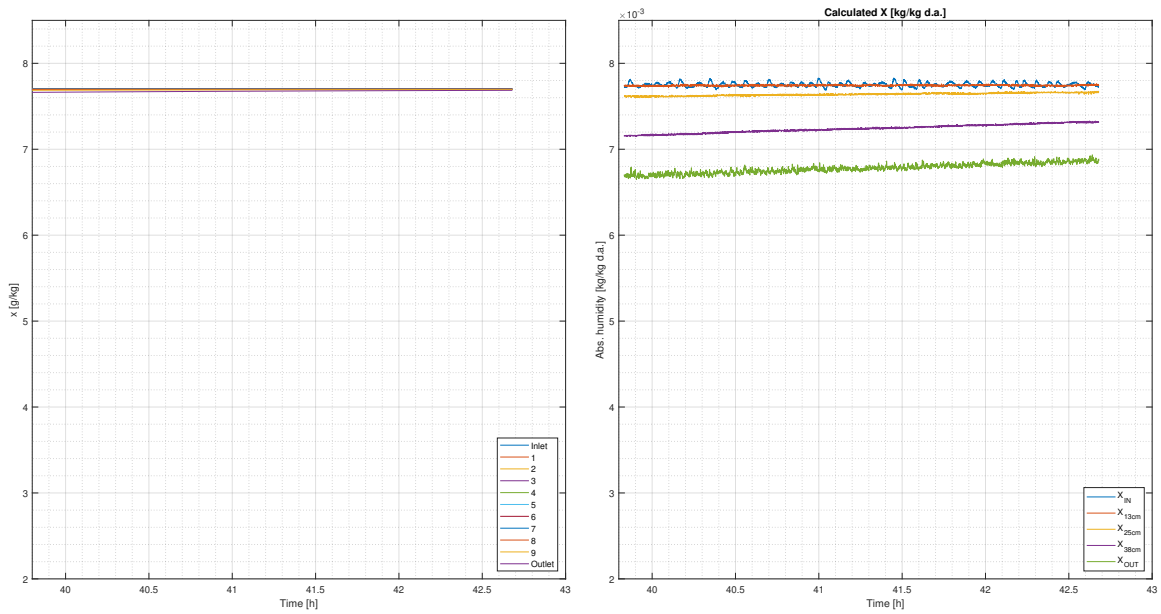

(a) (b)

Figure 5.10: Step input from 20 to 50 %RH: (a) PGC model results and (b) experimental results.

Long and short cycle

The complete set of numerical results compared to the results of Experiment 2 is presented in Annex C.

For the long cycle runs 5 up to 8, the numerical results are compared for one of the three cycles. Results are compared at first part of the packed bed ($13\ cm$), as well as at the outlet. For the short cycle runs 1 up to 4, the numerical results are compared to measurements at outlet.

The model is able to match experimental results for the short cycle. The step in absolute humidity after a step in inlet humidity is mainly determined by the latent heat, H_{ads}, in the model. Within the half cycle time of 1 hour, silica is not saturating. Different isotherms will not give different results.

A discrepancy is observed in the time constant of the humidity change. For the numerical results, the absolute humidity and temperature rise and drop faster than the experimental results.

An important observation is that model results for run 2 (sample 11/ mesoporous silica gel) match very good to experiments. This sample has small particle radius of $0.001\ m$. The impact of neglecting diffusion is smaller. This agrees to Ramzy et al. [10], stating the PGC model is acceptable for small particle diameters. Results for a SSR model, including intra-particle diffusion, are expected to match better to experimental results.

5.3 Discussion of numerical packed bed model

Most of the input parameters in the model are material properties. It is not reasonable to have large variations in material properties. An assumption is made regarding the bed porosity ϵ_{bed}. Varying this parameter does not have large influence on the numerical results.

The model proves to be sensitive to the inputted isotherm polynomial. The isotherm polynomial is the parameter determining the saturation of silica gel. The applied procedure for determining the isotherm polynomials has introduced uncertainties regarding the polynomial.

The difference between *primary* and *secondary* isotherms has introduced uncertainty to the polynomials. In Experiment 1 the primary adsorption isotherm is experimentally determined. In Experiment 2 the samples are loaded in dry state. After some cyclic behaviour, the samples are not following primary isotherm anymore. The fitting procedure itself introduces another uncertainty.

6 | Results and analysis

This section starts with analyzing the amount of (de)-humidification during Experiment 2.

Next, the Moisture Buffer Value (MBV) is calculated from this values for (de)-humidification. The MBV takes into account the timing of fluctuations in relative humidity.

6.1 Analysis of (de)-humidification in Experiment 2

The buffering performance is determined by the level of dehumidification of relatively wet air, and vice versa the level of humidification of relatively dry air. The (de)humidification is expressed as the difference between outlet and inlet air humidity: $x_{(de)hum} = x_{out} - x_{in}$. For short Run 2, this humidification is shown in Figure 6.1(b).

The absolute amount of moisture absorbed during time t is equal to following equation. Following the convention: the amount of adsorption ($+\Delta w$) in silica gel is equal to the amount of dehumidification ($-\Delta x_{air}$). This equation corresponds to the integral area of $x_{(de)hum}$ vs. $time$ plot, in Figure 6.1(b), times $\rho_{air} * Q$.

$$+\Delta w = m_{ads} = -(x_{(de)hum,average}) * t * \rho_{air} * Q \qquad [kg] \tag{6.1}$$

For Run 2, the calculated amount of water in kg adsorbed in the first half cycle equals:

$$+\Delta w = m_{ads} = 8.627e^{-4} * (3901 - 300) * 1.1987 * 0.001625 = 0.0061 \qquad [kg] \tag{6.2}$$

For all 8 half cycles of runs 1 up to 4, the amount of water adsorbed (+) or desorbed (-) in [kg] is shown in Table 6.1.

Runs 1 up to 4								
Run	*Half cycle 1*	*2*	*3*	*4*	*5*	*6*	*7*	*8*
1	+0.0073	-0.0112	+0.0103	-0.0112	+0.0102	-0.0112	+0.0102	-0.0113
2	+0.0061	-0.0076	+0.0073	-0.0077	+0.0073	-0.0077	+0.0074	-0.0077
3	+0.0074	-0.0109	+0.0103	-0.0109	+0.0103	-0.0109	+0.0103	-0.0109
4	+0.0085	-0.0116	+0.0116	-0.0116	+0.0116	-0.0117	+0.0116	-0.0116

Table 6.1: Moisture uptake and release in [kg] during half cycles of Experiment 2 - Short cycle.

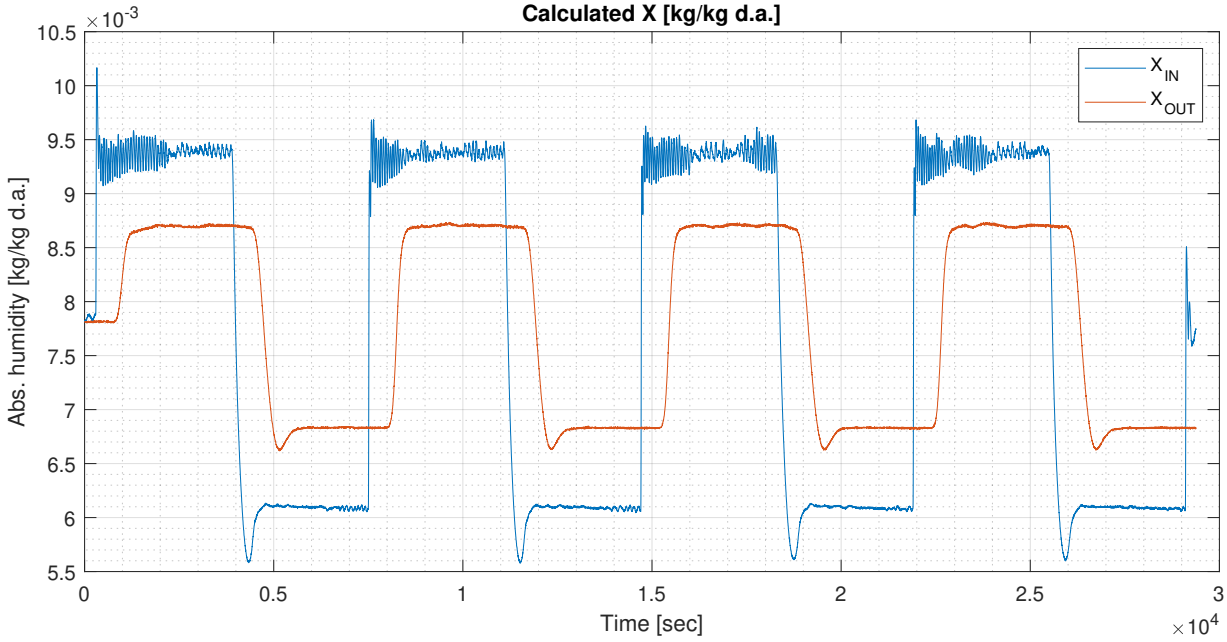

(a)

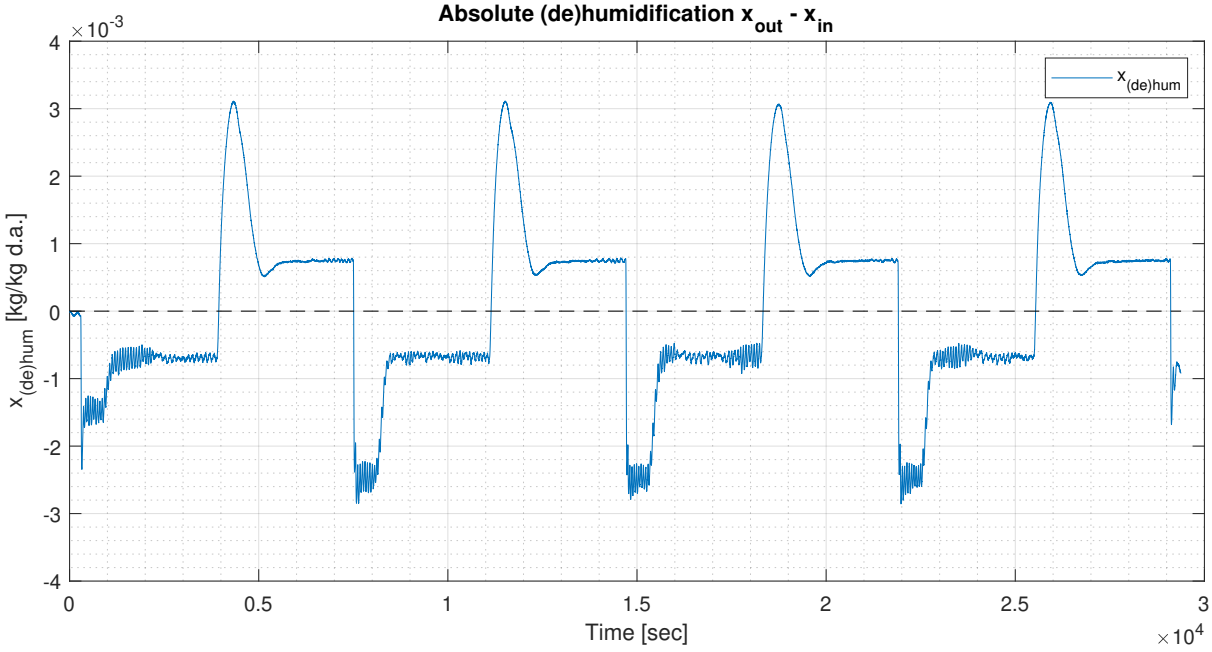

(b)

Figure 6.1: (a) Absolute air humidity at inlet and outlet of packed bed in run 2, and (b) Absolute (de)humidification of air leaving the packed bed.

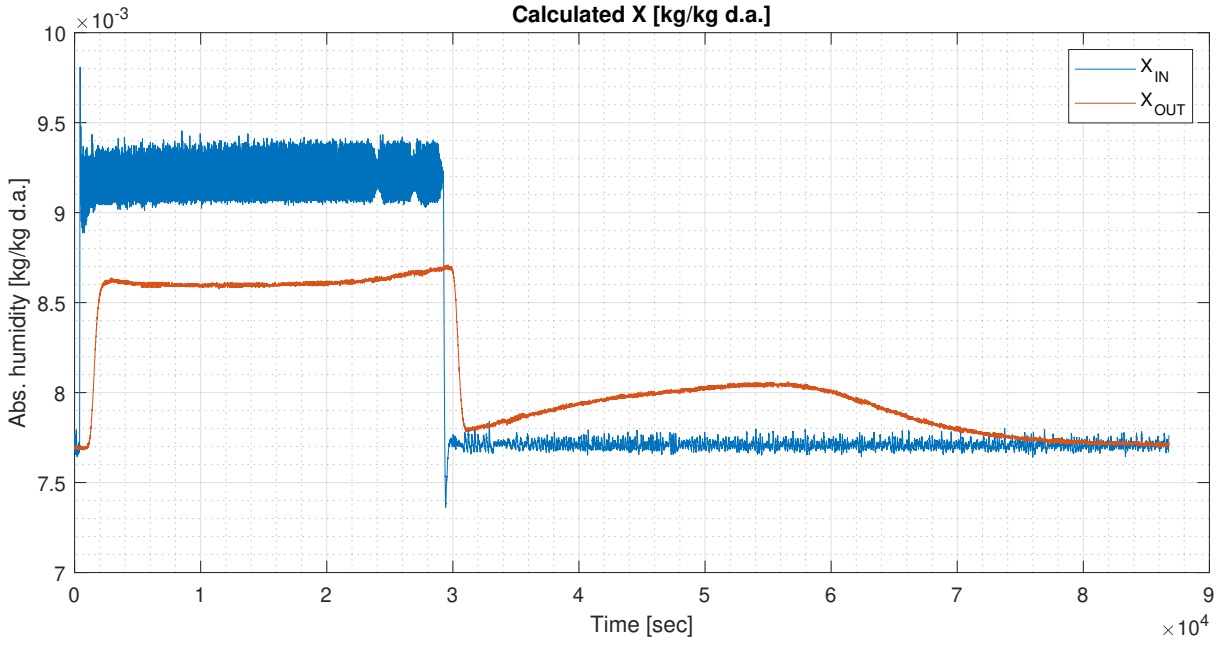

(a)

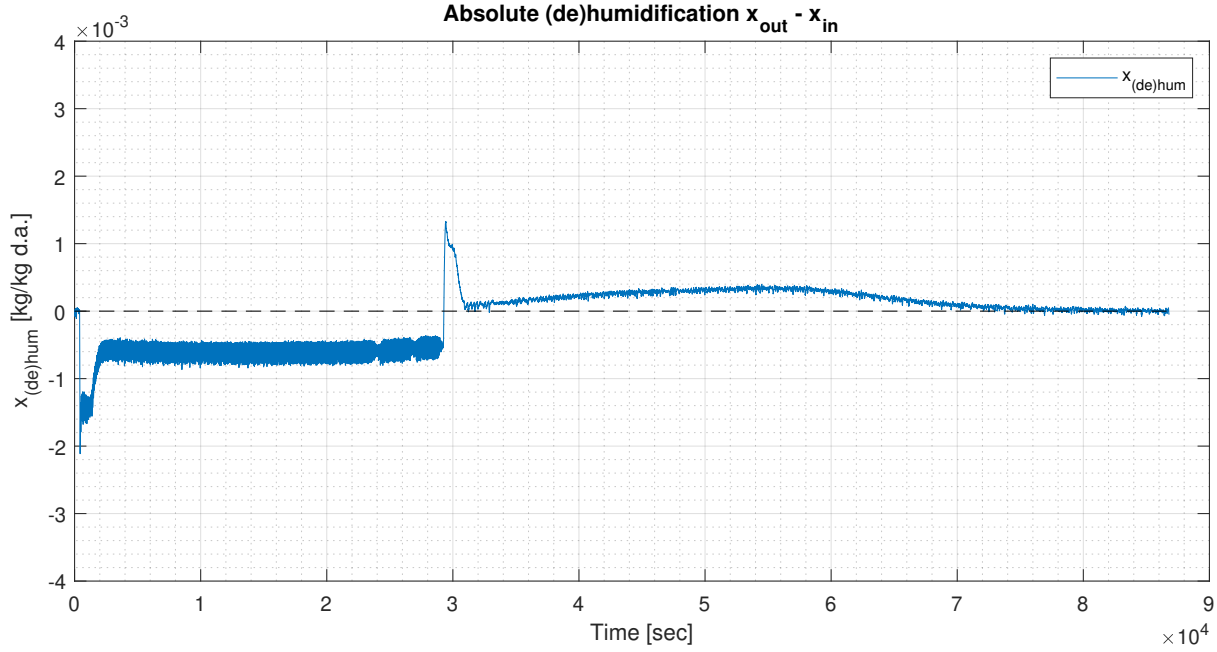

(b)

Figure 6.2: (a) Absolute air humidity at inlet and outlet of packed bed in run 7, and (b) Absolute (de)humidification of air leaving the packed bed.

The same calculation is done for long Run 7, cycle **1**, see Figure 6.2(b). During the 8 hour

high part of the cycle, the adsorbed amount of water equals:

$$+\Delta w = m_{ads} = 6.506e^{-4} * (29,286 - 400) * 1.1987 * 0.001725 = 0.0389 \qquad [kg] \tag{6.3}$$

The following isotherm, for sample 12, is solved for given RH values. Between 50 and 60 %RH equilibrium, the silica gel should take up Δw kg water per kg silica gel.

$$RH(w) = 0.782 - 16.74w + 157.4w^2 - 556.8w^3 + 700.1w^4 \tag{6.4}$$

$$RH = 0.50 \rightarrow w = 0.2714 \ kg/kg \tag{6.5}$$

$$RH = 0.60 \rightarrow w = 0.3109 \ kg/kg \tag{6.6}$$

$$\Delta w = 0.3109 - 0.2714 = 0.0395 \ kg/kg \tag{6.7}$$

This means the $3.193\ kg$ of silica gel could theoretically take up as much as $3.193 * 0.0395 = 0.1261 = 126.1$ gram of water. This is more than the actual amount of 38.9 gram adsorbed water. This means the silica is not near saturation. This fact agrees with Figure 6.2(a): The outlet absolute air humidity just starts to rise at the end of the 8 hours. A lot more water can be adsorbed.

The amount of water desorbed during the next 16 hours equals:

$$\Delta w = m_{ads} = -1.877e^{-4} * (86,793 - 29,286) * 1.1987 * 0.001725 = -0.0223 \qquad [kg] \tag{6.8}$$

For all three cycles of Runs 5 up to 8, the resulting moisture uptake (+) and release (−) is presented in Table 6.2.

Runs 5 up to 8						
Run	*Half cycle 1*	*2*	*3*	*4*	*5*	*6*
5	+0.0462	+0.0008	+0.0405	-0.0091	+0.0368	-0.0204
6	+0.0447	+0.0007	+0.0291	-0.0103	+0.0238	-0.0168
7	+0.0389	-0.0223	+0.0360	-0.0282	+0.0353	-0.0309
8	+0.0436	-0.0067	+0.0345	-0.0194	+0.0311	-0.0260

Table 6.2: Moisture uptake and release during half cycles of Experiment 2 - Long cycle.

6.2 Moisture Buffering Value

The moisture buffering by silica gel is quantified for the ProSorb, used in run 4 and 8.

The Moisture Buffering Value is an expression to quantify the moisture buffer potential of indoor finishes, used by [18]. In this expression the adsorbed and desorbed moisture mass, for a specified time, is normalised per m^2 and $\%RH$:

$$MBV_{8h} = \frac{m_{max} - m_{min}}{A * (\phi_{high} - \phi_{low})} \qquad [kg/m^2/\%RH] \tag{6.9}$$

Similarly, the moisture change in the experiments can be normalised per m^3 and $\%RH$:

$$MBV_{8h} = \frac{m_{max} - m_{min}}{V_{gel} * (\phi_{high} - \phi_{low})} \qquad [kg/m^3/\%RH] \tag{6.10}$$

The theoretical MBV between 40 and 60 %RH, when silica water content is at equilibrium, is derived from the equilibrium isotherm data from Figure 6.3:

$$MBV_{\infty} = \frac{(w_{60\%} - w_{40\%}) * \rho_{gel}}{V_{gel} * (60 - 40)} = \frac{(0.388 - 0.225) * 750}{1 * (60 - 40)} \approx \mathbf{6000} \qquad [g/m^3/\%RH] \tag{6.11}$$

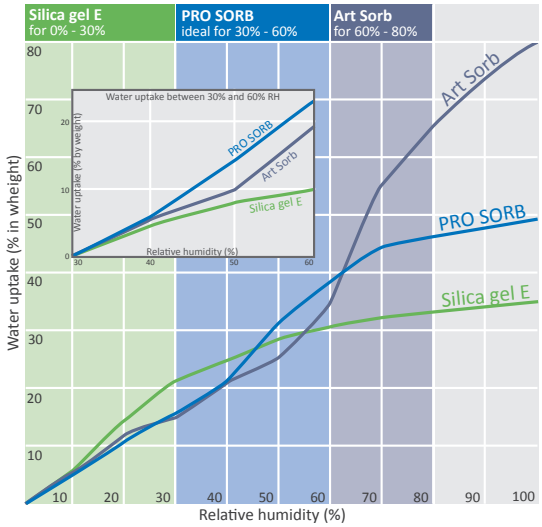

	Silica gel E		PRO SORB		Art Sorb	
Relative Humidity		30-60%		30-60%		30-60%
10%	7		6,2		6,5	
20%	14		10,6		11,5	
30%	20,5		16,2		16	
40%	25	10	22,5	22,6	22	19
50%	28,5		30,4		26	
60%	30,5		38,8		35	
70%	32		44,9		54	
80%	33		46		67	
90%	34		48		74	
100%	35		49		80	

Relative humidity (%)

Water uptake (% in wheight)

Figure 6.3: Equilibrium isotherm of ProSorb

In run 4, the effective mass change is 11.6 gram per hour, cf. Table 6.1. The MBV_{1h} equals:

$$MBV_{1h} = \frac{11.6}{0.0035 * (61.5 - 39.5)} \approx \mathbf{150} \qquad [g/m^3/\%RH] \tag{6.12}$$

In run 8, the moisture change converges to $\pm$ 29.0 gram per 8 hours, cf. Table 6.2. The MBV_{8h} equals:

$$MBV_{8h} = \frac{29.0}{0.0032 * (61.1 - 50.8)} \approx \mathbf{800} \qquad [g/m^3/\%RH] \tag{6.13}$$

The MBV calculations for other runs are tabulated in Figure 6.4. In this table, the second column contains $m_{max} - m_{min}$, which is the estimated value, or 'amplitude', the values in Tables 6.1 and 6.2 converge to.

Run	m_{max} - m_{min}	Height silica	V_{gel}	ϕ_{high}	ϕ_{low}	MBV_{1h}
	[g]	[m]	[m^3]	[-]	[-]	[g/m3/%RH]
1	*10.3*	*0.280*	*0.0032*	*61.2*	*39.0*	*146.6*
2	*7.5*	*0.310*	*0.0035*	*59.0*	*38.5*	*104.4*
3	*10.5*	*0.300*	*0.0034*	*60.9*	*40.4*	*151.0*
4	*11.6*	*0.310*	*0.0035*	*61.5*	*39.5*	*150.5*
						MBV_{8h}
5	*32.0*	*0.500*	*0.0057*	*58.3*	*48.3*	*566.2*
6	*19.0*	*0.310*	*0.0035*	*58.8*	*49.1*	*559.0*
7	*32.0*	*0.260*	*0.0029*	*61.1*	*50.9*	*1067.4*
8	*29.0*	*0.285*	*0.0032*	*61.1*	*50.8*	*873.9*

Figure 6.4: Moisture Buffer Values calculated for runs in Experiment 2.

7 | Discussion

The chapter starts with an overview of the lessons learned about using silica gel for passive humidity control. These takeaways are summarized in a List of Requirements, acting as a starting point for further design efforts. The chapter is concluded with a discussion of the followed research approach.

7.1 Discussion of moisture buffering in a packed bed

Experiment 2 has corroborated the hygric capacity of silica gel. The hygric capacity based on equilibrium isotherm is expected to be addressed when silica gel is able to reach equilibrium moisture content: $\xi_{theoretical}$.

However, for calculations on buffering it is not fair to account for the full hygric capacity. This is because the silica gel needs time to reach equilibrium moisture content. The required time to reach equilibrium is likely to exceed the half time period of the expected fluctuations ($\pm$ $8h$). Two major aspects determine the required time for all silica gel to reach equilibrium, which are schematically indicated in Figure 7.1:

- diffusion in the silica particles, and
- spatial organisation of the silica.

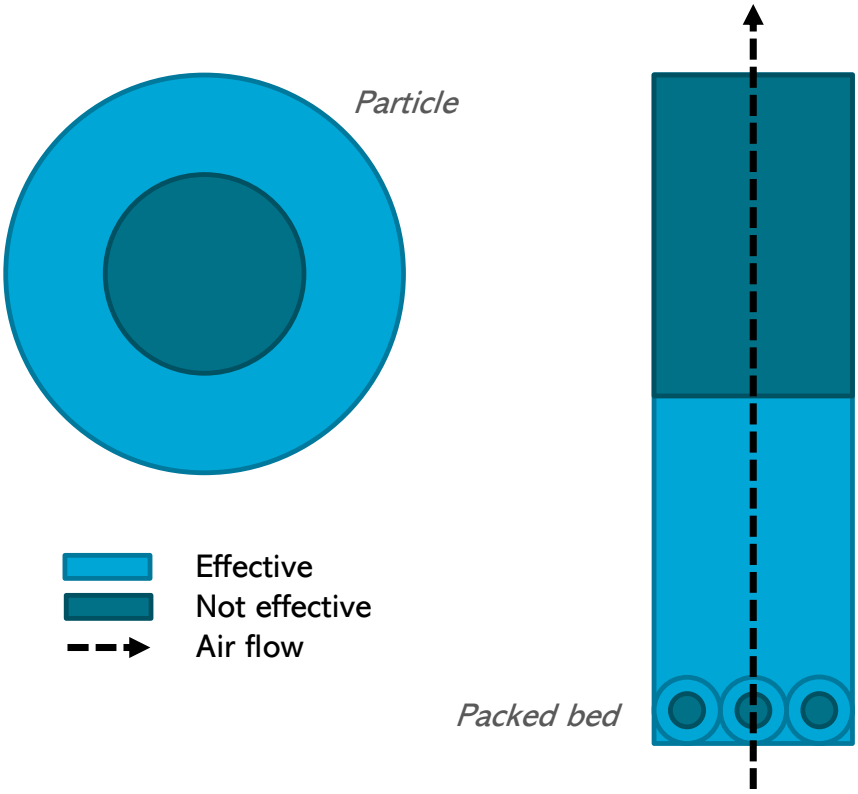

Figure 7.1: Effective volume of silica addressed for a specified humidity fluctuation.

Thus, for timed humidity fluctuations, only a fraction of the volume of silica is effectively addressed. This follows the logic of the theory on Effective Moisture Penetration Depth (EMPD), from Section 2.2 Given the boundary conditions of Experiment 2 (packed bed geometry, air velocity, RH fluctuations):

– for fluctuations of 20 %RH per 1h, only $150/6000 =$ **0.025** of the hygric capacity of silica gel is utilized:

$$\xi_{effective} = \frac{MBV_{1h,\ EXP}}{MBV_{\infty}} \cdot \xi_{theoretical} = 0.025 \cdot \xi_{theoretical} \tag{7.1}$$

- for fluctuations of 10 %RH per 8h, only $800/6000 =$ **0.133** of the hygric capacity of silica gel is utilized:

$$\xi_{effective} = \frac{MBV_{8h,\ EXP}}{MBV_{\infty}} \cdot \xi_{theoretical} = 0.133 \cdot \xi_{theoretical} \tag{7.2}$$

The MBV_{1h} and MBV_{8h} calculated from Experiment 2 correspond to an air velocity of $v = 0.13$ [m/s] and the specified difference in relative humidity. The MBV can likely be increased by increasing the velocity of air passing the silica gel.

Product design

Experiment 2 has pointed out important issues to consider when designing a device for passive humidity control using silica gel. A complete set of technical, and eventually aesthetical, design guidelines can be drawn up in the form of a List of Requirements. Aesthetical guidelines for application in a museum are not inventorized in this project. This should be done in a later stage.

In the field of engineering product design, a variety of models is available to guide the design process. A widely used model is the one proposed by Pahl and Beitz [7]. The first phase of product development is the **Planning and Task Clarification**. In this phase the task of the product is specified. The results is a List of Requirements, listing demands to be met at all times and wishes, to be met whenever possible. The first phase is followed by **Conceptual Design**, **Embodiment Design** and **Detail Design**.

The following table presents the List of Requirements to date. This list is not exhaustive and is intended to be continuously updated. It serves as a starting point for further product design efforts.

Planning and Task Clarification

Changes	**Requirements**	**Quantitative**	**Qualitative**
	Demands		
30/3	Maximize the surface-area-to-volume ratio, to utilize silica gel mass as effective as possible	max. $\frac{A}{V}$	
30/3	Minimize pressure drop in system (and consequential required fan capacity)	min. ΔP	
30/3	Reduce length of silica gel channel, to prevent delayed rises and falls		
30/3	Integrate provision to release heat from silica gel:		Preventing rise in temperature of silica gel enhances dehumidification. Preventing temperature drop enhances humidification.
30/3	Product is able to function without need to regenerate silica gel		
31/3	Sound pressure leaving the product should not exceed certain level	$L_{p,1m} \leq ...$	
04/4	The volumetric flow rate should be at least x m^3/h per m^2 $room$	$Q = ...$ m^3/h per m^2 $room$	
04/4	A filter should be integrated in the product to prevent dust from silica gel being mixed in the room air	Filter certificate?	
	Wishes		

Table 7.1: List of Requirements for the design of a passive moisture buffering device

7.2 Discussion of research approach

This section reflects on the research approach followed in this research.

Experiment 1

In Experiment 1, the equilibrium isotherm is determined for the relative humidity range of 20 to 80 %RH. A small sample of 20 grams is used for determination.

Knowing in advance the importance of the difference in primary and secondary isotherm, a better approach would have been to subject the sample to a few cycles between 20 and 80 %RH. This will ensure the determined isotherm is *secondary*.

With the numerical model in mind, it would have been more convenient to determine the complete isotherm between 0 and 100 %RH. This is not easy to do in the climate cabinet: it can not very well realise the ~ 0 %RH and ~ 100 %RH limits. It is more convenient to do this in a DVS apparatus.

Experiment 2

In retrospect, it would have been more consistent to start all runs in Experiment 2 with the same sample history. Since the silica will function under continuous cycles in practice, a good choice would be to have all samples following secondary isotherm.

The way to do this was to bring the large samples to $> \ 60\% RH$ equilibrium and back to $< \ 40\% RH$, at least one cycle. Time was lacking to do this using the experimental setup from Experiment 2. It was tried to store the silica gel containers (open) in a $65\ \% RH$ climate chamber, but moisture exchange was too limited to realize saturation.

An addition to Experiment 2 could have been to vary the mass flow rate blown through the packed bed. A higher air velocity is expected to increase moisture transfer. Experimental results for varying mass flow rates could indicate to what extent the '*effective hygric capacity*', ξ, could be increased.

Numerical model

Numerical results match better to measurements with small particle diameters. The assumption to neglect intra-particle diffusion is heavier for large particle diameters, where intra-particle diffusion is more dominant.

Two additions to the model are expected to improve the numerical results. The first addition is to include intra-particle diffusion in the model. Moisture exchange is no longer determined by a single mass transfer coefficient. The particle is divided in a number of shells, between which moisture is transported by diffusion. An elaborate description of the model improvement is presented in Appendix I.

The second proposed addition is to account for hysteresis in the model. In the PGC model, a single isotherm is used to describe the sorption behaviour of the silica gel. More realistic would be to use an adsorption and desorption isotherm. The sorption behaviour under small RH changes

is expressed by scanning curves, modelled with Pedersen's model. The proposed implementation of Pedersen's model is presented in more detail in Appendix J.

8 | Conclusion

In this chapter the conclusion to the main Research Questions is built from the answers to individual sub-questions. First, the (intermediate) conclusions to Experiment 1 (3.6), 2 (4.6) and the numerical packed model study are concisely repeated:

Experiment 1 has yielded adsorption and desorption isotherms for fourteen silica gel samples. The offset between adsorption and desorption isotherm exposed the difference in primary and secondary isotherm. Samples with favourable sorption behaviour are selected to use in Experiment 2. Isotherm data is used as input for the numerical packed bed model.

Experiment 2 has shown the hygroscopic capacity of silica gel is such, that it can significantly contribute to (de)-humidification of indoor air in the range of 40 to 60 %RH. The experiment and analysis have shown the geometry of the packed bed can reduce the effectiveness of the silica gel. It is preferred to make the silica gel as best available as possible.

The numerical packed bed model was able to calculate temperature and humidity of air, blown through a packed bed with silica gel. The model is particularly sensitive to the inputted isotherm polynomial, $RH(w)$. Improvements to the model are presented in Appendices I and J.

8.1 Research question 1

Is a silica gel packed bed able to dampen fluctuations in air relative humidity and how can it be modelled?

1. How can the equilibrium isotherm for water vapour - silica gel be determined and integrated in the packed bed model?

Two methods are suitable to determine the equilibrium isotherm of silica gel: uptake rate measurements or gravimetric determination in a Dynamic Vapour Sorption device. In this work the isotherm is determined by uptake rate measurements in a climatic cabinet. Isotherms can be derived from literature as well. However, since sorption kinetics depend very much on the conditions during manufacturing, it may differ per sample. Experimental determination is preferred.

For integrating the equilibrium isotherm in numerical modelling, it is necessary to know the equilibrium isotherm over the full humidity range. The absolute moisture content should be expressed against relative humidity, rather than the relative mass gain. A DVS device is better able to bring the sample in 'dry' state, compared to a climatic cabinet.

2. How can the values for the coefficients describing water uptake in silica gel be determined, and applied in the model?

The exchange of heat and mass between air and silica is described by heat transfer coefficient h_c and mass transfer coefficient h_m. Identical expressions for these coefficient are presented by Pesaran [12] and Antonellis [8]. Standard values for h_c and h_m apply in case of a Solid Side Resistance model, where intra-particle diffusion in the silica gel is taken into account. For the case of a Pseudo-Gas Controlled model, the intra-particle diffusion is neglected, and the values for h_c and h_m are adapted. The adapted values are used in the PGC model developed in this thesis.

When diffusion is taken into account, diffusion of water into the silica gel particle is described by the diffusion coefficient. Two mechanisms of diffusion are relevant in silica gel: Knudsen diffusion of gaseous water in the micro-pore and surface diffusion of adsorbed water along the micro-pore surface. The two contribution can be combined into an effective diffusion coefficient D_{eff}, as shown in Equation 2.13. Correlations to determine the values for Knudsen, surface and effective diffusion are presented by Pesaran [12], and shown in Equations 2.19 up to 2.23. This requires material properties of the silica gel, like particle porosity, gas tortuosity factor, cylindrical pore radius and surface tortuosity.

Effective diffusivity can be determined from a step experiment in a DVS device. The measured increase in moisture content can be fitted to the analytical solution of Fick's diffusion equation.

3. How can water vapour diffusion resistance in the adsorbent particles be accounted for in the packed bed model?

Including diffusion of water in the silica gel requires an SSR model. For the numerical model this means the silica can not be presented by a single volume V_{solid}. Instead, the silica gel volume has to be discretized into n_s control volumes of the particles, or shells. A mass balance can be

drawn up for each shell with the in- and outgoing diffusive fluxes. Figures 5.1 and I.2 present the schematics of PGC and SSR models.

4. How accurate do experimental results match numerical results for a cyclic RH-step input to a silica gel packed bed?

As mentioned in Section 5.3, the most important discrepancy is a shift in time between numerical and experimental results. In conclusion two major improvements are proposed to apply to the model. This has not been achieved within the time scope of this thesis.

The numerical and experimental results are qualitatively compared. The model appears sensitive to the applied isotherm polynomial. Careful determination of the secondary (!) isotherm could significantly improve numerical results.

The uncertainty related to the sorption isotherm is two-fold. On the one hand, the determined isotherm polynomial, based on Experiment 1, is primary. On the other hand, the samples in Experiment 2 do not follow strictly primary or secondary isotherm, as 'primary' hysteresis is ongoing during Experiment 2.

5. What is the impact on relative humidity levels and energy demand in the room model?

This thesis work has not focused on the model study of a complete room. The exhibition room model developed by Zhang [27] uses a simplified packed bed model that does not conflict with the PGC model. It is fair to say the results of Experiment 2 support the assumptions in this model. Conclusions presented by Zhang seem valid:

- *humidity fluctuations can be reduced by a factor of 2*
- *energy demand for (de)-humdification can be reduced by a factor 0.9*

In conclusion to Research Question 1: silica gel is well able to reduce fluctuations in relative humidity. The longer the packed bed of silica gel, the smaller the influence of inlet air humidity changes at outlet. Mind, the silica gel has a dampening function: strictly there is no (de)-humidification. Water stored in the silica will be released when air is relatively dry at a later moment.

A long packed bed of silica gel may introduce delayed rises or falls in relative humidity. These delayed rises in relative humidity occur when the end part of the packed bed is in desorption mode, but the inlet humidity becomes high. The temperature changes associated with adsorption and desorption have significant influence on the outlet air relative humidity. If the temperature changes associated with adsorption and desorption could be limited, the moisture buffering performance of silica gel could be improved.

A PGC model is able to simulate the outlet air temperature and humidity of a packed bed. Results are expected to be more accurate for a SSR model including intra-particle diffusion.

8.2 Research question 2

What can a preliminary prototype for moisture buffering device in museum rooms look like, and what is the performance?

6. Which type of silica gel can best be used in the device?

Values for moisture uptake per step are tabulated in Figure 3.3. Experiment 1 has shown the equilibrium isotherm of macroporous silica gel, samples 7-8, has a small slope compared to micro- and mesoporous silica gel. It is therefor less suitable for humidity buffering applications. For microporous silica gel, samples 1 - 6 and 12 - 14, the moisture uptake is particularly high between 40 and 50 %RH. Moisture uptake between 50 and 60 %RH is comparable for micro- and mesoporous silica gel. The moisture uptake in mesoporous silica gel, sample 11, is increasing for higher relative humidity values.

Desorption from silica between 60 and 50 %RH is high for sample 9 (irregular macroporous gel) and 11 (mesoporous gel). Between 50 and 40 %RH the desorption rate is particularly high for sample 14 (ProSorb). To have ideal sorption ánd desorption behaviour over the full range of 40 to 60 %RH, a solution could be to mix different types of silica gel.

7. Which technical and aesthetical design guidelines apply for packed bed moisture buffering devices in museum rooms?

Experiment 2 has pointed out several guidelines to take into account when designing a device for passive humidity control. Most important is to prevent a long length of silica gel, as it reduces the effectiveness of silica gel. Better is to have the hygric mass of silica gel spread out and easily available for room air. The second important take-away is that heating and cooling is expected to have a beneficial effect, during humidification and dehumidification of air, respectively.

8. How can the performance of a moisture buffering device be specified?

The moisture buffering capacity of silica gel is usually expressed as the amount of water (in grams) can be taken up or released from 1 litre of silica gel per 1%RH change. This value is also referred to as ξ $[g/dm^3$ *or* $kg/m^3]$. Mind, this expression is based on equilibrium moisture content. It is not an instantaneous change, since intra-particle diffusion spreads out the moisture transfer over time. Furthermore, moisture transfer at silica gel particle surface heavily depends on superficial fluid velocity, Reynolds number and gradient in humidity ratios.

Recommendations on how to include the moisture exchange between silica gel and room air in a room air moisture balance are given in Section 9.1.

In conclusion to Research Question 2: a device for passive humidity control should make the hygric mass, silica gel, as best reachable as possible for room air. This will ensure the silica gel is used as effective as possible, or: the effective hygroscopic capacity, $\xi_{effective}$ is increased in this way. Another important boundary condition to the design is that the pressure drop over the silica gel should be reduced. A high pressure drop will require a larger ventilator,

which will lead to higher associated sound levels.

Further design efforts are needed to develop a prototype. The effective hygroscopic capacity $\xi_{effective}$ of the silica gel is suitable for calculating the moisture buffering by silica gel. The effective hygroscopic capacity does account for the time period of humidity fluctuations. The reduction factor to multiply with the theoretical capacity, $\xi_{theoretical}$, can be determined based on experimental results or by using the numerical PGC model.

9 | Recommendations & further research

The first part of this chapter presents recommendations on how to use the outcomes of this research. The second part addresses recommendations on the further development of the idea air humidity buffering with use of silica gel. Several aspects of the current work can be taken as a starting point for further research.

9.1 Recommended use of research outcomes

Application of silica gel in a room for passive humidity control is best assessed by drawing up a room air moisture balance, as presented in Section 2.2:

$$\frac{V}{R_v T_i}\frac{\partial p_{vi}}{\partial t} = (p_{ve} - p_{vi})\frac{nV}{3600 R_v T_i} + G_{vp} - G_{buf} \tag{9.1}$$

In this model the buffering capacity, or moisture exchange with silica gel can be expressed as:

$$G_{buf} = V_{gel} \cdot \xi_{effective}\frac{\partial}{\partial t}\left(\frac{p_{vb}}{p_{v,sat}(T_b)}\right) \qquad [kg/s] \tag{9.2}$$

In this expression, the maximum hygroscopic capacity, based on equilibrium isotherm, can be multiplied with reduction factor rf:

$$\xi_{effective} = rf \cdot \xi_{equilibrium} \qquad [kg/m^3] \tag{9.3}$$

This reduction factor accounts for the time period of the expected humidity fluctuations. The value depends on the two aspects described in Section 7.1:

- diffusion inside the silica bead;
- spatial arrangement of the silica gel;

Furthermore, the moisture exchange in practice depends on air velocity and the imposed humidity fluctuations.

In this project, the reduction factor (and $\xi_{effective}$) was determined based on the measured moisture exchange in Experiment 2 and the theoretical hygroscopic capacity. Mind, that this value is unique for the boundary conditions applicable to Experiment 2: given geometry of container, air velocity and imposed humidity fluctuations.

To have a indicative value for the $\xi_{effective}$, the numerical model can be used to simulate moisture exchange for different boundary conditions. It is possible that the governing equations of the numerical packed bed model need adjustments before using for other geometries of the silica gel container.

$$\xi_{effective} = rf \cdot \xi_{theoretical} = \frac{MBV_{t_p,\ EXP/NUM}}{MBV_{\infty,\ theoretical}} \cdot \xi_{theoretical} \tag{9.4}$$

9.2 Further research

Model study

First of all, follow-up research can focus on the improvement of the current model of the packed bed. Two main improvements to the model are discussed in detail in Appendices I and J. The first major improvement is to include intra-particle diffusion. The model is then referred to as a Solid-Side Resistance (SSR) model. The second major improvement is to include both an adsorption and a desorption isotherm in the model. In the current model, a single isotherm is used to express the moisture content for a given relative humidity value, for adsorption as well as desorption mode. By using both an adsorption and desorption isotherm, it's possible to describe scanning curves using Pedersen's model.

Other then improving the structure of the model, model results could potentially better compare to experimental results when material properties are carefully assessed. These properties can be determined experimentally:

- Complete adsorption and desorption isotherm from 0 to 100 %RH in a Dynamic Vapour Sorption (DVS) apparatus.
- Diffusion coefficient D_{eff}, by step method in a DVS apparatus
- Heat of sorption H_{ads}, by determining two isotherms at different temperature in a DVS apparatus.
- Experimentally determine scanning curves in a DVS apparatus.
  - This allows fitting γ_a and γ_d parameters for Pedersen's model.

Large scale testing & modelling

An other direction for further research is to test the application of silica gel in an actual museum room. Roughly, the approach could be to place a prototype in a museum room and record temperature and humidity values of the room air. This data can be compared to either an identical room (if possible), or historical data of the same room. It is likely more convenient to focus on product design before the step of large scale testing. This could result in a prototype suitable to place in a museum room.

Parallel to large scale testing it is interesting to model the impact of silica gel as hygric mass in a room. In a previous thesis work [27], the impact of humidity buffering by silica gel on room air humidity levels and energy demand of the room is assessed. This model includes room characteristics and HVAC configuration, but not moisture exchange with indoor finishes. The room air moisture balance model presented in 2.2 includes moisture exchange with indoor finishes, but does not describe HVAC configuration. Further research efforts could focus on combining these aspects in a model. A case study could be very suitable as a research approach.

Bibliography

[1] P.N. Peralta; A.P. Bangi. Modeling wood moisture sorption hysteresis based on similarity hypothesis. part 1. direct approach. *Wood and fiber science*, 30(1):48–55, 1998.

[2] R.S. Barlow. Analysis of the adsorption process and of desiccant cooling systems - a pseudo-steady state model for coupled heat and mass transfer. *Solar Energy Research Institute, Colorado - USA*, 1982.

[3] L. D. Christoffersen;. Zephyr: Passive climate controlled repositories: Storage facilities for museum, archive and library purposes. 1996.

[4] H.L. Frandsen; S. Svensson; L. Damkilde. A hysteresis model suitable for numerical simulation of moisture content in wood. 2007.

[5] J. Carmeliet; M. de Wit; H. Janssen. Hysteresis and moisture buffering of wood. In *Symposium of building physics in the nordic countries*, pages 55–62. Citeseer, 2005.

[6] M.S. Owen (Ed). *ASHRAE Handb. HVAC Appl. SI Edition*, chapter ASHRAE, Museums, libraries and archives, pages 23.1–23.23. ASHRAE, Atlanta, 2011.

[7] G. Pahl; W. Beitz; J. Feldhusen; K.H. Grote. *Engineering Design*, chapter 5, 6. Springer, 2007.

[8] S. De Antonellis; L. Colombo; A. Freni; C. Joppolo. Feasibility study of a desiccant packed bed system for air humidification. *Energy*, 214, 2021.

[9] A. Ramzy; R. Kadoli. Experimental procedure to develop the isotherm equation for moisture adsorption of silica gel particles. *Journal of Multidisciplinary Engineering Science and Technology (JMEST)*, 2, 2015.

[10] A. Ramzy; T.P.A. Babu; R. Kadoli. Semi-analytical method for heat and moisture transfer in packed bed of silica gel. *International Journal of Heat and Mass Transfer*, 54(4):983–993, 2011.

[11] H.L. Schellen; B. Ankersmit; E. Neuhaus; M.H.J. Martens. Een bouwfysisch verantwoord binnenklimaat in monumenten met een museale functie. *Bouwfysica*, 4:2–11, 2009.

[12] A.A. Pesaran; A.F. Mills. Moisture transport in silica gel packed beds - i. theoretical study. *Int. J. Heat Mass Transfer*, 30, 1987.

[13] A.F. Mills. *Basic heat and mass transfer*. Pearson College Division, 1999.

[14] Y. Mualem. A conceptual model of hysteresis. *Water resources research*, 10(3):514–520, 1974.

[15] T. Padfield. The role of absorbent building materials in moderating changes of relative humidity. *Department of Structural Engineering and Materials, Lyngby, Technical University of Denmark*, 150, 1998.

[16] C.R. Pedersen. Combined heat and moisture transfer in building constructions. *Thermal Insulation Laboratory, Technical University of Denmark*, 214, 1990.

[17] K.S. Rao. Hysteresis in sorption. iii. permanence and scanning of the hysteresis loop. silica gel–water system. *The Journal of Physical Chemistry*, 45(3):513–517, 1941.

[18] H. Janssen; S. Roels. Qualitative and quantitative assessment of interior moisture buffering by enclosures. *Energy and Buildings*, 41(4):382–394, 2009.

[19] D.M. Ruthven. *Principles of Adsorption and Adsorption Processes*, chapter 5.3, 7. John Wiley & Sons, 1984.

[20] J.G. Salin. Inclusion of the sorption hysteresis phenomenon in future drying models: Some basic considerations. *Maderas. Ciencia y tecnología*, 13(2):173–182, 2011.

[21] G. Thomson. *The Museum Environment*, chapter 2. Butterworth-Heinemann Ltd., 1986.

[22] C. Tien. *Adsorption Calculations and Modelling*, chapter 5.3. Butterworth-Heinemann Ltd., 1994.

[23] R.P. Kramer; A.W.M. van Schijndel; H.L. Schellen. Energy impact of ASHRAE's museum climate classes: a simulation study on four museums with different quality of envelopes. *Energy Procedia*, 78, 2015.

[24] R.P. Kramer; A.W.M. van Schijndel; H.L. Schellen. Dynamic setpoint control for museum indoor climate conditioning integrating collection and comfort requirements: Development and energy impact for europe. *Building and Environment*, 118, 2017.

[25] S. Weintraub. Demystifying silica gel. *AIC Objects Specialty Group Postprints*, 9, 2002.

[26] P. Rajniak; R.T. Yang;. A simple model and experiments for adsorption-desorption hysteresis: Water vapor on silica gel. *AIChE journal*, 39(5):774–786, 1993.

[27] L. Zhang. Evaluation of high capacity hygroscopic materials on air conditions and energy performance in renovated historic buildings. *MSc thesis*, 2020.

A | Matlab script used in Experiment 1

The following Matlab script is used in the processing of raw data acquired in Experiment 1. Equivalent code is used for other steps than 20 to 30 %RH. The script reads raw data from Excel file *EXP 1A - SORPTION.xlsx*.

Listing A.1: *results2030.m*

```
clear all;
close all;
clc

mass = zeros(7,14);
t = xlsread('EXP 1A - SORPTION.xlsx','handled','E7:K7');
mass(:,1) = xlsread('EXP 1A - SORPTION.xlsx','handled','E12:K12');
mass(:,2) = xlsread('EXP 1A - SORPTION.xlsx','handled','E14:K14');
mass(:,3) = xlsread('EXP 1A - SORPTION.xlsx','handled','E16:K16');
mass(:,4) = xlsread('EXP 1A - SORPTION.xlsx','handled','E18:K18');
mass(:,5) = xlsread('EXP 1A - SORPTION.xlsx','handled','E20:K20');
mass(:,6) = xlsread('EXP 1A - SORPTION.xlsx','handled','E22:K22');
mass(:,7) = xlsread('EXP 1A - SORPTION.xlsx','handled','E24:K24');
mass(:,8) = xlsread('EXP 1A - SORPTION.xlsx','handled','E26:K26');
mass(:,9) = xlsread('EXP 1A - SORPTION.xlsx','handled','E28:K28');
mass(:,10) = xlsread('EXP 1A - SORPTION.xlsx','handled','E30:K30');
mass(:,11) = xlsread('EXP 1A - SORPTION.xlsx','handled','E32:K32');
mass(:,12) = xlsread('EXP 1A - SORPTION.xlsx','handled','E34:K34');
mass(:,13) = xlsread('EXP 1A - SORPTION.xlsx','handled','E36:K36');
mass(:,14) = xlsread('EXP 1A - SORPTION.xlsx','handled','E38:K38');

%%
p0 = zeros(14,3);
for i=1:14                  %OR set only one sample (1-14);
p0(i,:)=[1 1 mass(1,i)];
g = fittype( @(a,b,c,x) a*(1-exp(-b*x))+c);
[f{i,1} gof{i,1}]=fit(t',mass(:,i),g,'StartPoint',p0(i,:));

fv(i)=f{i,1}.a+f{i,1}.c;
c(i)=f{i,1}.c;
b(i)=f{i,1}.b;
a(i)=f{i,1}.a;

```

```
figure;
plot(f{i},t,mass(:,i));
grid on;
title( ['Mass sample ' num2str(i) ' , 20 to 30 %RH'] )
xlabel('Time [h]');
ylabel('Sample mass [g]');
legend('Experimental data','Fitted curve','Location','northwest');
end

%% Goodness of fit results
GoF = {'SSE';'R-Square';'dfe';'Adjusted R-Square';'RMSE';'c';'a';'End value';'b';};
Var = {'Sample 1';'Sample 2';'Sample 3';'Sample 4';'Sample 5';'Sample 6';'Sample ...
    7';'Sample 8';'Sample 9';'Sample 10';'Sample 11';'Sample 12';'Sample 13';'Sample 14';};
values=zeros(14,9);

for i=1:14
values(i,:) = [gof{i,1}.sse gof{i,1}.rsquare gof{i,1}.dfe gof{i,1}.adjrsquare ...
    gof{i,1}.rmse c(i) a(i) fv(i) b(i)];
T(i,:) = table(values(i,:));
end
figure;
uitable('Data',T{:,:},'Units', 'Normalized', 'Position',[0, 0, 1, 1]);

%% Write end values to Excel
filename = 'Results Experiment 1A.xlsx';
xlswrite(filename,fv','final values','D3:D16');

%write table GoF results to separate Excel-file;
writetable(T,'Goodness of Fit.xlsx','WriteVariableNames',0,'Sheet',1,'Range','B2:P15')
```

B | Matlab script used for plotting isotherms

The following Matlab script is used for plotting isotherms with the data acquired in Experiment 1. The script reads end values from Excel file *Results Experiment 1A.xlsx*.

Listing B.1: *isotherms.m*

```
clear all;
close all;

humid1 = xlsread('Results Experiment 1A','final values','C2:I2'); %sorption
humid2 = xlsread('Results Experiment 1A','final values','M2:S2'); %desorption
%absolute sorption in [g]
% sorp_abs = xlsread('Results Experiment 1A','final values','C4:I17');
% desorp_abs = xlsread('Results Experiement 1A',''final values','M4:S17'

%percentual sorption in [%]
sorp_perc = xlsread('Results Experiment 1A','final values','C19:I32')/10;
desorp_perc = xlsread('Results Experiment 1A','final values','M19:S32')/10;

%%
for i=1:14
    figure;
    plot(humid1,sorp_perc(i,:));
    hold on;
    plot(humid2,desorp_perc(i,:));
    title( ['Equilibrium isotherm sample ' num2str(i) ''] )
    grid on;
    axis([10 90 -5 60])
    legend('sorption','desorption','Location','northwest');
    xlabel('Target relative humidity [%]');
    ylabel('Relative mass gain wt-%');
end
```

C | System characteristics of packed bed

The following Matlab script is used for theoretical analysis of the pressure drop over a packed bed.

Listing C.1: System characteristics of packed bed

```
clear all;
close all;

%% parameters
D = [0.125 0.160 0.250];    %column diameter (m)
%D = 0.160;
L = 0.40;                   %column length (m)
A = pi.*(D/2).^2;           %cross sestion area (m2)

%Q = 0.0016;
Q = logspace(-4,-2,50);     %volumetric flow range (m3/s)
U = zeros(length(Q),length(D));

for n=1:length(D)
U(:,n) = Q'./A(n);          %superficial air velocity (m/s)
end

Rp = 0.001;                 %particle radius (m)
eps = 0.35;                 %bed voidage (-)

rho_f = 1.1987;             %fluid density (kg/m3)
mu_f = 18.17e-6;            %fluid dynamic viscosity (Pa.s)

rho_s = 700;                %density silica gel (kg/m3);
%% Calculations pressure drop.
for k=1:length(D)           %for all diameters...
for i=1:length(Q)           %for range (n=50) of flow rates...
    Re_p(i,k) = (2*Rp.*(U(i,k))*(rho_f))/((mu_f)*(1-eps));
    f(i,k) = 150/Re_p(i,k) + 1.75;
    dP(i,k) = L*f(i,k)*(rho_f * U(i,k)^2 * (1-eps))/(2*Rp*eps^3); %N/m2;
end
end

Qh = Q*3600;                %volumetric flow range (m3/h)
```

```
35 plot(Qh,dP);
36 title('System curve packed bed, Rp = 0.002 m');
37 legend('d=125mm','d=160mm','d=250mm','Location','northwest');
38 xlabel('Volumetric flow Q (m3/h)');
39 ylabel('Pressure drop over column (Pa)');
40
41 %% Calculations flow discharge.
42 F_ls = zeros(5,3);
43 Vel = zeros(5,3);
44 m = zeros(1,3);
45 T = [1 3 5 7 10];                        %residence time air in column (s)
46 for j=1:length(D)
47     V(j) = (D(j)*10/2)^2*pi*(L*10);                %volume column (dm3)
48     F_ls(:,j) = V(j)./T;                           %volume flow (dm3/s)
49     Vel(:,j) = (F_ls(:,j)/1000)./((D(j)/2)^2*pi);  %air velocity;
50     m(1,j) = V(j)*rho_s/1000;                      %mass silica
51 end
52 F_ch = F_ls*3.6;                                  %volume flow (m3/h)
```

D | Calibration procedure

This section described the detailed procedure of the calibration of Telaire T9602 temperature and relative humidity sensors.

Telaire T9602 sensor measures relative humidity in the range 0 to 100 %RH, and sends a 14-bit value. The theoretical conversion formula is thus:

$$\frac{RH\ sensor\ value}{2^{14}} * RH_{scale} + RH_{offset} = \frac{RH\ sensor\ value}{16.384} * 100.00 + 0.00 \tag{D.1}$$

The temperature is measured between -40 and + 125 ^oC, and expressed in 14 bits as well. Following theoretical conversion formula applies:

$$\frac{RH\ sensor\ value}{2^{14}} * T_{scale} + T_{offset} = \frac{RH\ sensor\ value}{16.384} * 165.00 - 40.00 \tag{D.2}$$

Next, the sensor output without conversion is measured ($Scale = 1.00$ and ($Offset = 0.00$). This will give a number between 0 and 1. Results are shown in Figure D.1.

	Rotronic display RH		
	30.1	***40.9***	***59.5***
Telaire 1	0.30176	0.40479	0.58105
Telaire 2	0.30542	0.40625	0.58081
Telaire 3	0.30737	0.40942	0.58447
Telaire 4	0.29443	0.39819	0.57959
Telaire 5	0.29687	0.40332	0.57104

(a)

	Rotronic display T		
	16.9	***22.4***	***24.7***
Telaire 1	0.34656	0.37964	0.39392
Telaire 2	0.34607	0.37946	0.39368
Telaire 3	0.34576	0.37826	0.39221
Telaire 4	0.34704	0.37943	0.39331
Telaire 5	0.34701	0.37915	0.39294

(b)

Figure D.1: Measured unconverted sensor output for (a) relative humidity and (b) temperature, at three distinct points.

The display value of RH and T are plotted against the measured sensor output. A linear fitting curve is fitted to this plot. Figures D.2 and D.3 present the fitted curve and the resulting conversion formula.

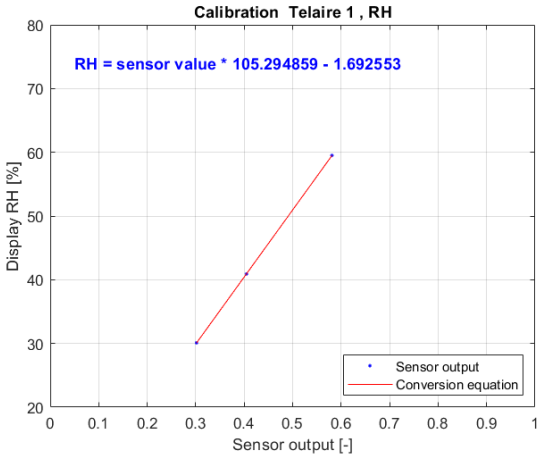

(a)

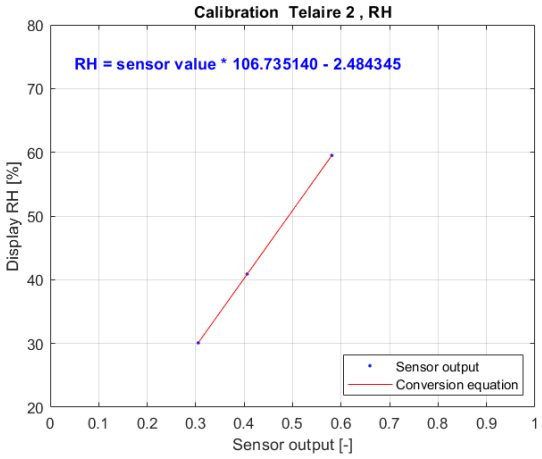

(b)

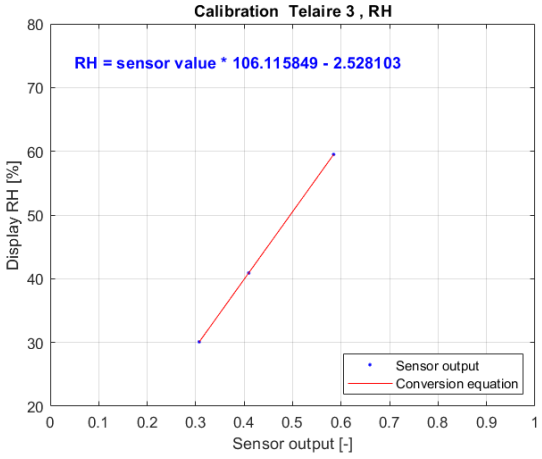

(c)

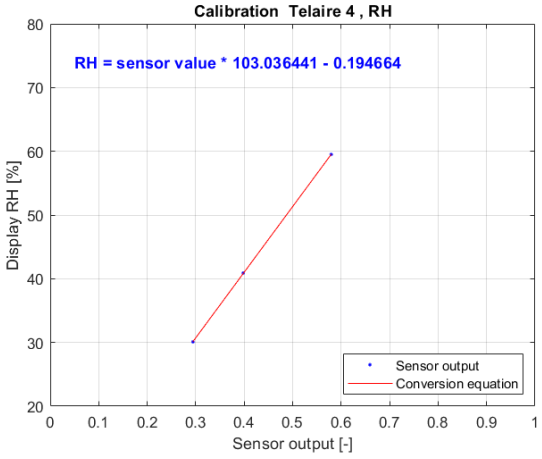

(d)

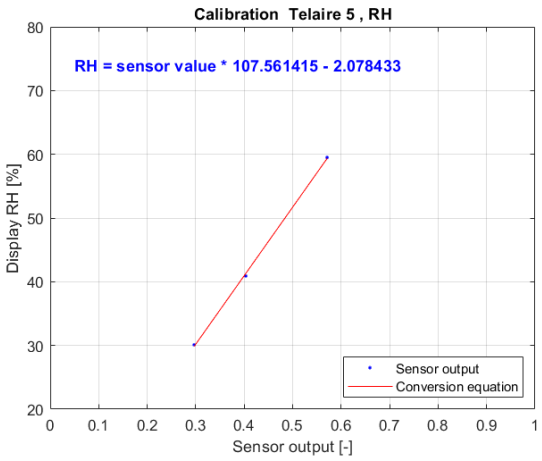

(e)

Figure D.2: Relative humidity calibration of Telaire 1 to 5.

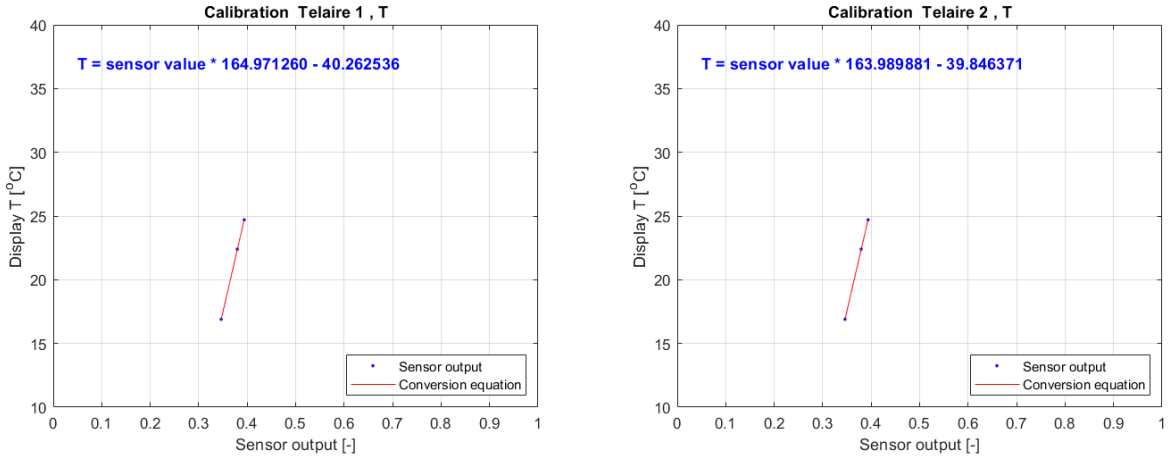

(a)

(b)

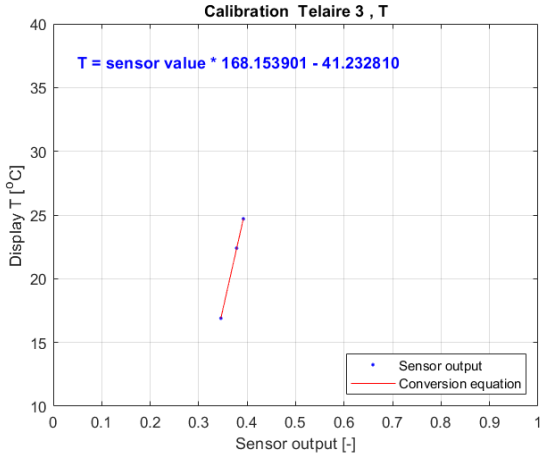

(c)

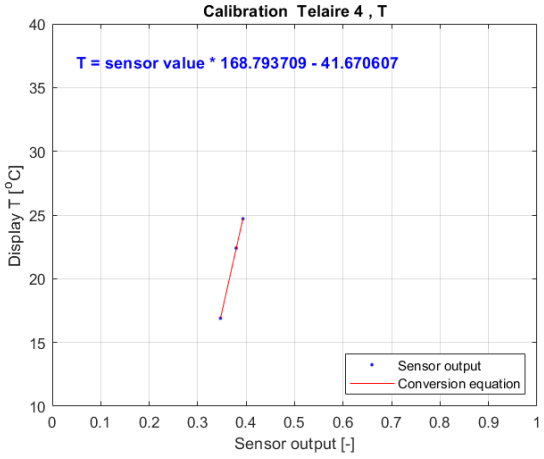

(d)

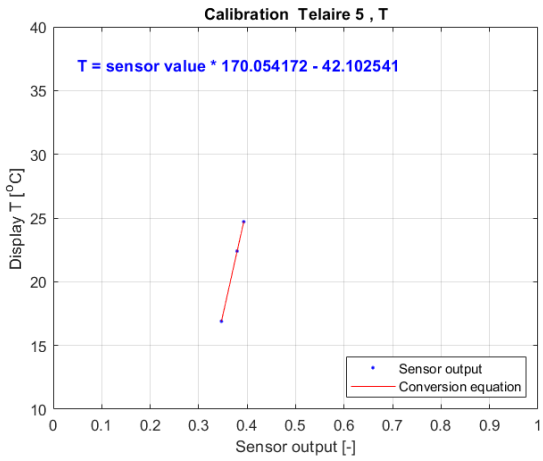

(e)

Figure D.3: Temperature calibration of Telaire 1 to 5.

The presented conversion formulae are applied to the microcontroller. At two new arbitrary points, the converted sensor output is read as presented in Fig. D.4. It can be concluded the sensor calibration is acceptable.

	Point 1 [%RH, C]		Point 2 [%RH, C]	
Display	*51.5*	*19.5*	*38.3*	*20.8*
Telaire 1	51.54	19.49	38.41	20.78
Telaire 2	51.46	19.52	38.46	20.78
Telaire 3	51.44	19.51	38.43	20.78
Telaire 4	51.40	19.55	38.50	20.77
Telaire 5	51.41	19.52	38.26	20.79

Figure D.4: Sensor readings at arbitrary points

Figure D.5: T/RH sensors hanged together in climatic cabinet for calibration

E | Matlab script for data acquisition

The following Matlab script is used for data acquisition in Experiment 2. The script reads all data received from the microcontroller. It adds the elapsed time in the experiment, and the current system time. This information combined is written line by line to a *.txt* file defined by *file_name*.

Listing E.1: Matlab script to log sensor data

```
clear all;
close all;

delete(instrfind); %close possible open COM-ports;
%%
file_name = 'sample12_5060_step_1.txt';
sObject = serial('COM3','BaudRate', 38400,'Terminator','LF');   % create serial object;
fopen(sObject);                              % open serial port;
tic;
fid = fopen(file_name,'wt');                 % Insert name of file!
while(1)
    data = fscanf(sObject);                  % received sensor data;
    abstime = datestr(datetime('now'));      % print current system time;
    reltime = ["," + num2str(toc)];          % print elapsed time since tic;
    acq = strcat(data,abstime,reltime);
    C = fprintf(fid,'%s\n', acq);
    pause(2);
end
fclose(fid);
fclose(sObject);
```

F | Matlab script for Experiment 2

The following Matlab script reads data acquired in Experiment 2 from the defined *.txt* file. It stores data in a matrix D, available for processing.

Listing F.1: Matlab script to process sensor data

```
%% Read data from txt.file
clear file_name;
fid = fopen('16mar_sample6_5060_longcycle3.txt','rt'); % Insert name of file!
C = textscan(fid,'%f%f%f%f%f%f%f%f%f%f%f%f%f%f%s%f','Delimiter',',');
fclose(fid);

%% Store data
D = cell2mat(C(1:14));
relT = C{1,16,1};
absT = C{1,15,1};

% Remove potential outliers!
% D(709,:)=[];
% relT(709)=[];
% D(12820,:)=[];
% relT(12820)=[];

RH = zeros(14486,5);
RH = [D(:,1) D(:,3) D(:,5) D(:,7) D(:,9)];
TEMP = [D(:,2) D(:,4) D(:,6) D(:,8) D(:,10)];

%% Calculate absolute humidity;
n=length(D(:,1));
xsat = zeros(n,5);
xs = zeros(n,5);
for j = 1:5
for i = 1:length(D(:,1))
    xsat(i,j) = 0.622*10^-5*611*exp(17.08*TEMP(i,j)/(234.18+TEMP(i,j)));
end
xs(:,j) = xsat(:,j).*RH(:,j)/100;
end

%% Plot RH and T;
figure;
plot(relT,xs(:,1)); title('Calculated X [kg/kg d.a.]');
hold on;
grid on; grid minor;
```

```
plot(relT,xs(:,2)); plot(relT,xs(:,3));
plot(relT,xs(:,4)); %plot(relT,xs(:,5));
xlim([0 35000]); ylim([0.005 0.011]);
xlabel('Time [sec]'); ylabel('Abs. humidity [kg/kg d.a.]');
legend('X_{IN}','X_{13cm}','X_{25cm}','X_{OUT}','Location','northeast');

figure;
plot(relT,RH(:,1)); title('Sensor output RH [%]');
hold on;
grid on; grid minor;
plot(relT,RH(:,2)); plot(relT,RH(:,3));
plot(relT,RH(:,4)); %plot(relT,RH(:,5));
xlim([0 35000]); ylim([33 68]);
xlabel('Time [sec]'); ylabel('Rel. humidity [%]');
legend('RH_{IN}','RH_{13cm}','RH_{25cm}','RH_{OUT}','Location','northeast');

figure;
plot(relT,TEMP(:,1)); title('Sensor output T [^oC]');
hold on;
grid on; grid minor;
plot(relT,TEMP(:,2)); plot(relT,TEMP(:,3));
plot(relT,TEMP(:,4)); %plot(relT,TEMP(:,5));
xlim([0 35000]); ylim([18 24]);
xlabel('Time [sec]'); ylabel('Temperature [^oC]');
legend('T_{IN}','T_{13cm}','T_{25cm}','T_{OUT}','Location','northeast');

figure;
plot(relT,D(:,11));
grid on; grid minor;
xlim([0 35000]); ylim([0 120]);
title('Flow in SLM');
xlabel('Time [sec]'); ylabel('Air flow [dm^3/min]');
legend('Air flow','Location','northeast');
```

G | Matlab script for PGC model

The following Matlab script is used to define time-invariant variables in the PGC model.

Listing G.1: *PGCmodel_m.m*

```
clear all;
close all;
clc

D = 0.120;                  % diameter column [m]
L = 0.500;                  % length column [m]
A_bed = pi*(D/2)^2;         % cross section column [m2]
eps = 0.36;                 % porosity of packed bed [-]

n = 10;                     % Control Volumes in column [-]

Q = 1.667e-3;               % volumetric flow through column [m3/s]

% material properties;
rho_air = 1.1987;             % density air [kg/m3]
rho_gel = 700;              % mass density of dry silica gel (kg/m3)
mu_air = 18.17e-6;            % dynamic viscosity air;
c_air = 1000;               % specific heat of dry air;
c_vap = 1860;               % specific heat capacity of water vapour (J/kg.K)
c_gel = 1000;               % specific heat capacity of dry silica gel (J/kg.K)
c_liq = 4184;               % specific heat of liquid water ();
H_ads = 2.50e6;             % latent heat of vaporization of water (J/kg)

V_cv = A_bed*(L/n);         % volume of 1 C.V. [m3]
V_gel = (1-eps)*V_cv;     % volume of adsorbent in C.V. [m3]
V_air = eps*V_cv;         % volume of air in C.V. [m3]

Rp = 0.002;                 % particle radius (m)
U = Q/A_bed;                % superficial air velocity m/s;
Re = 2*Rp*U*rho_air/(mu_air*(1-eps));               % Reynolds number [-]

hm = 0.704*U*rho_air*Re^-0.51;    % mass transfer coefficient;
%hc = 0.683*c_air*U*rho_a*Re^-0.51;

Ap = 4*pi*Rp^2;             % surface area 1 particle;
Vp = 4/3*pi*Rp^3;           % volume of 1 particle;
np = V_gel/Vp;            % number of particles in 1 C.V.;
p = np*Ap;                  % Wetted Perimeter in 1 C.V.

```

```
%% initial conditions and inputs
% input flow:
T_in1 = 22;                 % high temperature in cycle [C]
T_in2 = 21;                 % low temperature in cycle [C]
x_in1 = 0.0077;             % high humidity in cycle [kg/kg]
x_in2 = 0.0030;             % low humidity in cycle [kg/kg]

T0e = 21;                   % initial air temperature in column [C]
x0e = 0.0030;               % initial air humidity in column [kg/kg]

% RH is calculated from initial T and abs. humidity m0e, acc. to psychrometric
% relations. Assumed: silica temperature equals air temperature in column.
T0s = T0e;                  % initial temperature silica gel [C]
pd = (101.33*x0e)/(0.622+x0e);      % partial vapour pressure [kPa];
pds = 0.813*exp(T0e/17.6) - 0.2;    % saturated vapour pressure [kPa];
RH_start = pd/pds;          % initial RH, appearing in the column;

% initial RH, corresponds to water content w [kg/kg] and C [kg/dm3].
% Equilibrium between air humidity and water content is assumed at start!;
w = [204.226 -124.478 24.16554 -0.05759 0.0078-RH_start];       % isotherm polynomial;
wroots = roots(w);
wroots1 = wroots(imag(wroots)==0);       % Save only the real roots
w_init = wroots1(1);
C0 = w_init * rho_gel;      % initial water content column [kg/m3]

%% help matrix advective flow:
S_help=zeros(n,n+1);
for k=1:n
    S_help(k,k)= 1;
    S_help(k,k+1)= -1;
end
```

H | Simulink script for PGC model

The complete overview of the Simulink part of the PGC model is shown in Figure H.1. It consists of the following parts:

- Humidity and temperature input (*yellow*)
- Mass balances for air and silica (*red*)
- Heat balances for air and silica (*magenta*)
- Heat - mass transfer coupling coefficients (*green*)
- Output graphs for absolute humidity, relative humidity and temperature (*blue*)

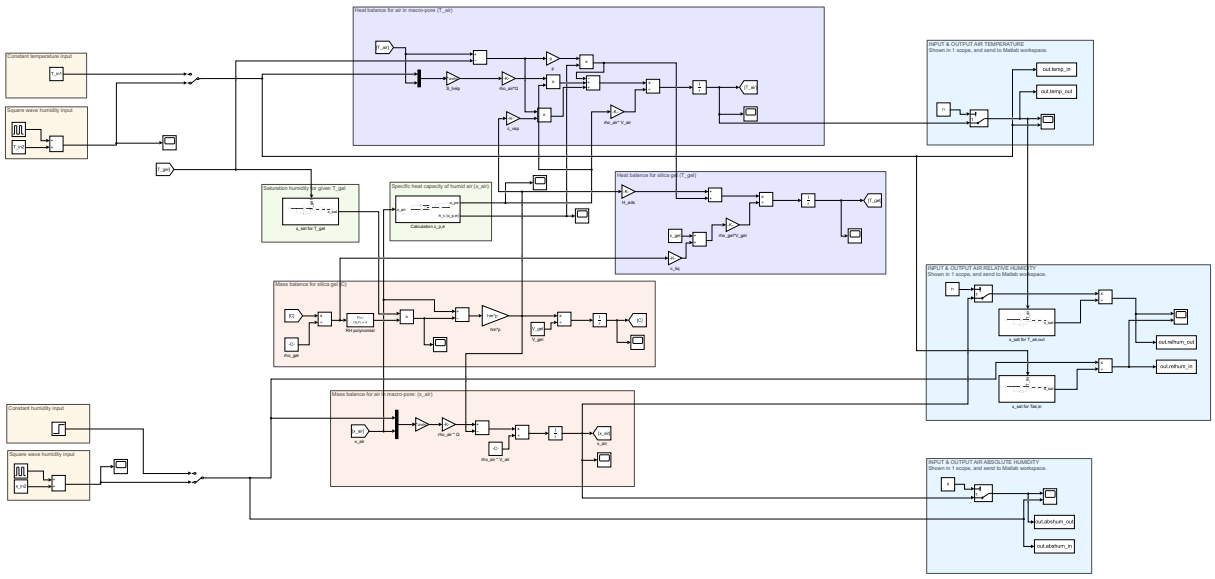

Figure H.1: Overview of Simulink part of PGC model.

Hereafter, the parts are shown in more detail.

Humidity and temperature input

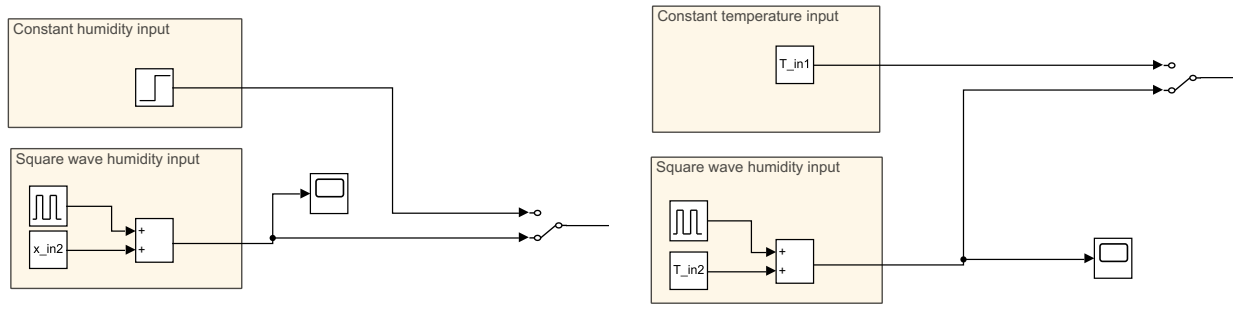

Figure H.2: Model input: (a) inlet air humidity and (b) inlet air temperature.

Mass balance for silica gel and air

The following figure shows the graphical presentation of the mass balance for silica gel, as given by:

$$V_{gel}\frac{\partial C}{\partial t} = h_m\ p(x_{air} - x_{gel}) \tag{H.1}$$

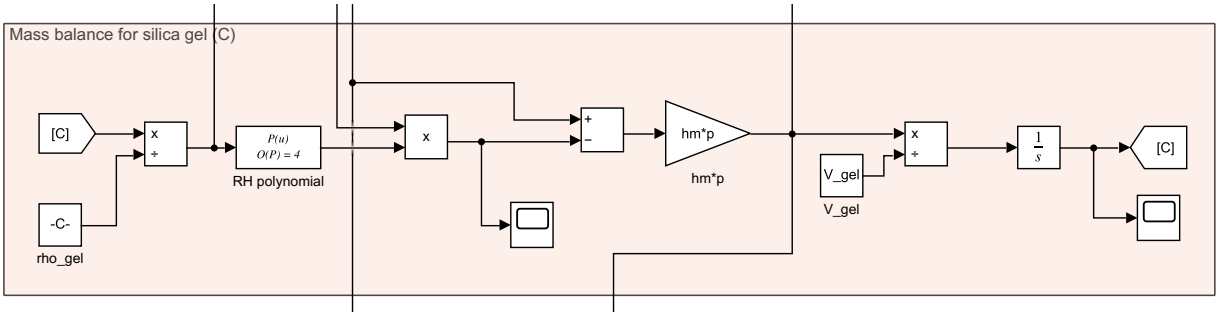

Figure H.3: Mass balance for silica gel.

The following figure shows the graphical presentation of the mass balance for air in the macro-pores of the packed bed, as given by:

$$V_{air}\frac{\partial x_{air}}{\partial t} = -h_m\ p(x_{air} - x_{gel}) + \rho_{air}Q(x_{v,in} - x_{air}) \tag{H.2}$$

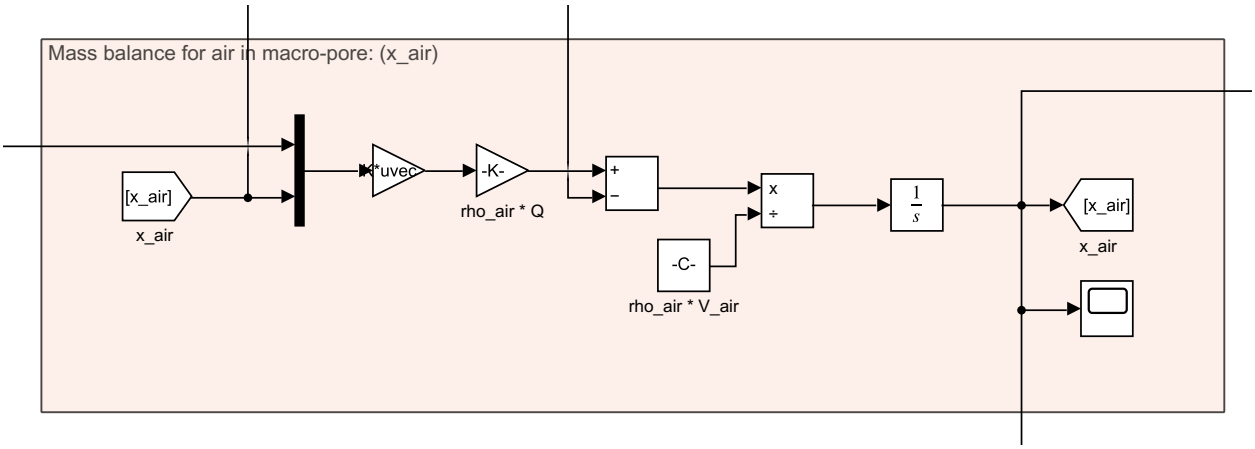

Figure H.4: Mass balance for air in packed bed.

Heat balances for air and silica gel

The following figure shows the graphical presentation of the heat balance for silica gel, as given by:

$$\rho_{gel}(c_{gel} + w * c_{gel})V_{gel}\frac{\partial T_{gel}}{\partial t} = h_c\ p(T_{air} - T_{gel}) + H_{ads}h_m\ p(x_{air} - x_{gel}) \tag{H.3}$$

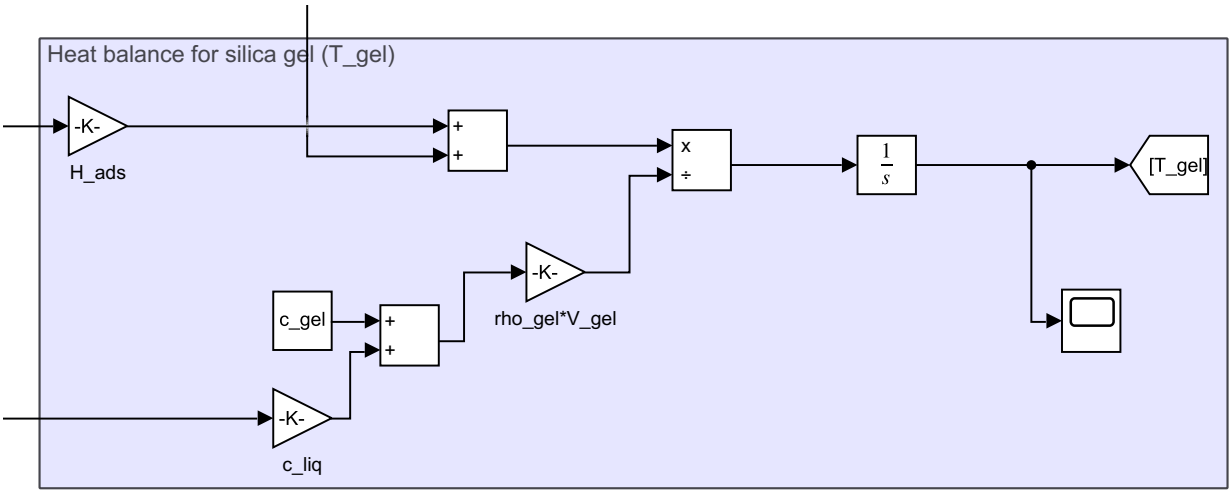

Figure H.5: Heat balance for silica gel.

The following figure shows the graphical presentation of the heat balance for air in the macro-pores of the packed bed, as given by:

$$\rho_{air}c_{p,e}V_{air}\frac{\partial T_{air}}{\partial t} = +\rho_{air}Qc_{air}(T_{in} - T_{air}) - h_c\ p(T_{air} - T_{gel}) + c_{vap}h_m\ p(x_{air} - x_{gel})(T_{air} - T_{gel}) \tag{H.4}$$

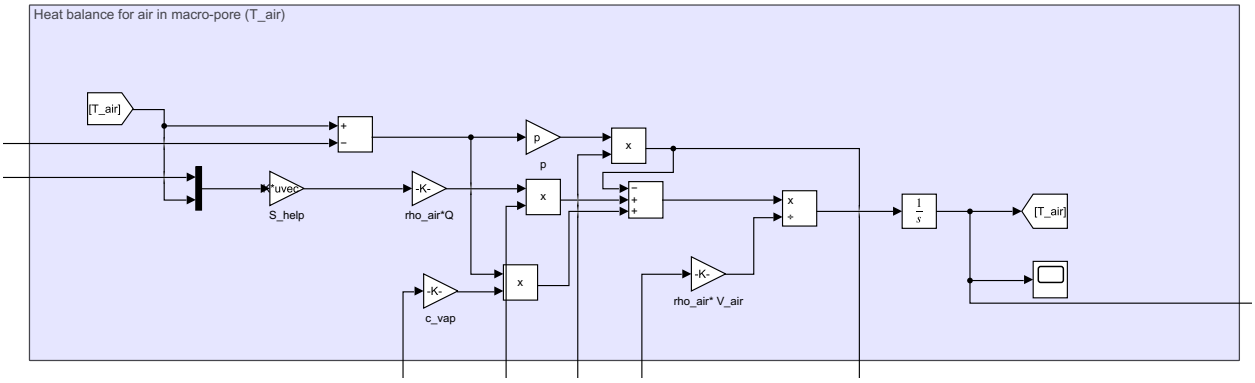

Figure H.6: Heat balance for air in packed bed.

Heat and mass transfer coupling coefficients

Heat and mass transfer are coupled by two coefficients. x_{sat} is determined using silica gel surface temperature T_s, according to following equations, and displayed in Figure H.7(a).

$$P_{sat}(T_{gel}) = 611 * exp\left\{\frac{17.08\ T_{gel}}{234.18 + T_{gel}}\right\} \qquad [Pa] \tag{H.5}$$

$$x_{sat}(T_{gel}) = 0.622 * 10^5 * P_{sat}(T_{gel}) \qquad [kg/kg\ d.a.] \tag{H.6}$$

The second coupling coefficient is the specific heat of humid air, $c_{p,e}$, which depends on the humidity $x_{1,e}$, expressed in following equation, and displayed in Figure H.7(b).

$$c_{p,e} = 1884 * x_{air} + 1004 * (1 - x_{air}) \qquad [kJ\ kg^{-1}\ K^{-1}] \tag{H.7}$$

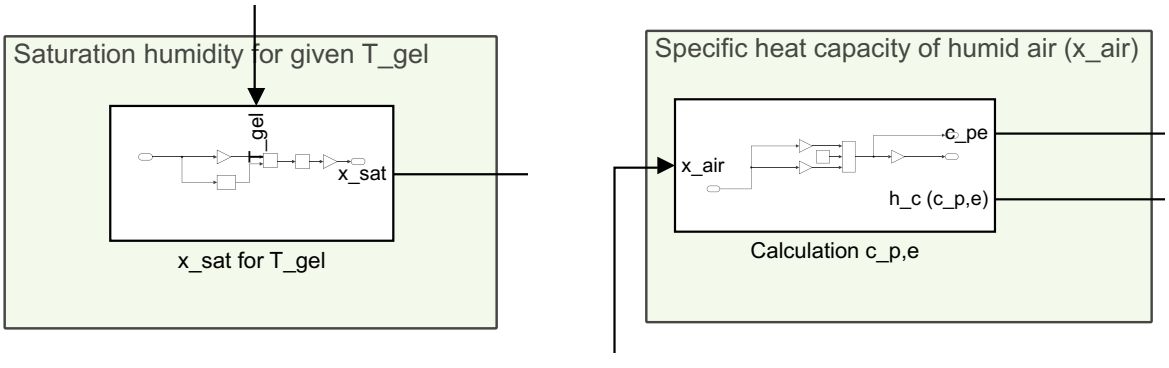

(a) (b)

Figure H.7: Calculation of coupling coefficients (a) saturation humidity x_{sat} and (b) specific heat of humid air.

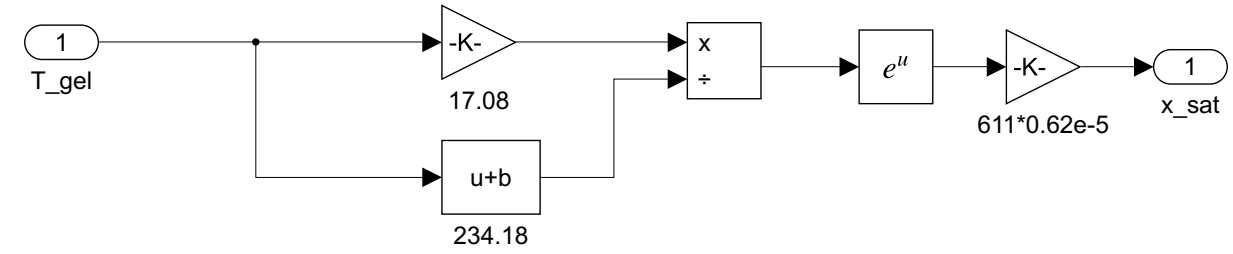

(a)

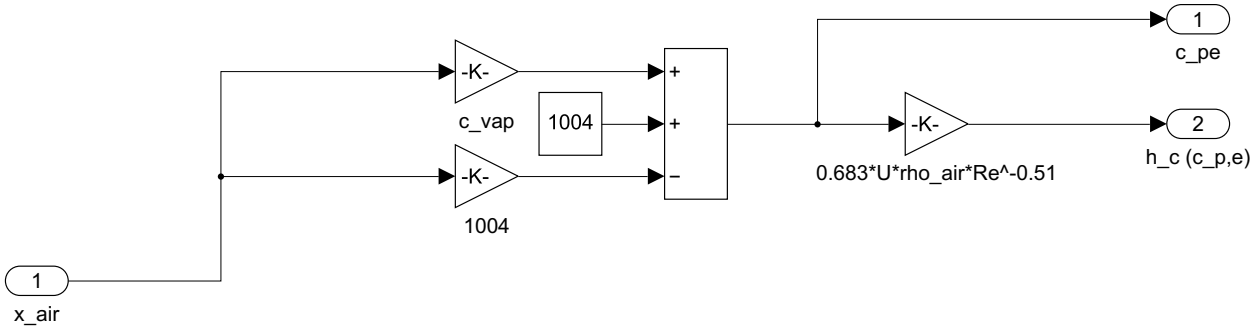

(b)

Figure H.8: Content of sub-system for calculation of (a) saturation humidity, x_{sat}, and (b) specific heat of humid air, $c_{p,e}$.

Output graphs for absolute humidity, relative humidity and temperature

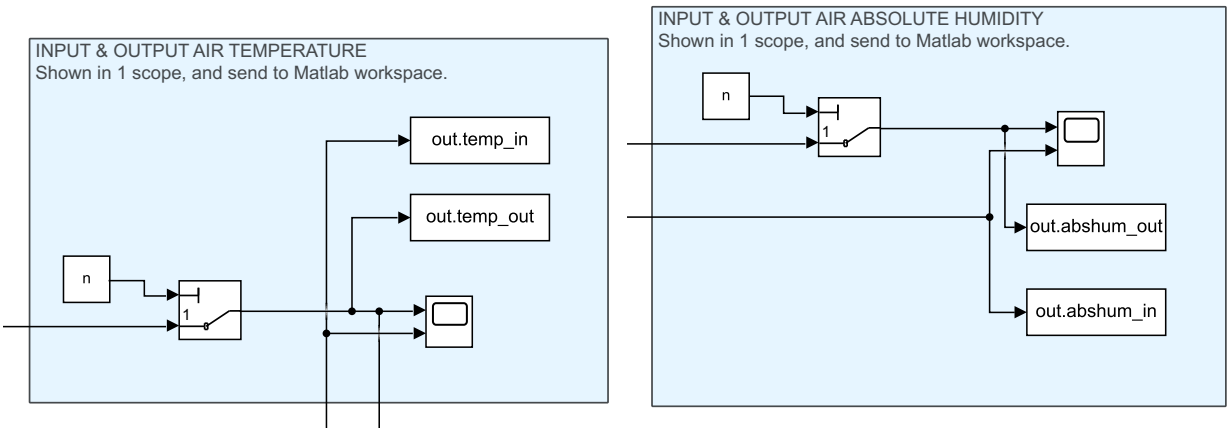

Figure H.9: Graph displaying inlet and outlet conditions for: (a) air temperature, and (b) air absolute humidity.

For inlet and outlet air, the saturation humidity is determined using air temperature T_e. The relative humidity is determined using the following equation:

$$RH = \frac{x_{v,e}}{x_{v,sat}} \tag{H.8}$$

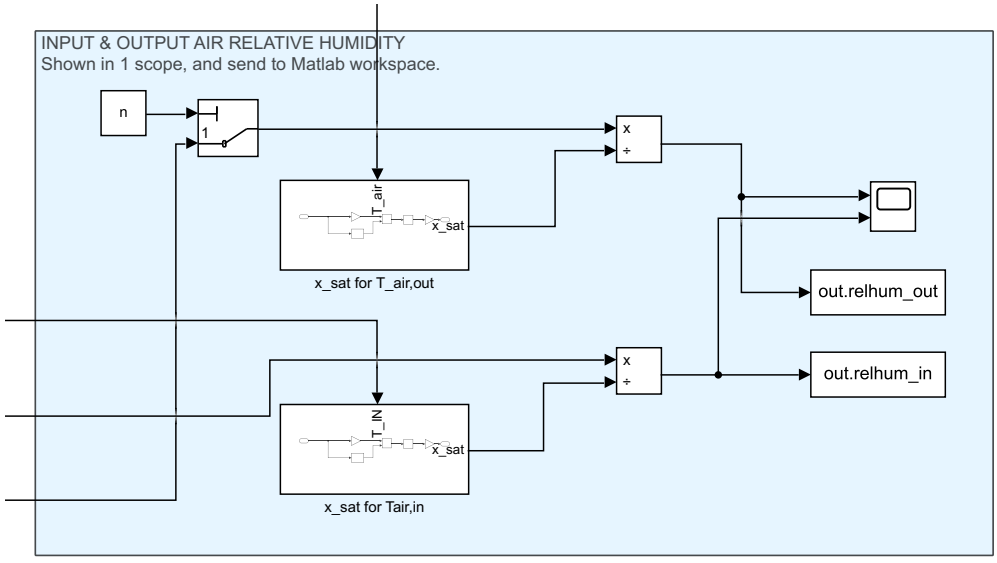

Figure H.10: Graph displaying inlet and outlet conditions for air relative humidity.

I | Model addition 1: Solid- side resistance model (SSR)

Intra-particle diffusion can be added to the model. The model is then labelled a Solid-Side Resistance (SSR) model.

A schematic overview of the SSR model is presented in Figure I.2. Diffusion in the particle is described by Fick's law for diffusion, equation I.1, and below presented for the SSR model:

$$\frac{\partial C}{\partial t} = \frac{1}{r^2}\frac{\partial}{\partial r}\left(Dr^2\frac{\partial C}{\partial r}\right) \tag{I.1}$$

Next, the particle will be reviewed in detail. Following the same method, the particle can be discretized in n_s control volumes, or shells. For these shells, the mass balances can be drawn up. The mass balance of a shell is presented in Figure I.1. Fick's law for diffusion is the equivalent of Fourier's heat law. For diffusion:

$$j\Big)_{r_i+\frac{\Delta r}{2}} = -D\frac{\partial C}{\partial r}\Big)_{r_i+\frac{\Delta r}{2}} \tag{I.2}$$

The following assumptions are made regarding the volume and surface of a particle shell:

$$V_{shell\ i} = \frac{4}{3}\pi * (R_i^3 - R_{i-1}^3) = 4\pi * r_i^2 * \Delta r \tag{I.3}$$

$$A_{shell\ i,outer} = 4\pi * (r_i + \frac{\Delta r}{2})^2 \tag{I.4}$$

The mass balance is constructed as follows: the change in moisture content of a shell is expressed by the partial derivative of the concentration times the volume of a shell. This is equal to the difference in influx and outflux multiplied by the corresponding surfaces:

$$\frac{\partial C_i}{\partial t}(4\pi r_i^2)\Delta r = 4\pi\left(-j\Big)_{r_i-\frac{\Delta r}{2}}\left(r_i - \frac{\Delta r}{2}\right)^2 + j\Big)_{r_i+\frac{\Delta r}{2}}\left(r_i + \frac{\Delta r}{2}\right)^2\right) \tag{I.5}$$

$$\frac{\partial C_i}{\partial t}(4\pi r_i^2)\Delta r = 4\pi\left(+D\frac{\partial C}{\partial r}\Big)_{r_i-\frac{\Delta r}{2}}\left(r_i - \frac{\Delta r}{2}\right)^2 - D\frac{\partial C}{\partial r}\Big)_{r_i+\frac{\Delta r}{2}}\left(r_i + \frac{\Delta r}{2}\right)^2\right) \tag{I.6}$$

Diffusion coefficient is assumed constant. 4π can be eliminated. The equation is divided by r_i^2.

$$\frac{\partial C_i}{\partial t} = \frac{D}{r_i^2}\left(\frac{+\frac{\partial C}{\partial r}\Big)_{r_i-\frac{\Delta r}{2}}\left(r_i - \frac{\Delta r}{2}\right)^2 - \frac{\partial C}{\partial r}\Big)_{r_i+\frac{\Delta r}{2}}\left(r_i + \frac{\Delta r}{2}\right)^2}{\Delta r}\right) \tag{I.7}$$

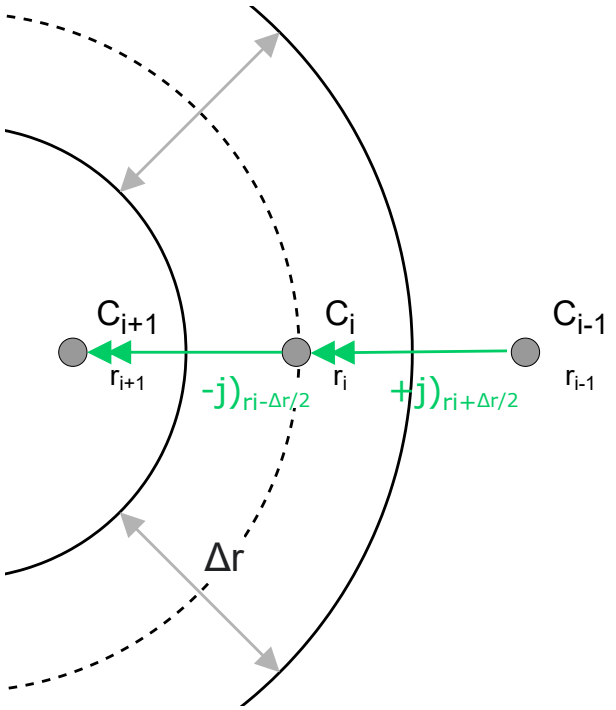

Figure I.1: Mass balance of particle control volume.

$$\frac{\partial C_i}{\partial t} = \frac{D}{r_i^2}\left(\frac{\frac{C_{i+1}-C_i}{\Delta r}\left(r_i - \frac{\Delta r}{2}\right)^2 - \frac{C_i - C_{i-1}}{\Delta r}\left(r_i + \frac{\Delta r}{2}\right)^2}{\Delta r}\right) \tag{I.8}$$

$$\frac{\partial C_i}{\partial t} = \frac{D}{r_i^2}\left(\frac{C_{i+1}-C_i}{\Delta r^2}\left(r_i - \frac{\Delta r}{2}\right)^2 - \frac{C_i - C_{i-1}}{\Delta r^2}\left(r_i + \frac{\Delta r}{2}\right)^2\right) \tag{I.9}$$

The most inner control volume, or sphere, has only influx. The mass balance simplifies to:

$$\frac{\partial C_n}{\partial t} = \frac{D}{r_n^2}\left(-\frac{C_n - C_{n-1}}{\Delta r^2}\left(r_n + \frac{\Delta r}{2}\right)^2\right) \tag{I.10}$$

The most outer control volume sums the outgoing diffusive flux and the incoming convective mass exchange with the air.

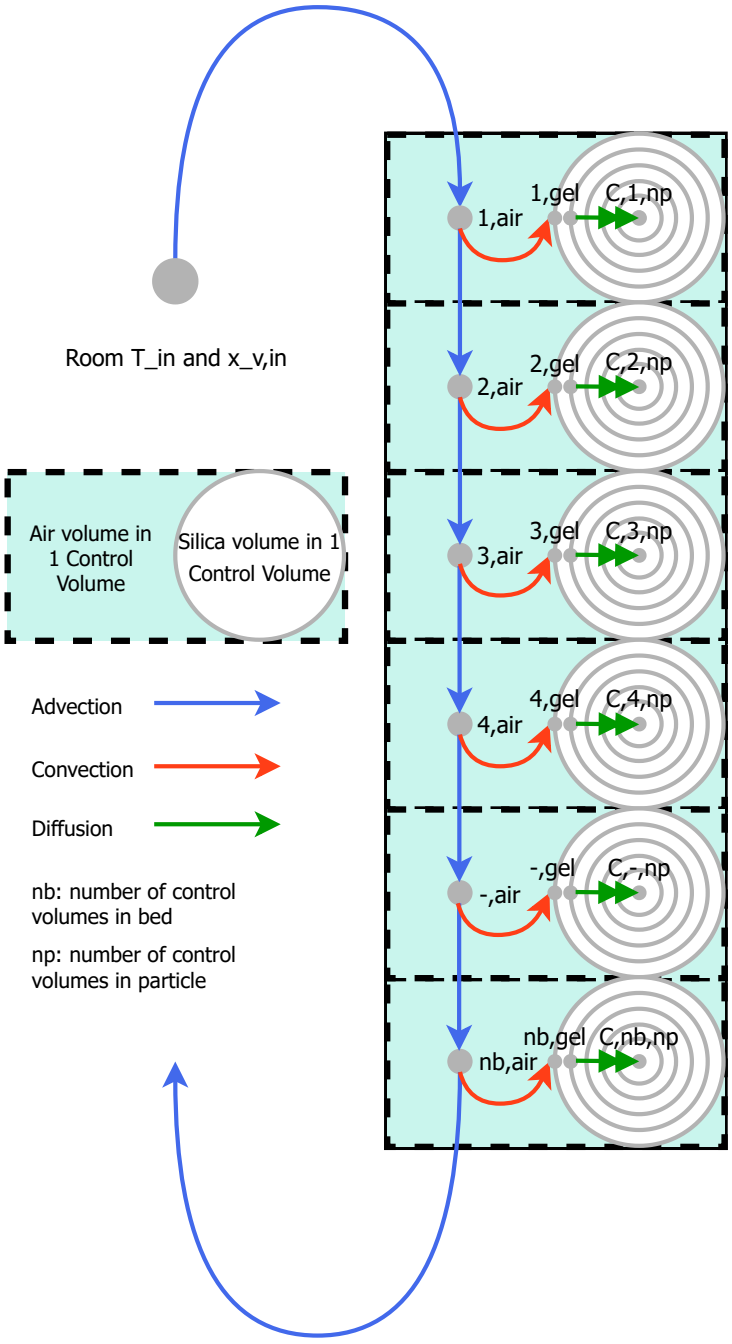

Figure I.2: Schematic overview of the Solid-Side-Resistance model.

J | Model addition 2: Hysteresis-accounted model (Pedersen)

In the before mentioned models, for every numerical time step the partial differential equation describing water content C ($\equiv$ w) is solved, yielding a new value for C and w. This new value for water content is used to calculate the new relative humidity appearing at the silica gel surface. This is done using the isotherm polynomial. Taking into account hysteresis in the model means the relative humidity can not be determined by a single polynomial.

Pedersen's model is included to determine the new appearing RH using the boundary adsorption and desorption isotherms, the adapted isotherm slope $\xi_{hys,ads}$ or $\xi_{hys,des}$, the mode of adsorption or desorption, current value of RH and w and the change in water content, Δw.

Pedersen's model described by Carmeliet [5] uses the transposed expression $w(RH)$. In the model developed in this thesis, the adsorption and desorption isotherms are expressed by fourth order polynomials $RH_{ads}(w)$ and $RH_{des}(w)$, respectively. The scanning curves follow the course as described by Rao et al. [17], sketched in Fig. J.1 for the transposed plot.

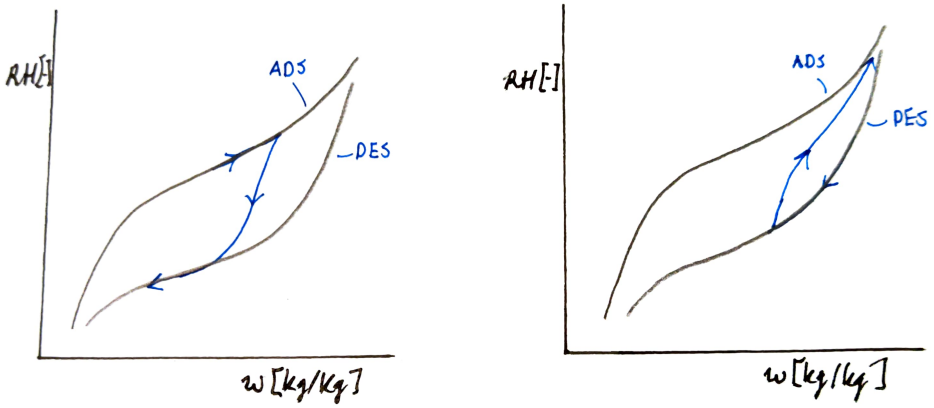

Figure J.1: Scanning curves shown in a $RH(w)$ plot, for desorption following adsorption (left) and adsorption following desorption (right).

Depending on the mode of adsorption or desorption, the isotherm slope is determined. The parameters γ_a and γ_d adjust the slope to adsorption or desorption mode. This is because the

scanning curve follow a course depending on this mode.

$$\xi_{hys,ads} = \frac{\gamma_a(RH - RH_{ads})^2\xi_{des} + (RH - RH_{des})^2\xi_{ads}}{(RH_{des} - RH_{ads})^2} \tag{J.1}$$

$$\xi_{hys,des} = \frac{(RH - RH_{ads})^2\xi_{des} + \gamma_d(RH - RH_{des})^2\xi_{ads}}{(RH_{des} - RH_{ads})^2} \tag{J.2}$$

In the model the following steps have to be integrated. Figure J.2 helps to clarify these steps.

1. Initial w_t and RH_t on the adsorption or desorption isotherm are known.
2. The adsorption or desorption mode from previous time step should be tracked. At current time step, the mode is determined by:
   - $(x_{1,e} - x_{1,s}) > 0 \; - Adsorption$
   - $(x_{1,e} - x_{1,s}) < 0 \; - Desorption$
3. Based on the mode, the slope is chosen, $\xi_{hys,ads}$ or $\xi_{hys,des}$.
4. The new RH_{t+1} is determined using this isotherm slope. w_{t+1} will follow from the solved mass balance. For desorption following adsorption:
   - $(w_{t+1} - w_t) = \Delta w$
   - $\Delta RH = RH_{t+1} - RH_t$
   - $\Delta RH = \Delta w * \xi_{hys,des}$
   - $RH_{t+1} = (\Delta w * \xi_{hys,des}) + RH_t$

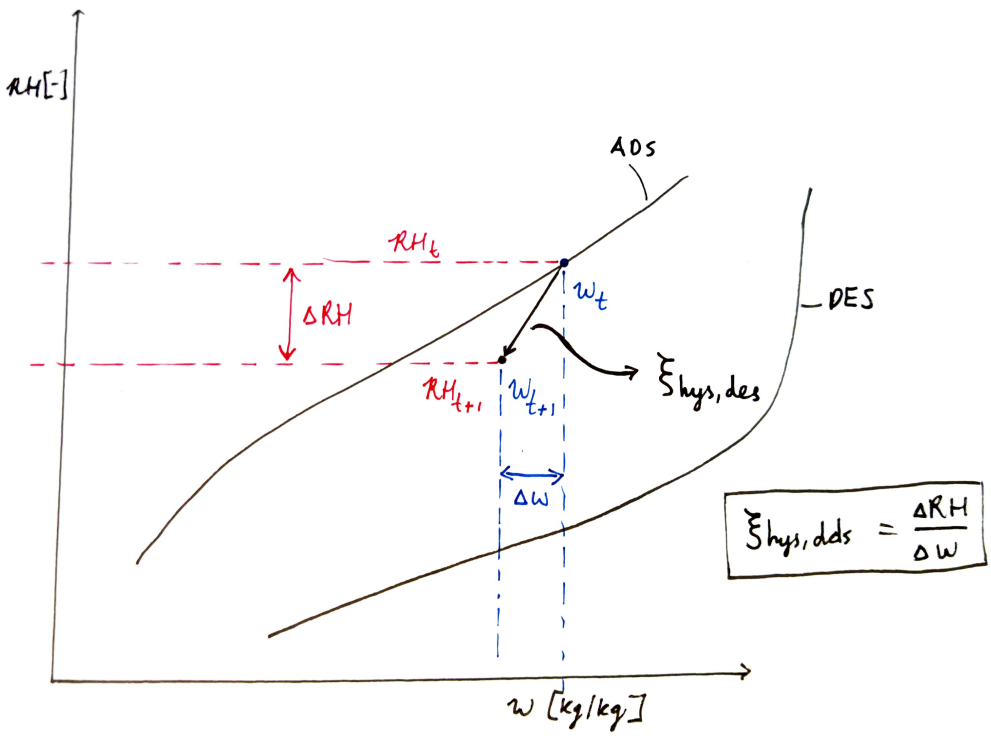

Figure J.2: Calculation of RH_{t+1}, presented for the case of desorption following adsorption.

List of Figures

List of Tables